A Novel Method of Determining Sediment Transport using Ultrasonic Wireless Sensors

by

Archie John Watt, B.Sc.

Director of Studies: Dr Carlene Campbell

Supervisors: Prof. Ian Wells, Prof. Mike Phillips, Dr Stephen Hole

Submitted in partial fulfilment for the award
of the degree of Doctor of Philosophy

University of Wales Trinity Saint David

School of Applied Computing
Faculty of Architecture, Computing and Engineering

2019

Abstract

Doctor of Philosophy

Climate change can result from human activities and natural fluctuations, and has been identified as a significant contributor to several storm events over recent years. As sea levels are predicted to increase because of global warming, and since most of the warming is absorbed by the oceans, sea level rise has resulted in increased concerns about coastal erosion.

Therefore, monitoring of the shoreline, coastal processes and in particular sediment movement, given the dynamic nature of coastal systems, is vital to ensure that erosion response is appropriate. Ideally, monitoring should take place regularly over long periods with data collected for both the visible beach and submerged parts of the littoral zone. Consequently, two current limitations to effective coastal monitoring are: 1. data acquisition is largely manual and 2. measurements are limited to the visible beach. This results in an incomplete picture of what is happening due to the inability to gather data beneath the sea surface. To overcome these limitations, a novel method was developed to monitor sediment transport using a combination of ultrasonic distance measurement and Wireless Sensor Network (WSN) technologies. This technique will enable effective coastal monitoring via regular acquisition of underwater data over a long period of time.

Practical results from proof of principle testing were obtained from laboratory experiments, with air-based validation of the system being undertaken. Importantly, results showed this novel approach enabled comparisons to be made between different types of sediment, an important requirement for monitoring coastal environments. The ZigBee communication protocol transmitted sediment movement data and results demonstrated the capability and potential effectiveness of the system, as well as its limitations. High levels of accuracy (upwards of 95%) were achieved for all experiments. In summary, this research represented the first stage in development of a novel coastal monitoring system that has potential global impact. It will facilitate a greater understanding of sediment movement via real time data acquisition and transmission, which in turn will enable the development of more effective coastal management strategies.

Acknowledgements

First and foremost I want to express my deepest gratitude to my director of studies Dr Carlene Campbell, who inspired me as an undergraduate student to undertake a research degree. Throughout this work she has been a constant source of motivation and encouragement, and without her incredible support I would not have even come close to completing it. Her passion for research, insight, clarity, and high standards make anybody fortunate to have the opportunity to carry out research under her guidance, as does her unwavering devotion to supporting the well-being of her students. I was no doubt frustrating to supervise at times, but she never let that show and was always there for support and to set me back on track. Academically and personally, she will always remain one of my biggest sources of inspiration. Thank you Carlene.

I want to thank my lead supervisor Professor Ian Wells for his support and enthusiasm, as well as his innovative previous work with the ASTEC project which informed this research. Without his technical expertise this work would not have been possible.

I am incredibly grateful to Professor Mike Phillips for taking an interest in my research and securing funding for this work. His environmental and coastal knowledge added an exciting new discipline to this project and enabled it to move beyond theory to something that can have real-world application.

My thanks go to Dr Stephen Hole, who contributed many useful ideas and has always been full of support and encouragement. I am also grateful to him for providing financial support by giving me teaching hours during my first year.

No student could ask for a better supervisory team than the people above. I feel extremely fortunate to have undertaken my PhD under their supervision, and I will owe a major part of any success I have in the future to what they have made possible for me over the last four years.

I want to thank all the staff in the School of Applied Computing for making study at UWTSD such an enjoyable and rewarding experience. Throughout my undergraduate and postgraduate study, many of them have provided me with help and support, and without it I wouldn't be where I am today. I also want to thank past and present fellow research students, especially Arya, Ethan, and Mabrouka,

the original members of the Computer Networks & Communications group, for fostering such a fantastic research environment.

Many others who have given invaluable advice and help during this work and I am very grateful to them all. In particular I would like to thank Professor Peter Charlton whose knowledge of ultrasonics was instrumental in determining a way forward at the start of this research, and also Dr Tony Thomas for his expertise in coastal monitoring.

I want to thank my family for their unconditional support throughout the completion of this work, especially my parents, Fiona and Ron, and my sisters Caitlin, Evie, and Martha. Now that it's finished I will hopefully have the time to properly explain what I've actually been doing for the last few years.

Finally, I offer my regards to all of those who supported me in any respect during the completion of this project. I will always be grateful.

Contents

List of Figures

List of Tables

Abbreviations

ADC	**A**nalogue to **D**igital **C**onvertor
API	**A**pplication **P**rogramming **I**nterface
AT	**A**pplication to **T**ransparent
DoC	**D**epth **o**f **C**losure
DSP	**D**igital **S**ignal **P**rocessor
EM	**E**lectro**m**agnetic
GPS	**G**lobal **P**ositioning **S**ystem
GSM	**G**lobal **S**ystem for **M**obile Communications
IDE	**I**ntegrated **D**evelopment **E**nvironment
MAC	**M**edium **A**ccess **C**ontrol
LOS	**L**ine **o**f **S**ight
LST	**L**ongshore **S**ediment **T**ransport
SLR	**S**ea **L**evel **R**ise
UWSN	**U**nderwater **W**ireless **S**ensor **N**etwork
WLAN	**W**ireless **L**ocal **A**rea **N**etwork
WPAN	**W**ireless **P**ersonal **A**rea **N**etwork
WSN	**W**ireless **S**ensor **N**etwork

Chapter 1

Introduction

1.1 Background

Due to their rich resources, coastal zones have always attracted humans. Our uses of these regions are many and varied, but can broadly be classified under one or more of the following six categories defined by Ketchum [1]:

1. Living space and recreation
2. Industrial and commercial
3. Waste Disposal
4. Food Production
5. Natural Preserves
6. Special Government Uses

These uses of the coastal zone regularly conflict not just with each other, but also with natural processes. Developments in and around coastal zones have greatly

increased in recent decades, and this is a trend that is expected to continue in the future. Population density around the coast is significantly higher than in non-coastal areas, and the rates of population growth and urbanisation outstrip those of the hinterlands [2]. This is expected to increase the pressure on coastal and marine environments, whilst storm events and rising sea levels will also put communities along the coast at risk.

Sea level rise is attributable to global warming and in particular to two main factors: added water from melting ice, and thermal expansion as the temperature of sea water increases [3]. It has been determined that between 1990 and 2010, global mean sea levels have risen approximately 0.19 m, at a rate of nearly 1.7 millimetres per year, one that is expected to increase in the future as a result of rising global temperatures [4]. Ice sheets around the world hold enough water to raise sea levels by several meters, with the two largest ice sheets in the world, Antarctica and Greenland, containing nearly 99% of freshwater ice. It has been estimated that the melting of Greenland's ice sheet could result in sea levels rising by approximately 6 metres, and the melting of Antarctica's 60 metres [5].

Sea level rise leads to greater quantities of sediment being removed from beaches and less amounts being deposited, causing coastal erosion, which is becoming a increasingly common and destructive occurrence worldwide. There are several possible responses to mitigate the impacts of coastal erosion, and these are discussed in Chapter 2. However, in order for coastal engineers to determine the optimal response to take, they require the long-term ability to monitor and measure the movement of sediments so that their decisions are informed by both historical and current data.

Collection of data on the movement of sediments has to date largely centred upon surveying and measuring exposed coastal areas such as beaches. Whilst this makes it possible to quantify the effects of coastal erosion, the inability to measure what

is occurring beneath the surface of the sea means that only a partial understanding of the processes involved is achieved. Furthermore, current monitoring techniques are largely manual and are therefore often unable to collect data at the desired regularity. This thesis proposes a new approach to overcome these limitations of existing methods, using a combination of ultrasonic distance measurement and wireless sensor network (WSN) technology, both of which are briefly introduced below and are discussed in greater detail in Chapter 3.

The use of acoustics to measure ocean depth dates back to the early 1900s and was gradually refined throughout the 20th century. Today, it is the most common means of depth sounding, involving a transmitter sending a pulse of energy which reflects off the seabed and returns to a receiver. The time taken between transmission and receiving, together with knowledge of the current sound velocity, is used to establish the distance measured [6].

WSNs [7] are an emerging and fast growing technology, with their growth primarily attributable to the new applications they enable. WSNs are made up of "nodes", which can range from several to hundreds or even thousands in number, each of which is connected to one or more sensors. These nodes collaboratively collect data and transmit it to a central point, usually called the "sink". From there, data can be transmitted to its final destination, where it can then be processed and analysed. They have two main abilities that make them a promising approach to overcoming the aforementioned limitations in existing methods of coastal monitoring. Firstly, they can be deployed in and withstand harsh environments. Secondly, they are able to operate for long periods of time with minimal human intervention, which makes them particularly suitable for deployment in areas which are not easily reached.

These two technologies form the basis of this research, which takes one older, established technology and combines it with a newer, emerging one, in order to

initiate a new pathway of research in the area of coastal monitoring.

1.2 Problem Statement

In order to respond to the growing threat of coastal erosion, it is necessary to establish a better understanding of the associated sediment transport processes. Since coastal environments represent highly dynamic natural systems, observation and measurement of the relevant processes requires the collection of data regularly over long periods of time, from monitoring both the visible beach and the submerged portions of the coastal zone. Systems developed for coastal monitoring need to have the ability to operate for long periods of time with minimal human intervention. Considering this, existing coastal monitoring techniques have two significant limitations:

- They are limited to the visible beach and do not have the ability to monitor beneath the sea's surface. This means that only a partial understanding of the relevant processes is achieved due to the absence of this important data.
- They require largely manual operation, and are therefore unable to gather data with the desired level of automation or regularity.

There is therefore a need to establish a new method of monitoring sediment transport in the submerged portions of the coastal zone and furthermore, one that can operate for extended periods of time with minimal human intervention.

1.3 Motivation

The primary motivation for this work is derived from the need to establish a better understanding of coastal erosion, which is becoming increasingly common and a threat to coastal communities. In particular, the work in this thesis is motivated by the following issues:

- Coastal populations have greatly increased in recent years and the impact of this will continue to rise in the years to come. 1.4 billion people worldwide (20% of the population) live within 25 km of the coastline and a further 2.8 billion (40% of the population) within 100 km [8]. Furthermore, the population levels in and around the coast is expected to continue to increase in the future [2], which in turn increases the number at risk of the effects of eroding coastlines.

- Beaches are the most popular destination in travel and tourism, the world's largest industry, and therefore have tremendous economic value [9], contributing much needed revenue to the GDP of a country. For example, tourism in Greece provides 24% of GDP [10]. In Spain, beaches produce 10% of GDP despite the fact they contribute only 0.001% of land surface [8]. Erosion of the coastlines is therefore a significant economical threat locally, nationally and globally.

- There is a need for strategic options to address the threat of coastal erosion to be evaluated based on quality data. Indeed, it has been argued, for example by Williams and Alvarez [11], that this should be mandatory. However, as specified in Section 1.2, current monitoring techniques are lacking in the ability to gather data from beneath the surface of the sea, where key processes related to coastal erosion occur. Therefore, as it currently stands,

evaluation of the strategic options in the case of coastal erosions is only partially based on quality data.

Research in the field of WSNs for monitoring coastal processes is not new to the research group. The ASTEC (Automated Sensing Technologies for Coastal Monitoring) project is the most significant previous example of a WSN deployed for monitoring underwater sediment transport. This project therefore forms the basis of this work and is discussed in detail in Chapter 3. The approach taken is critically analysed and shortcomings identified are used to inform development of the new approach presented in this thesis.

More broadly, this work is motivated by the global interest in exploration of the world's oceans. It is the largest biosphere on Earth, covering more than two thirds of its surface, with an average depth of 4000 metres. The oceans significantly contribute to making this planet habitable, for example through rainwater supply and climate regulation, but despite this, they remain largely unexplored [12], with it being estimated that only approximately 5% has been explored to date [13]. Exploration of oceans enables the gathering of a great deal of data relating to phenomena such as climate change and natural disasters, as well as history of the planet.

1.4 Aims and Objectives

The main aim of this thesis is to initiate a new research pathway in the field of coastal monitoring, which will ultimately lead to a technique capable of monitoring underwater sediment movement, and specifically to determine depth of closure (DoC) in order to establish the seaward limit of sediment transport and advance the knowledge and understanding of the coastal environment. This aim is expressed in terms of the following objectives:

1. To develop a theoretical base for the coastal environment and the relevant processes that occur (Chapter 2)
2. Identify the challenges faced in monitoring coastal processes and the limitations of existing methods and how these can be overcome (Chapters 2 and 3).
3. Devise a new method to overcome the limitations identified Chapter 4.
4. Develop a prototype system and setup an experimental arrangement to test the proposed new method and evaluate its performance (Chapter 4).
5. To critically analyse the results and provide suggestions for future work (Chapters 5 and 6).

1.5 Contributions to Existing Knowledge

This thesis contributes to the fields of computer science and coastal engineering through the application of the former to the latter. This was achieved by designing a novel automated method of measuring sediment movement, whereby the point at which there is absence of significant sediment movement (depth of closure) can be identified using ultrasonic sensors. The contributions to knowledge can be summarised as follows:

1. **An analysis of current methods of coastal monitoring and their limitations**

   Chapter 2 critically evaluates literature related to current methods of monitoring the coastal environment and sediment transport. Based on the deficiencies identified, Chapter 3 introduces the sensor and wireless networking technologies, with emphasis on their features that address that can overcome problems that were identified with current methods.

2. **Formulation of a new method ultimately to be capable of monitoring underwater sediment movement**

   Based on the critical analysis of existing literature, a novel method is presented which combines ultrasonic distance measurement and wireless sensor networks to determine sediment movement based on changes in depth measurement. The novelty of this method is in the way it is applied in this thesis; although ultrasonics are a well established means of depth measurement, no previous examples could be found of it being applied to monitoring sediment transport. This thesis represents the first step in the the development and application of this method, which ultimately will result in the ability to gather previously unobtainable data relating to movement of sediments underwater. Furthermore, its approach of deploying sensors on the

sea's surface rather than the seabed will overcome a number of significant maintenance and energy related restrictions that were inherent in previous systems developed for similar applications.

3. **A lab-based evaluation of the developed system**

   Following the introduction of the new method, a prototype system was built and an evaluation was carried out in a lab environment in order to test its feasibility. In-air validation of the system is achieved, with recommendations made for extending this to the underwater environment. Testing was conducted across three sediment mixes: sand, shingle and a mix of both. High levels of both accuracy (97.25% for sand, 95.75% for shingle, and 97.41% for mixed sediments) and precision (average standard error was calculated below 0.2 for all experiments) were achieved in all cases.

1.6 Approach

The work in this thesis forms part of a larger research project, the ultimate aim of which is to produce a floating sensor network capable of monitoring underwater sediment transport, from which the data gathered would be used to develop a computational model to predict future patterns of sediment movement.

In order to establish a structured approach, this project has been divided into six stages, as shown in Table 1.1.

Stage 1	**Stage 2**	**Stage 3**	**Stage 4**	**Stage 5**	**Stage 6**
Initial prototype and in-air testing	Prototype for water testing	Wave tank tests	Sea trials	Final deployment	Development of predictive computational model

Table 1.1: Research Stages

In order to keep the work in this thesis focused, it was decided to concentrate on Stage 1, or an initial prototype along with in-air validation of the method, which sets the stage for progress of the remaining stages. It is expected that the remaining stages of this research project will involve at least two further PhD candidatures. The ultimate aim of this research (as detailed in Section 1.4) is therefore still a long way away. However, the work carried out in this thesis has resulted in the fulfilment of that aim being one step closer.

The initial stages of this research focused on a review of relevant literature, including books, research papers in the form of conference proceedings and peer reviewed journals, standards and white-papers, in order to critically review:

1. The coastal environment and the relevant processes that occur in this region. Additionally, current coastal monitoring approaches are investigated with the aim of identifying their limitations in terms of addressing the problem identified in Section 1.2.

2. Ultrasonic sensor and wireless sensor network technology, with a view to determining how they can overcome the limitations identified in the first stage of the literature review.

In order to continue work already undertaken within the research group, analysis is then conducted on a previous system developed for the same application (the aforementioned ASTEC project), considering such factors as deployment type, protocols, and ease of maintenance. The findings from this are used to inform development of the new system documented in this thesis.

The design and implementation of a WSN capable of measuring sediment movement is then undertaken. Since the work in this thesis is proof-of-principle, care was taken to minimize the cost of the system at each stage. The method developed utilizes ultrasonic sounding sensors to determine the distance from sensor to sediment which is used to identify a point where sediment motion has occurred, relative to a previously established datum/baseline. Data is collected by individual sensor nodes which co-operatively transmit the measurements obtained to the sink (central) node using the ZigBee protocol. To demonstrate the concept, a simple prototype consisting of three nodes (one sink and two for gathering data) was built in a lab environment and tested using different types of sediment. Lab experiments demonstrated high levels of both accuracy (upwards of 95% in all cases) and precision (standard error of below 0.2) of measurements.

1.7 Thesis Structure

Including this introduction, this thesis is comprised of six chapters. The contents of each are summarised below:

- Chapter 1 introduced the background to this research and the necessity of developing a system for monitoring underwater sediment transport. The main problems associated with existing systems were highlighted, and a solution based on echo sounding techniques and WSNs was proposed, from which the research aim, objectives and methodology are derived.

- Chapter 2 introduced the coastal environment and relevant environmental processes, with a focus on the process of sediment transport, and in particular the current methods available for monitoring it. The primary limitation identified was the inability to monitor sediment transport beyond the visible beach. Depth of closure (DoC) and its importance is also introduced. This highlighted the need for a system for monitoring underwater sediment transport.

- Chapter 3 introduces the relevant sensor technologies, along with a discussion of the relevant background theory, as well as the principles of WSNs, highlighting key features that suit them to this research, as well as potential constraints that needed to be considered. They are then critically compared with existing coastal monitoring technologies to highlight shortcomings in the latter. Finally, the aforementioned ASTEC project is discussed, with the shortcomings identified forming the basis for this work.

- Chapter 4 introduces the novel method of monitoring sediment transport using ultrasonic distance sensors and WSNs. It then proceeds to outline the hardware and software equipment that was utilized in order to develop and build a prototype to evaluate the proposed system.

- Chapter 5 describes the experimental procedure that was followed to evaluate the prototype system developed in Chapter 4. It then presented and analysed results obtained from the set of experiments that were conducted, with a view to ascertaining validity of the developed system.

- Chapter 6 presents conclusions drawn from this research as well as recommendations for future work.

Chapter 2

The Coastal Environment

2.1 Introduction

In order to develop a system to monitor sediment transport, it is first important to establish an understanding of the coastal environment and key physical processes which occur. Accordingly, this chapter commences with an overview of the coastal zone and the concepts of sediment transport and depth of closure (DoC) (Sections 2.2, 2.4 and 2.5). Current methods of monitoring the coast are then discussed in order to identify their limitations and how this research can overcome them 2.4.2. Climate change and its link to sea level rise and erosion of coastlines is also discussed (Section 2.3).

2.2 The Coastal Zone

There is no uniform definition of the coastal zone, which in a broad sense is generally considered to be the area between land and the marine environment. In the context of coastal engineering, where more specific definitions are required, the coastal zone is generally divided into two sections, defined by Davidson-Arnott

[14] as offshore zone and littoral zone, a definition that this thesis will adopt for discussion of the coastal zone that follows.

The offshore zone describes the region that is inactive with respect to significant wave-induced movement of sediment. Conversely, the littoral zone (sometimes referred to as the nearshore zone) is where wave action results in sediment being transported, leading to changes in beach morphology. These two zones are divided by a contour known as Depth of Closure (DoC) [15], an important concept that is further discussed later in this chapter (Section 2.5). The littoral zone is often subdivided into several smaller sub zones, as illustrated in Figure 2.1. The nearshore zone extends from the DoC to the shoreward limit of breaking waves, and sediment that is transported in this zone is generally done so by wave action and currents. Orbital velocity of the waves results in the sediment being lifted from the seabed and being transported in the prevalent direction of the currents.

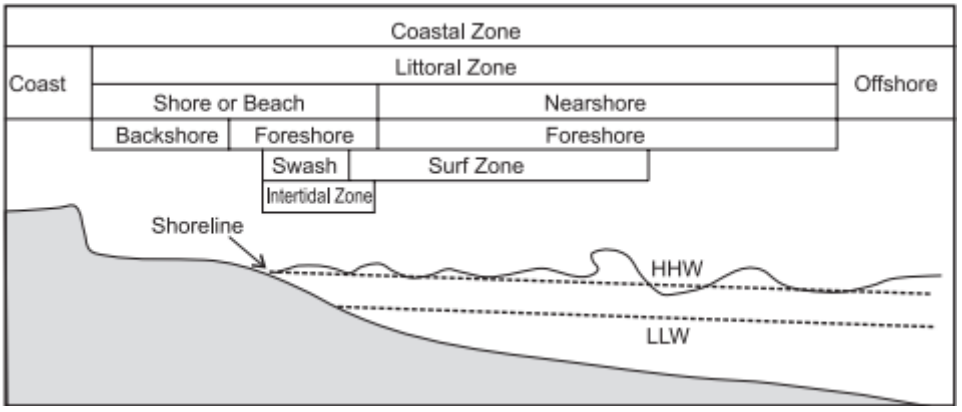

FIGURE 2.1: Schematic Diagram of the Coastal Zone [15]

When waves break in the surf zone, they continue to move in, and eventually run up the front of the beach; this results in a turbulent layer of water known as swash. The transport of sediment that takes place in the swash zone is responsible for determining whether sediment remains onshore or is transported and lost offshore [16], and consequently this process plays a large part in shaping the face of beaches. Given the non-linear conditions of flow that occur, sediment transport processes can be extremely complex to understand [17]. This has resulted in many studies

over the years which has focused upon sediment transport in the swash zone, including those by Turner and Masselink [18], Pritchard and Hogg [19], Alsina et al. [20], and Ruju et al. [21]. A recent review of methods of modelling swash zone sediment transport is given by Bakhtyar et al. in [22]. Approaches to modelling and measurement of coastal processes are further discussed in Section 2.4.2.

The beach can be defined as the region that is subaerial for extended periods and is susceptible to regular wave action [17]. In terms of wave action, the beach is generally subdivided into the foreshore and backshore. The foreshore is subjected to wave action during regular conditions, whilst the backshore is not generally encroached upon by waves, although exceptions do occur in storm conditions. As such, the backshore is often defined as the "beach" in terms of recreational activities as it is not affected by regular wave conditions. There are four principle types of beach, which are categorised according to the sizes of sediment present: shingle, shingle upper/sand lower, shingle/sand mixed and sand, as shown in Figure 2.2.

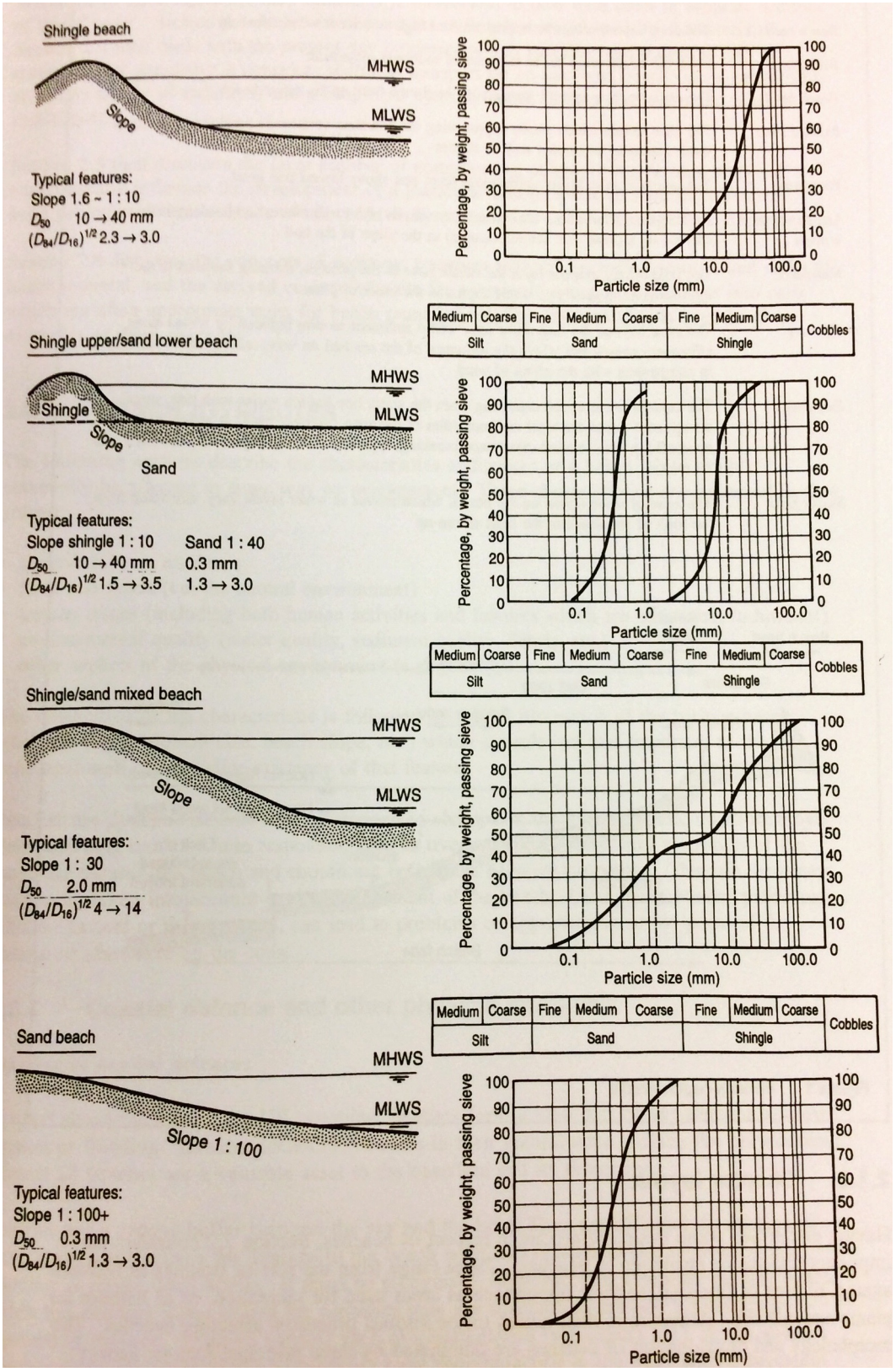

FIGURE 2.2: Beach Classifications [23]

2.3 Climate Change, Sea Level Rise and Coastal Erosion

It is widely accepted among climatologists that climate change is an issue that needs to be addressed. Although climate change can results from both human activity and natural fluctuations, the former, in particular population growth and industrialisation has been identified as a significant contributor to several climatic events that have occurred in recent years [24]. Indeed, a recent study by Mann et al. suggests that 13 out of the 15 warmest years on record would not have occurred were it not for emissions resulting from the burning of oil and coal [25].

Repeated visits to any section of coastline illustrates that it is not a permanent, fixed feature, but rather a highly dynamic one that is constantly reshaped by the wind and waves. Considering this, coastal erosion itself is a natural process that has shaped coastlines all over the world. It has always occurred and will continue to occur in the future. However, human influence, in particular the aforementioned contributions to global warming and climate change, as well as urbanisation and economic activities in and around the coast, has resulted in what was once a natural phenomenon becoming an increasingly common and destructive problem of growing intensity, with a 2004 Eurosion report [26] highlighting that in Europe, coastal erosion induced by human activity has surpassed that induced by natural factors.

A key factor in causing coastal erosion is sea level rise (SLR), and future ocean levels are predicted to rise in the future as a result of global warming, since most of the warming is absorbed by the oceans. This in turn has led to increased concerns about eroding coastlines. There are two primary factors related to global warming that result in sea level rise: water is added from ice sheets and glaciers that have melted, and thermal expansion as the sea water gets warmer.

Erosion of coastlines can be responded to in a number of ways, which Leatherman identifies [27] as:

- Retreat from the shore
- Armouring of the coast
- Beach nourishment

Appropriate responses to coastal erosion are strongly dependant on site-specific factors, and therefore any general coastal response due to climate change is not particularly meaningful as each case is different. However, responses that are based on results of a detailed study and availability of long-term coastal change data can be implemented with a higher degree of confidence. Additionally, there are economic and political factors to consider; for example, whilst retreating from the shore would be the preferred approach for a sparsely developed and/or populated area, it would not be a realistic option for highly urbanised locations.

2.4 Sediment Transport

Sediment transport plays a major role in many coastal situations that impact human activity, and consequently has been subject of much study over the last century. Movement of sediments on coastlines can result in significant erosion or accretion occurring, which can in turn affect important facilities or structures in the area. For example, excessive deposition of sediments may interfere with port and harbour operations, whilst erosion may undermine structures on the coastline. Timescales for such occurrences vary greatly, from a few hours (as a result of storms or floods) to decades (resulting from climate change, itself a result of both natural and human influence) [28]. Thus, study of sediment transport processes is one of great importance when researching coastal engineering and management.

Coastal sediment transport is typically divided into two components, that which occurs perpendicular to the coastline (cross-shore) and parallel to the coastline (longshore, sometimes also known as littoral transport). The affects of cross-shore transport are largely limited to causing a redistribution of sediment in the beach profile, whilst longshore transport has a significant impact on the long-term evolution of the coastline.

This section will discuss the basic principles of sediment transport; further detail can be found in the work of Fredsøe and Deigaard [29], Soulsby [30], Reeve et al. [28], and the references therein.

Although sediments can be transported by unbroken waves and/or currents, the majority of sediment transport processes occur in the surf and swash zones [31]. The process of transporting sediments in a mobile fluid can be simply described in the following three steps [17]:

1. The incorporation of sediment into a fluid flow, also known as entrainment.
2. Transport of entrained sediment.
3. Settling and deposition of transported sediment.

Sediment transport occurs as a result of being acted upon by by two forces: mobilising and stabilising (or resisting), as illustrated in Figure 2.3.

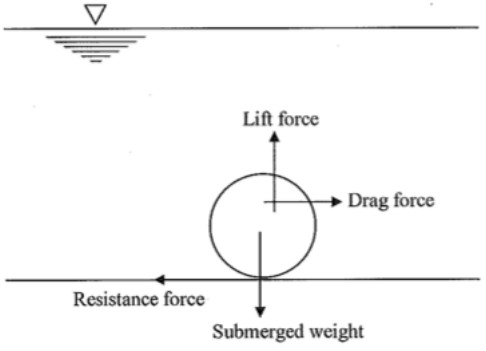

FIGURE 2.3: Forces acting upon sediments [32]

If mobilising forces are greater than stabilising, sediment will start to move. Drag and lift forces act as mobilising forces, whilst gravity is generally the stabilising force (although in some cases, for example, on a sloping bed, it can also act as a mobilising force). As such, transport of sediment can only occur if mobilising forces exceed a certain critical value, known as the sediment threshold [33].

Many sediment threshold theories exist, the first of which was presented by Shields, who in 1936 [34] studied sediment particle mobility and introduced a now well-known mobility threshold (τ_*), the eponymous Shields parameter, the formula for which is shown in Equation 2.1.

$$\tau_* = \theta = \frac{\tau}{(\rho_s - \rho)gD} \tag{2.1}$$

Where:

- τ is a dimensional shear stress;
- ρ_s is density of the sediment;
- ρ is density of the fluid;
- g is acceleration as a result of gravity;
- D is a characteristic particle diameter of the sediment.

There have been a number of extensions and adaptations that have been proposed for the Shields parameter since its publication; Soulsby and Whitehouse [35], for example, extended it for very fine sediment grains. Many transport formulae have been proposed throughout the last century, ranging from Meyer-Peter and Muller (1948) [36] to Nielsen (1992) [37]. These formulae derive a rate of transport from the difference of the flow Shield's parameter to the critical Shield's parameter,

which requires a calculation of the force of fluid against the bed, otherwise known as bed shear stress [38], as shown in Equation 2.2.

$$\tau = \gamma \; DSw, \tag{2.2}$$

Where:

- τ is shear stress (N/m^2);
- γ is water weight density ($N/m^3, lb/ft$);
- D is average water depth (m, ft);
- Sw is the water surface slope (m/m, ft/ft).

Many of these formulae have two characteristics that restrict their applicability in the coastal environment. In their original form, the majority of these sediment transport models were developed for steady flow in channels, using a time independent channel friction formula. An oscillatory friction formula must be found in order to apply these models to the coastal environment where an oscillatory flow, such as in waves, will be present [38]. A summary of these models adapted for coastal use can be found in [35]. Secondly, many earlier sediment transport models assume the presence of a homogeneous mix of sediment. Realistically, the sediment sizes on a seabed may vary, and different sizes will lead to different rates of flow. Accordingly, a number of studies have investigated differential rates of transport that occur when varying sizes of sediment are present, of which the work of Armanini and Di Silvio [39] is among the earliest examples. Later in 1996 Pender and Li [40] developed a numerical model of mixed sediment transport, which individually modelled different sized sediment fractions, allowing numerical sediment sorting, thereby allowing the time-varying composition of the sediment mix to be determined.

2.4.1 Modes of Transport

Once sediment motion has begun there are various modes in which it can be transported. Each mode of transport has different characteristics and the mode will therefore determine the morphological response. There are two modes of sediment transport that are generally recognised in the coastal environment [23]:

1. Bed load transport occurs during low velocities. In this mode, sediment rolls or slides whilst being fully supported by the bed.

2. Suspended load transport involves suspension of sediment in a water column during high velocity situations.

Some authors differentiate further, for example Dean and Dalrymple [41] who identify Swash load (movement occurring in the swash zone) as a third mode of transport. Reeve et al. [31] identify two modes of transport in addition to the above primary two, namely washload and sheetflow. The washload comprises sediment consisting of very fine particles which are suspended but do not originate from the bed; rather, they enter the system from river tributaries. Sheetflow occurs during higher rates of transport when more than one layer of sediment travels along the bed. As such, this could be viewed as an extension of bed load transport. Bed load transport is the dominant mode for low velocity flows and/or when large grain sizes are present in the sediment, whilst the opposite is the case for low velocity flows and small grain sizes [31]. Efforts to model the process have suggested that suspended load is more important within the surf zone, but since bed load transport is very difficult to measure under field conditions, there is little if any consensus on the subject [42].

2.4.2 Monitoring and Measurement

Monitoring is an essential undertaking in order to collect such data on any coastline where flooding or erosion is occurring or is a potential risk [43]. The process of monitoring a beach generally begins with a baseline survey, the results of which are used to establish an understanding of the beach's physical characteristics, and should therefore be as detailed as possible. On occasion, there may not be sufficient information available to use as a starting point for a baseline assessment. Such cases may necessitate original survey work [23], in order to establish a baseline against which future change can be measured. This work should be undertaken over several years in order to allow for any natural fluctuations that may occur, thereby allowing for a more comprehensive and accurate prediction of potential impacts. Given the dynamic nature of coastal systems, monitoring needs to be an ongoing exercise in order to enable comparisons of monitoring data with that obtained from the initial baseline survey.

There are many methods that have been used in order to attempt to measure sediment transport, ranging from field measurements to detailed statistical analysis, and much literature exists on the subject. Summaries of monitoring methods can be found in [44], [45] and [46]. Common approaches include:

- **Sediment budgets** utilize historical data on topography and bathymetry in order to assess evidence of morphological change. By combining measurements of losses and gains with knowledge of coastal processes, a picture can be built of rates of change over a given period.
- **Sand traps**, also known as sediment traps, are intended to capture sediments moving in the surf zone and assess the gross sediment transport at specific points.

- **Tracers** can be used to determine the direction of longshore sediment transport (LST) by releasing them and at least partially recovering them later. They exist in various different forms, both natural and artificial. Natural sediments can be tagged in various ways such as dyeing and geochemically in order to allow them to be identified later, whilst artificial sediments can be made to a specific density and grain size.

In past monitoring programmes, the most common means of capturing data is the use of total station theodolite combined with a data logger. Most do not require manual recording of data, although much of the operation of the equipment is manual. However, accuracy is degraded as the distance from the instrument increases. Additionally, operational problems occur during low-light conditions, which can be significant when surveying in early morning or evening over low-water periods [42].

More recent developments largely centre around the Global Positioning System (GPS), which was originally developed by the United States Department of Defence in 1973, initially for military purposes, but was allowed for use by civilians in the 1980s. Morton et al. [47] made use of kinematic GPS for monitoring beaches as part of an attempt to devise methods that could be "rapid, reliable, relatively inexpensive, and maintain or improve measurement accuracy". They went on to devise a method of collecting data which used a moving vehicle to collect data from large areas of coastline. Results indicated that variations in topography were generally more pronounced cross-shore than parallel [42]. Accordingly, surveys are usually carried out in the form of cross-shore profile surveys, with survey points recorded every second and profile line spacing generally being between 25m and 50m depending on the site that is being studied. It was correctly predicted that GPS techniques would replace conventional profiling as the preferred method for future beach monitoring. GPS is now used extensively for field data collection.

Its primarily advantage over other techniques is the speed at which data can be captured, making it particularly suitable for repetitive surveys.

The main limitation of existing monitoring methods is that they are restricted to the visible beach. As can be observed in Figure 2.1, the coastal zone extends beyond this to beneath the sea's surface as well. Therefore, it is also necessary to be able to monitor underwater occurrences in order to build a complete picture of the coastal processes that are taking place. Furthermore, despite the benefits GPS has brought to beach monitoring, its operation remains largely manual which restricts the frequency with which monitoring activities can be carried out. An automated means of beach monitoring is therefore desirable as well.

2.4.3 Prediction

Sediment transport rates are considered in terms of the longshore and cross-shore components previously discussed in Section 2.4, and the majority of previous work has focused on longshore sediment transport (LST) [42], largely because this has a more significant impact on the evolution of the coastline. Esteves et al. [48] identify three ways of estimating LST:

1. Direct measurements
2. Empirical formulae
3. Inference of net LST from observed large-scale changes

The former and latter of these approaches require considerable resources in order to gather the necessary data, and therefore investigators may not have access to all the equipment to measure the parameters that are required by the formulae. Furthermore, As a result of this, the majority of LST studies are reliant solely on empirical predictions, which, when considering large time and/or spatial scales

can result in large errors. Although accurate measurements can often be attained by physically modelling conditions in a lab environment, uncertainties associated with scaling can make interpreting the results problematic [49].

A number of formulae exist for the purpose of calculating both cross-shore and longshore transport, however, agreement between the derived formulae and field measurements is rare. Bayram et al. conducted a study of six sediment transport formulae for cross-shore prediction and compared them to field measurements, and found that for all six formulae, the measured and calculated transport differed by a factor of 5 or more in 20% of the cases studied [50]. Even the direction of cross-shore sediment transport remains difficult to predict [51]. Although in the case of longshore transport the direction is often obvious, large differences have nevertheless been found to exist between the calculated and measured transport [52]. As such, it is generally agreed among coastal scientists that field measurements are the most reliable approach [53] [54] [55].

2.5 Depth of Closure

The littoral zone is an area in which important sediment transport processes occur, and this area ultimately forms a beach [56]. In this area a zone extends across the whole beach into the water, eventually reaching a depth where sediment transport is less active [55]. The depth at which there is little or no significant movement of sediment is often referred to as the depth of closure (DoC), which was first defined in concept by Hallermeier [57] in 1978 and later described in detail by Krauss as [58]:

"The depth of closure (DoC) for a given or characteristic time interval is the most landward depth seaward of which there is no significant change in bottom elevation and no significant net sediment transport between the nearshore and the offshore."

DoC is a fundamentally important concept in coastal engineering, as it can be used as an indicator of the seaward limit of significant sediment transport. As such, it is crucial for establishing sediment budgets as well as associated applications such as beach nourishment [59]. For example, by providing an estimate how far offshore morphological change is likely to occur, coastal engineers can better assess the volume of sediment that will likely be required in order to nourish a specific section of the coast. Its importance has been further identified in relation to the design and construction of structures in the coastal region, such as groynes and piers [60].

Despite its importance, DoC is a somewhat vague concept [61] [62], largely as a result of insufficient hard data being available for analysis due to the aforementioned limitations in current monitoring methods, as discussed in Section 2.4.2. DoC is generally accepted to range between 4 and 6 metres [63], an estimate literature seems to agree with; a study involving repetitive surveying of 555 beach profiles over a 5 year period, Wang and Davis [64] found an average DoC of 4.9 metres in areas absent of direct control of the regional hard bottom. However, there are exceptions, as demonstrated in a case study conducted by Marsh et al. [65], which found that DoC can be as high as 10 metres over long periods of time.

A lack of accurate DoC measurement results in only a partial understanding of sediment transport processes being achieved due to the inability to monitor underwater processes. This in turn results in a lack of important data for planning optimal and appropriate responses to coastal erosion. The development of an approach to measure depth of closure is therefore highly desirable, and such an approach will be made in this thesis.

2.6 Chapter Summary

This chapter has discussed principles of the coastal environment and the growing problem of coastal erosion. In particular, this chapter has examined sediment transport and the concept of depth of closure (DoC), with a focus on methods of monitoring and predicting this process. Two main limitations in existing monitoring techniques were identified: the inability to monitor beneath the sea's surface, and the fact that they lack automation, meaning that monitoring needs to be manually undertaken.

Accordingly, Chapter 3 will examine how these two limitations can be overcome using ultrasonic sensors and Wireless Sensor Network (WSN) technology, each of which addresses one of the above limitations. The findings from this will then inform the development of a novel automated means of measuring underwater sediment transport.

Chapter 3

Sensors and Wireless Networks

Following a review in Chapter 2 of methods currently available to assist in monitoring of coastal erosion, the two main limitations identified were the inability to monitor beneath the sea's surface, and that their operation is largely manual. Therefore, an alternative approach was sought in an attempt to overcome limitations of current methods. Specifically, the aim was to identify a method capable of monitoring underwater sediment transport processes relevant to coastal erosion, and furthermore, one that can do this on a regular basis and long-term. Considering these requirements, ultrasonic sensors in combination with Wireless Sensor Network (WSN) [66] [67] [68] [69] are viewed as a solution.

This chapter is divided into two sections. The first discusses ultrasonic sensor technology along with the relevant background theory, and then outlines the technique of echosounding, which has been used for measuring ocean depth since the 1950s. Following this, WSN technology is presented, with a focus on the key features that make them suitable for this work, as well as their advantages over existing approaches.

The ASTEC (Automated Sensing Technolgies for Coastal Erosion) project is then discussed in detail, as the primary previous example of applying WSN technology to monitoring underwater sediment transport. The deployment approaches of underwater sensor networks are critically compared with those of a floating echosounding equivalent, in order to ascertain the benefits of this approach over the previous attempt in this field.

3.1 Sensors

Sensors are used to capture data about the environment being monitored. Sensors are a form of transducer which translate physical conditions into electrical signals which can then be interpreted and analysed. Depending on the output that they produce, they can be classified as either analogue or digital devices. Sensors are typically described based on the parameter(s) that they monitor, such as pressure, temperature, magnetism, sound, etc (e.g. a pressure sensor or motion sensor).

Broadly, sensors can be divided into three different categories [71]:

- **Passive, omnidirectional sensors** measure physical quantities of environmental conditions without manipulating the environment in any way. Furthermore, they do not have any sense of "direction" in measurements they take. Examples of these sensors include those that measure light, vibration, humidity, and chemical concentrations. The vast majority of the literature reviewed assumes the use of passive omnidirectional sensors.

- **Passive, narrow-beam sensors** differ from omnidirectional sensors in that they have a well-defined direction of measurement, but otherwise share the same characteristics. A camera, for example, is a narrow-beam sensor, as it takes "measurements" in a given direction.

- **Active sensors**, in addition to measuring parameters, also actively probe the environment, and therefore need to be continuously powered. Sonar and radar are common examples of active sensors.

3.1.1 Ultrasonic Sensors

Ultrasonic sensors operate by measuring the time between sending a sound pulse and receiving the reflection of the transmitted pulse [72]. By applying the formula shown in Equation 3.1 to the time taken, the distance (d, measured in cm) between the sensor and the reflecting object can be determined.

$$d = vt/2 \tag{3.1}$$

Where:

- v (m/s) is the velocity of the sound wave.
- t (seconds) is time between the sound pulse being transmitted and received. This is divided by two to account for the two way journey taken.

3.1.1.1 Ultrasound

Ultrasonics are a branch of sound waves that occur at frequencies above 20 kilohertz (Khz). It does not differ from audible sound in terms of physical properties, except that it cannot be heard by humans [73]. Like all sound waves, they consist of mechanical vibrations which travel through a given medium at a specific velocity, and are reflected or transmitted when they encounter a boundary with a different medium [74].

The most important properties of propagating sound waves are:

- **Frequency (Hz)** - all sound waves oscillate at a specific frequency, which refers to the number of vibrations or cycles per second.

- **Velocity (m/s)** - the speed of a sound wave, most commonly measured in metres per second (m/s), which will differ depending on the medium through which it travels. Velocity of a sound wave can be determined as per Equation 3.2

$$V = f\lambda \tag{3.2}$$

  where f is the frequency, λ is the wavelength and V is the velocity.

- **Wavelength (mm)** refers to the distance between two corresponding points in the wave cycle. This is shown in Figure 3.1, where the distance AB is equal to the wavelength λ.

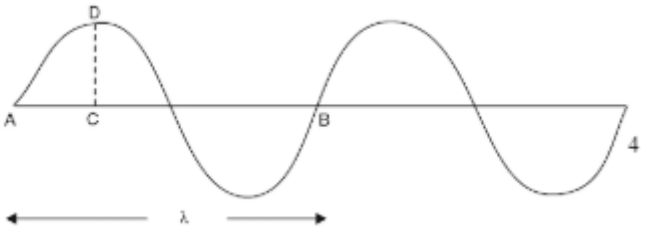

FIGURE 3.1: Wavelength [75]

The relationship between the above three properties is shown in Equation 3.3.

$$\lambda = \frac{v}{f} \tag{3.3}$$

As can be observed, a change in frequency will in turn result in a change in wavelength. In terms of object detection, a shorter wavelength resulting from an increase in frequency will generally result in increased resolution, but at the cost of reduced range, and increased risk of the sound wave scattering. As such,

determining the optimal frequency will often involve the need to achieve a balance between the positive and negative results of the selection. This is further discussed in Section 3.1.2.

3.1.1.2 Boundary Reflection

When a propagating sound wave encounters a boundary with another material, a portion of the associated energy will be reflected and a portion will be transmitted through. Energy that is reflected is known as the reflection coefficient and is related to the relative acoustic impedance of the two materials [76]. Generally speaking, hard and homogeneous materials reflect sound waves better than those that are soft or granular, although scattering (see Section 3.1.2) tends to increase when the materials are coarsely structured, especially at high frequencies. Acoustic impedance (Z, measured in Ω) refers to the extent to which the propagation of the sound wave is resisted and is calculated as [74]:

$$Z = pV \tag{3.4}$$

where p is the density of the material in question (grams/cm^3) and V is the sound velocity (m/s).

The reflection coefficient (R) can therefore be calculated as [74]:

$$R = \frac{(Z2 - Z1)^2}{(Z2 + Z1)^2} \tag{3.5}$$

where Z1 is the acoustic impedance for one medium and Z2 is the same value for the other.

3.1.1.3 Beam Spread

The energy of an ultrasonic pulse is transmitted in a conical shape along the axis of the transducer. As a pulse is generated it propagates through the medium in front of the transducer, and spreads outwards in the form of a three dimensional cone, which is initially narrow, but then spreads over an increasingly larger area, as illustrated in Figure 3.2. Objects capable of reflecting sound (see Section 3.1.1.2) that are in this conical area will be detected by the sensor.

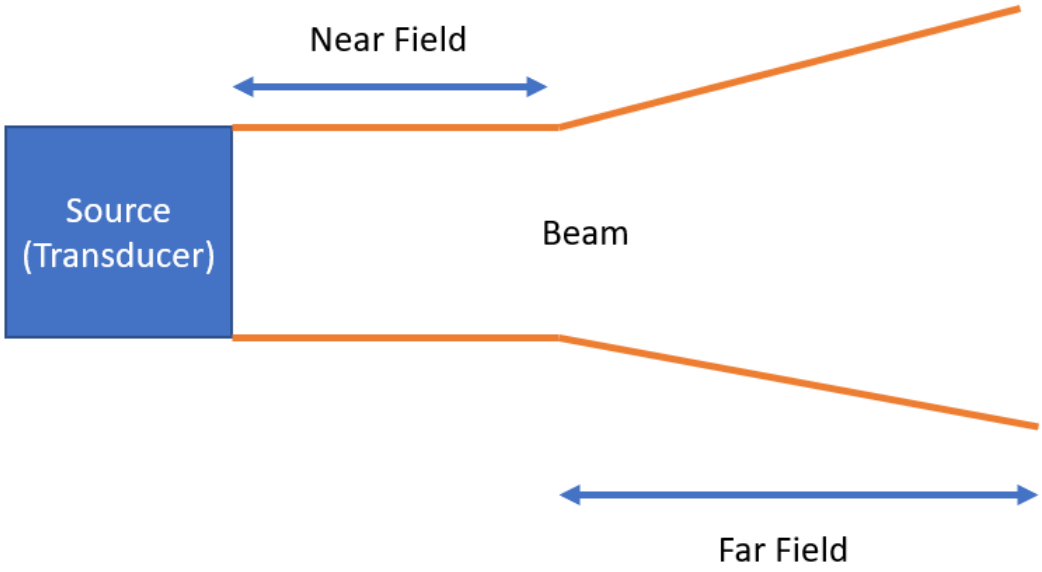

FIGURE 3.2: Beam Width

As can be observed in Figure 3.2, the pulse begins with a narrow, cylindrical beam width (W), approximately equal to the width of the source transducer. This is known as near field, or the Fresnel zone [77], which can be calculated as per Equation 3.6:

$$W = \frac{\mathrm{d}^2}{4\lambda} \tag{3.6}$$

where d is the diameter of the transducer and λ is the wavelength of the ultrasonic beam.

Beyond the Fresnel zone the beam takes a conical form, known as the far field, or Fraunhofer zone [77], which begins at distances $> \frac{d^2}{4\lambda}$. At this stage, the beam starts to spread over an increasingly large area, which causes the spatial resolution of the sensor to deteriorate. Considering the wave equation of $\lambda = \frac{v}{f}$, introduction in Section 3.1.1.1, the Fresnel zone length can be rewritten as follows:

$$W = \frac{d^2}{4\lambda} = \frac{d^2 f}{4v} \tag{3.7}$$

This demonstrates, as can be observed in Figure 3.3, the length of the Fresnel zone is increased as the wave frequency increases. Higher frequencies therefore, offer improved resolution, at the cost of being more vulnerable to attenuation of the beam, which is discussed in detail in Section 3.8.

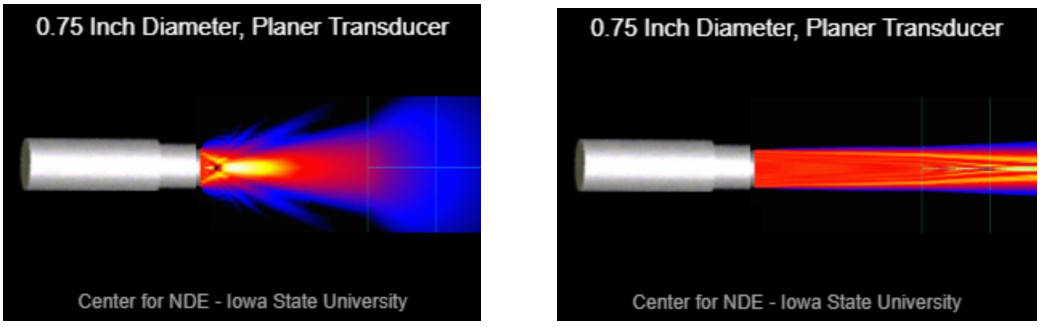

(a) Beam Spread at 1MHz (b) Beam Spread at 9MHz

FIGURE 3.3: Beam Spread Comparison

3.1.2 Limitations

3.1.2.1 Attenuation

When sound travels through a medium, the intensity of the signal diminishes as the distance travelled by the sound wave increases. Further effects that weaken the signal are produced through interaction of the sound wave with materials (unless the materials are idealized rather than natural), which are known as attenuation, which is the combined effect of two effects: scattering and absorption [78]. Attenuation is typically measured in decibels (dBs) and can be calculated according to Equation 3.8.

$$A = A_0 e^{-\alpha r} \tag{3.8}$$

where A_0 is the incident amplitude, A is the amplitude after travelling r distance, and α is the attenuation coefficient [74]

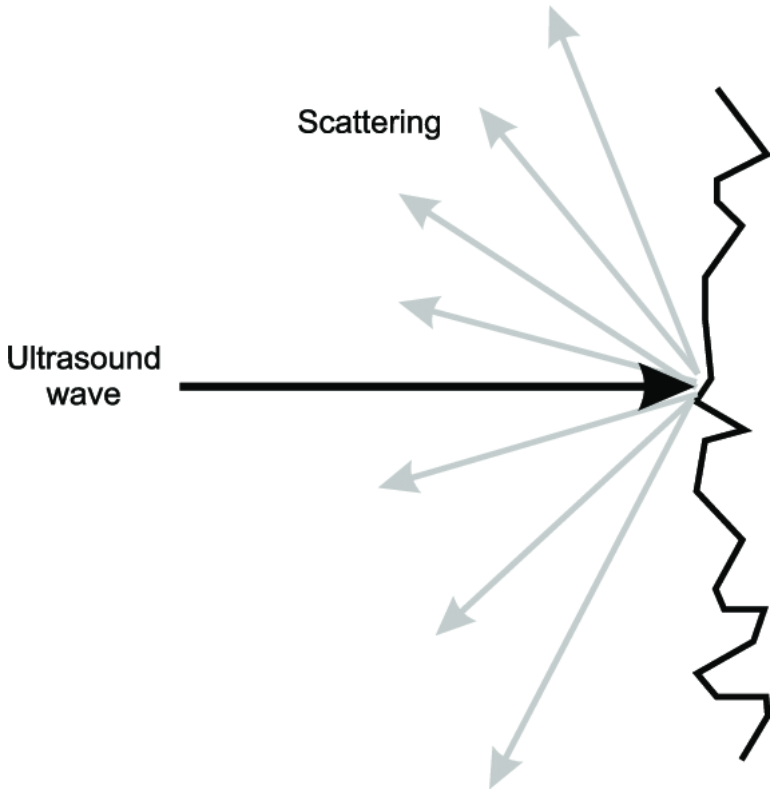

FIGURE 3.4: Scattering of an ultrasonic wave [79]

Scattering, as depicted in Figure 3.4, occurs when sound waves are reflected in a direction other than the original direction of propagation, which happens due to inhomogeneities, such as pores, contained in the material(s), in this case sediments. Even when the sediments being measured are homogeneous, they can still generally be considered an inhomogeneous material from the perspective of sound wave propagation because it is not isotropic (i.e. the properties are not the same in all directions). Absorption generally increases the higher the frequency and results in sound energy being converted into heat, which can be caused by several processes such as heat conduction and internal friction [74].

Both of these effects can negatively limit the interaction of a sound wave with materials, though scattering is the effect that is particularly problematic, not just because it results in numerous "false" echoes with which true echoes may get confused, but also because of the limited means to alleviate it. The problem of

absorption can be counteracted by increasing the transmitter voltage and amplification, but this solution cannot be applied to scattering, as it would worsen the effect, since an increase in initial energy would in turn cause an increase in the false echoes. Thus, utilising lower frequencies is the only way to reduce scattering, which in turn limits the level of detectability that can be achieved [74]. The extent to which this is a hindrance is application dependent, but it is potentially a major limitation for an application where high resolution is required.

3.1.2.2 Blind Zone

The blind zone, also known as the dead zone [80] is an inherent issue with ultrasonic sensors. It refers to distance between the sensor and its minimum sensing range. This principle is illustrated in Figure 3.5.

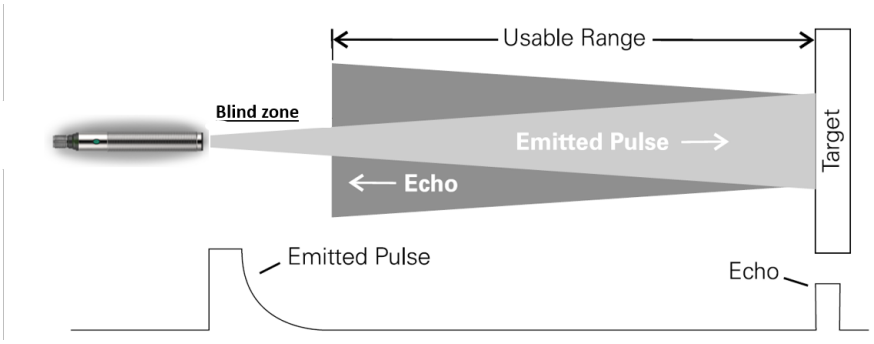

FIGURE 3.5: Blind Zone [81]

An ultrasonic sensor has a transducer that both emits sound waves and detects the echo that is reflected, and the transducer alternates between these two functions. Once a sound wave has been emitted the transducer then needs to switch from transmitting to receiving mode so that the returning echo can be detected. The time delay that this process causes translates into a distance within which measurements are not reliable, i.e. the blind zone. As such, the minimum distance of measurement must be considered when determining the placement of sensors and when interpreting results.

3.1.2.3 Crosstalk

Crosstalk is a common problem that arises when multiple ultrasonic sensors are operating in close proximity, and is often the source of incorrect measurements [82]. It occurs when one sensor receives an echo that originated with an adjacent sensor. Since the sensor receiving the echo has no way to determine that it did not originally emit the sound wave, this leads to an incorrect measurement. Crosstalk has been investigated by many researchers over the years, with a number of different solutions proposed. Most of these have sought to improve sensor performance by adding information to the ultrasound signal, for example by means of frequency modulation and pulse modulation [83]. If each sensor was configured with a different frequency, crosstalk could be easily eliminated, but this is not a realistic approach in most cases due to bandwidth limitations, and additionally due to the fact that frequency ranges for most transducers are small [84]. Furthermore, this would mean each sensor would have a different resolution, which would result in accuracy and precision of measurements being inconsistent across different sensors.

The most basic method to avoid crosstalk is to simply ensure that each sensor transmit in sequence; in other words, no two sensors simultaneously send and receive [85]. Since ultrasonic pulses are sent at different times, the possibility of one sensor mistaking another's echo as their own is eliminated. This is also known as multiplexing, a functionality incorporated by many ultrasonic sensors. Since the study in this thesis only focuses on proof-of-principle and does not require real-time performance, this is an adequate solution in this case. However, more efficient methods of crosstalk elimination would need to be investigated in the event that future developments of this research required higher performance, for which simple multiplexing of sensors may be insufficient.

3.1.3 Echo-Sounding

The term "Sounding" is the term used in reference to all types of depth measurement. It is derived from the old English word "sund", meaning swimming, water and sea; it is not related to sound in the physical sense of oscillation or vibration. Earliest methods of directly measuring water depth involved the use of lead lines and sounding poles, which remained in use for many centuries due to their principles of operation being very straightforward. Despite this, these methods of depth measurement were very time consuming, especially when measuring very deep bodies of water.

Sounding lines were a simple method of lowering a weighted line over the side of a boat and measuring the length of the line output when the line hit the bottom. This was useful not only for depth measurement but also for navigation, since it made it possible to detect shallow water away from land. This is illustrated in Figure 3.6. Sounding machines (Figure 3.7) were later developed which used reels to deploy sounding lines and measure the output which increased the speed and accuracy of measurements, particularly in deeper water.

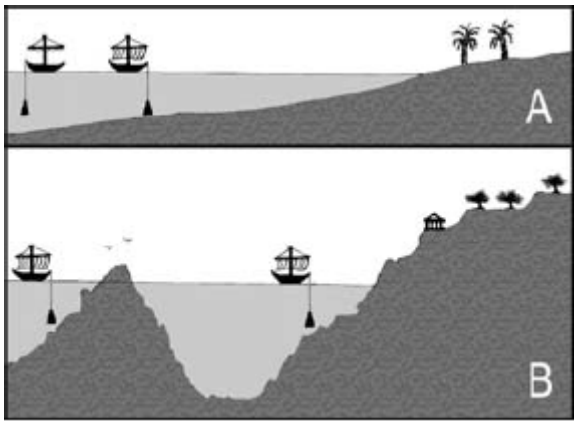

FIGURE 3.6: Use of sounding lines for water depth (A) and safety indicators (B) [86]

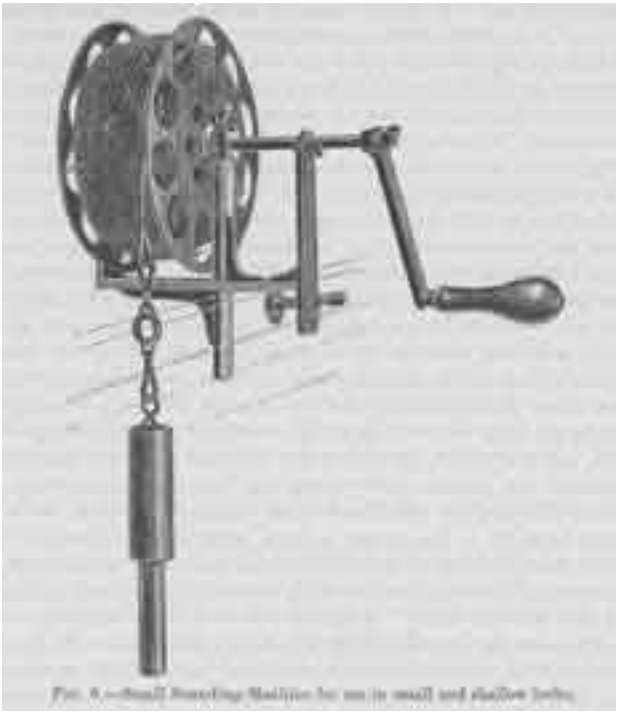

FIGURE 3.7: Sounding machine developed circa 1895 [87]

Aristotle (384 - 322 BC) is thought to be the first to note that sound could be heard underwater as well as in air. Nearly 2000 years later in 1490, Leonardo da Vinci wrote that *"If you cause your ship to stop, and place the head of a long tube in the water and the outer extremity to your ear, you will hear ships at a great distance from you"* [88]. This was the first known example of what is now known as passive sonar, however, it did not give any information about direction or intensity of targets. The first mathematical theory on how sound travels was published in 1687 by Sir Isaac Newton in *Philosophiae Naturalis Principia Mathematica*. Although it focused on sound travel in air, the basic principles of Newton's theory can also be applied to sound travelling underwater [89]. The modern study of underwater acoustics began in the early 19th century, with the first quantitative measurements of underwater sound being made on Lake Geneva in 1826 by Daniel Colladon and Charles Sturm. Their experiment consisted of striking an underwater bell, and generating a flash of light that could be seen over the horizon (Figure

3.8) . The elapsed time between seeing the flash of light and hearing the bell was measured at approximately ten seconds.

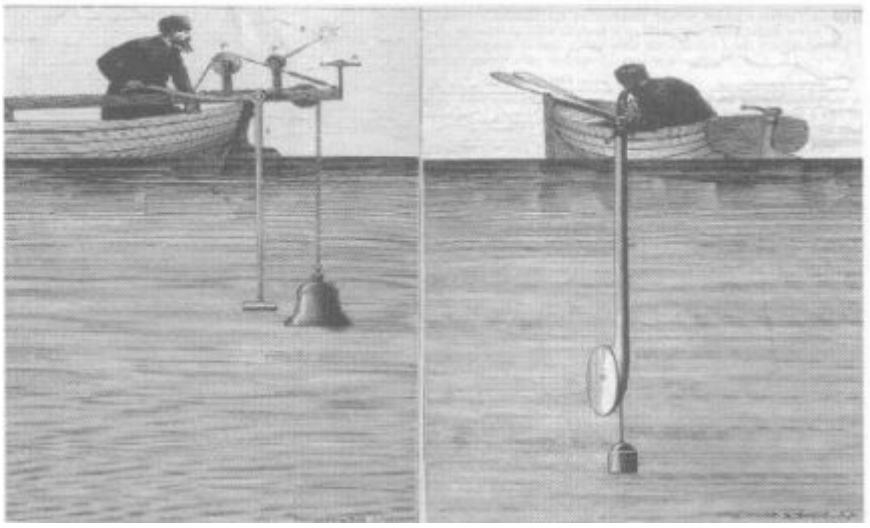

FIGURE 3.8: First measurements of speed of sound [90]

From this experiment, Colladon and Sturm determined the speed of sound underwater with surprising accuracy; their calculation of 1435 m/s is only three meters less than today's accepted values. Their study also demonstrated another important characteristic of underwater sound, namely its ability to travel great distances without significant dissipation [90]. However, it was soon realised that speeds in waters varied significantly depending on such parameters as temperature, pressure, and the amount of dissolved salts present (salinity).

It was during the two World Wars that underwater acoustic technologies were heavily developed due to their use in submarine warfare. The simple method of listening underwater as specified by Leonardo da Vinci was retained and applied with a second tube, which made it possible to determine direction and bearing of the target. Between World War I and II, these technologies were also adapted and developed for peacetime use, resulting in inventions such as the fathometer, a ship location system, and seismic prospecting [90]. Furthermore, advances in electronics advanced the ability to amplify, process and display acoustical data. As a result

of these advances, by the time World War II began, many ships were equipped for underwater listening and echo ranging. Further development in underwater acoustics was primarily concerned with locating and tracking German U-boats, with acoustic mines and homing torpedoes being among the resulting inventions.

Echo-sounders, specifically single-beam echo-sounders (SBES), are derived from the aforementioned military sonar equipment, and were a major development in depth measurement and have been used for this purpose in hydrographic surveying since the 1950s, which was only possible following improvements in transducer technology [91]. This has seen further major developments since, particularly over the last decade with the development of such techniques as multi-beam echo-sounders and airborne laser sounding, which make it possible to provide near-total seafloor coverage, enabling the gathering of massive bathymetric data sets.

Despite these more recent developments, SBES remain the dominant means of hydrographic surveys worldwide. Higher accuracy and precision has been achieved as a result of transitioning from analogue to digital recording, which has made them interoperable with technologies such microcontrollers and the Global Positioning System (GPS).

3.1.3.1 Basic Principle

The sonar process is initiated by an electrical pulse, which is then applied to the transducer. Transducers are normally made from piezoelectric ceramic, which, under the application of the electrical pulse, expands and contracts to generate an acoustic pulse in the water. This pulse is propagated through the water and is reflected and scattered by the seabed or by other objects present in the water column. A proportion of the scattered energy is reflected back to the transducer, which converts the acoustic pulse into an electrical signal which is then detected and amplified by the receiver [92]. A control unit regulates the sonar process and

usually incorporates a means of displaying and/or recording returned signals. The sonar process is summarised in Figure 3.9.

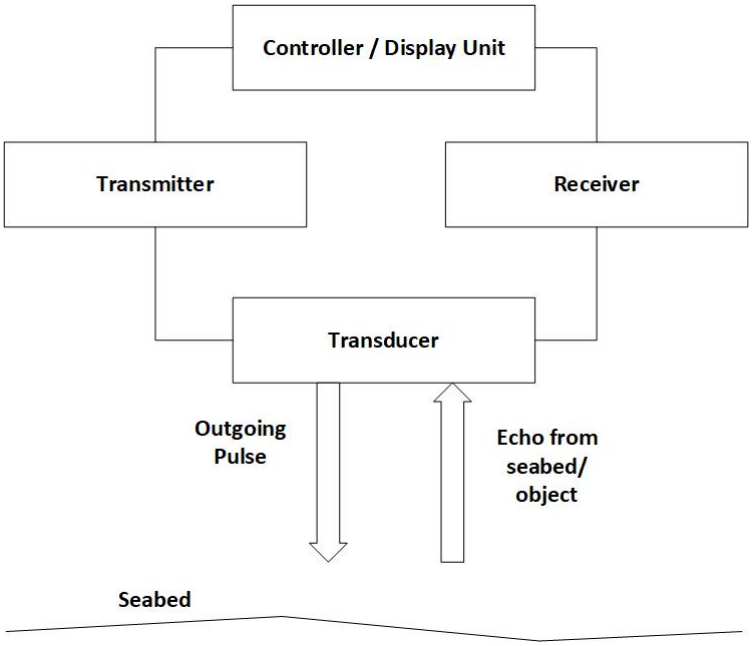

FIGURE 3.9: Elements of a sonar system

3.2 Wireless Sensor Networks

A Wireless Sensor Network (WSN) is a collection of smart devices, otherwise known as sensor "nodes", the numbers of which can range from a few to several hundred or even thousands, depending on the application for which the WSN is deployed. Sensor nodes are typically inexpensive, small, low powered devices, making it easier to deploy them in large quantities.

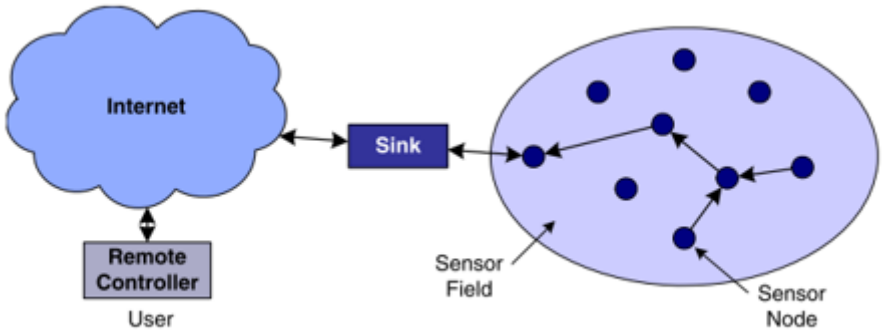

FIGURE 3.10: Wireless Sensor Network Architecture [93]

Figure 3.10 depicts a typical WSN architecture. Sensor nodes in a WSN perform three basic tasks; the collection, processing and transmission of data relating to physical or environmental conditions, for example pressure or temperature. The nodes co-operatively transmit the collected data through the network to its destination, which is normally a "sink" node (also known as a base station), a device capable of performing more complex data processing. Finally, processed data can be transmitted to a computer where it can then be analysed.

Initial development of WSNs was motivated by their use in military applications, such as battlefield surveillance and intrusion detection [94]. However, their use expanded and they are now for a diverse range of applications, areas of which include environmental monitoring, health monitoring, and the control and monitoring of industrial processes (e.g. manufacturing). Table 3.1 provides a summary of the main types of WSN applications along with some typical examples.

Category	**Example Applications**
Military / Security	-Intrusion detection -Battlefield surveillance
Industrial Control	-Intelligent buildings -Predictive maintenance -Improving productivity
Environmental	-Temperature -Soil moisture -Wind speed -Wind direction -Pressure -Water quality / Pollution distribution -Monitoring situations such as wildfires, floods etc.
Home Automation	-Smart homes -Personal digital assistants
Agriculture	-Improve food quality -Measurement of energy and light absorbed by plants
Medicine / Health Care	-Medical sensing, detecting signals such as thermal, optical, and chemical. Used in combination with signal processing algorithms to estimate a persons health status. -Workflow efficiency in hospitals. -Wearable sensors for monitoring various parameters such as heart rate.

Table 3.1: WSN Applications

3.3 Key Features

WSNs have a number of features that make them suitable for a wide range of applications. In this section, these are discussed with a focus on features that make WSNs suitable in the context of this research.

3.3.1 Mesh Topology

Nodes in a WSN require the ability to communicate with their neighbours on the network, as well as the sink node which serves as the gateway between the WSN and the final destination. This is especially true when the deployment conditions of the WSN are such that the topology changes regularly, which could occur in two main scenarios:

- Additional sensor nodes are regularly added to the network.
- Sensor nodes are deployed in a location where they are subject to being moved from one location to another.

If the network topology regularly changes, a path through which data is routed on one occasion may not be available on another. As a result, a WSN is typically deployed in the form of a mesh topology [95], an example of which is depicted in Figure 3.11. This results in the ability of the WSN to route data between sensor nodes by relaying data from node to node until the destination is successfully reached, a technique often referred to as **multihop communications** or **multihop routing**, which allows all nodes in the network to communicate not only with the sink node but also with each other. This gives rise to a key benefit, **self-healing**, which ensures that in the event of a node failure, data can be routed around the failed node, preserving connectivity and avoiding data loss even in the event of hardware failure, thereby improving the overall network reliability.

Shrestha and Xing [96] note that this process has high cost in terms of energy consumption, and therefore in some cases it may be more efficient to allow the WSN to "die", rather than attempting network reconfiguration. However, they also determined that mesh networking provided the highest level of reliability when compared to other topologies.

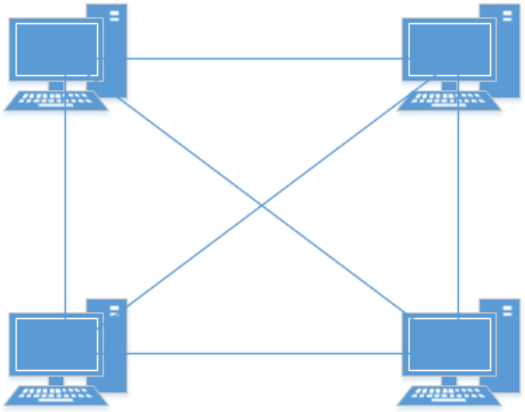

FIGURE 3.11: Mesh Topology

The capability of multihop routing is particularly important considering the application of this research. A WSN deployed in a highly dynamic and often turbulent environment such as the sea is very likely to be subject to regular topology changes, and therefore must be able to adapt to such conditions quickly. Furthermore, deployment in salt water is problematic from a communications standpoint; salt water is electrically conductive, and will therefore result in greater attenuation to the radio waves that the sensor nodes use to communicate. Provided that there is sufficient node density, multihop communications can contribute towards overcoming problems of attenuation; routing data between nodes results in the effective communication range being increased.

3.3.2 Scalability

Scalability refers to the network's ability to meet future growth requirements. In the case of WSNs, it refers to the ability of the network to cope with an increasing number of sensor nodes being added to the network over time [97]. There are two primary features of WSNs that enable them to adapt in response additional nodes being added to the network and the greater volume of traffic that will pass through the network as a result. Firstly the mesh topology previously discussed in Section 3.3.1 enables new sensor nodes to easily connect to the WSN and configure themselves appropriately. Additionally, since all nodes in the network are able to communicate with each other, this allows theoretically unlimited range [98]. Secondly, sensor networks can be programmed with specialized protocols designed to cope with managing communication between a large number of sensor nodes.

Scalability is an important consideration when deploying a sensor network for coastal monitoring; given the dynamics of many of the environmental processes, it may become necessary to rapidly expand the WSN in order to monitor a larger area. As such, the ability of WSNs to scale makes them an advantageous approach when compared to traditional beach monitoring technologies, which are typically only able to monitor one location at once, when in many cases it is highly desirable to be able to monitor multiple simultaneously in order to provide a more complete view of the site and the coastal processes occurring.

3.3.3 Expandability

Expandability refers to the ability of the nodes in a WSN to have their functionality expanded to include additional features that were not included originally. There are two ways a sensor node can be expanded, which can broadly be defined as software-based expansion and hardware-based expansion. Software based

expansion involves programming the node's controller unit to perform additional functions in relation to how the device will respond in specific scenarios to data, whether it be sensor data or network traffic. The extent to which software-based expansion can be implemented varies according to the type of controller that is utilized. Microcontrollers, for example, are the most common type of controller and are generally easy to program, whereas application specific circuits usually cannot be reconfigured once they are built.

Hardware-based expansion can be implemented in many different ways. For example, hardware-based expansion to improve power efficiency might involve the addition of solar harvesting capabilities. For this research, the WSN may be deployed to determine water depth initially, but it may be desirable to later add the ability to monitor other parameters as well, such as temperature or water levels, in order to provide a better range of data on which decisions can be based. As such, a system that takes into account not only the initial requirements, but future requirements as well, is highly advantageous.

3.3.4 Non-Intrusive

The ability to monitor locations in a non-intrusive manner makes WSNs particularly suitable for monitoring conditions in areas that might be adversely affected (and by extension, the validity of any data obtained) by excessive human presence. This is particularly true of many animal habitats, as many animals are very sensitive to human interaction. This has led to a number of WSN deployments designed to non-intrusively monitor animal habitats, the first major example being the Great Duck Island Network in Maine [99], which was able to remain in operation without issue for a six month period following deployment, enabling the collection of valuable data which would not have been possible by other means.

ZebraNet [100] is another example deployment created for the purpose of monitoring zebra migration patterns. Additionally, this project features a number of innovations that are useful for a wide range of future deployments, particularly in relation to node mobility and GPS integration, as well as energy efficiency through the use of rechargeable batteries with solar cells, allowing them to be recharged using solar energy, hence maximizing network lifetime. This approach may not be feasible for many WSNs monitoring coastal processes as the nodes may not be deployed in a location where they can easily pick up solar energy from the sun, for example underwater. However, in deployments where this was a possibility, it would contribute greatly towards the longevity of the network, and hence enable a better variety of data to be collected.

Considering the use case of this research, coastal process monitoring, the non-intrusive aspects of WSNs are particularly beneficial. Most beaches are important recreational resources [101], and therefore an intrusive or obstructive method of data collection would likely have adverse effects in terms of less people visiting the beach. Not only could this impact the local economies as a result of less visitors, but it could potentially also impact data validity, in the event that processes being monitored are influenced by the activities of beach-goers, or by changes made to the beach to accommodate them (e.g. construction) [102] [103] [104]. As such, it is highly desirable that coastal monitoring equipment be able to operate in a manner that has as little impact as possible on the coastal environment, both in terms of natural processes and in terms of human activity.

3.4 Potential Constraints

3.4.1 Energy

Energy efficiency is perhaps the most prevalent challenge in WSN operations, due to typically finite resources of sensor nodes. Although other constraints discussed in this section can cause significant problems, all are worsened by the broader problem of excessive consumption of limited energy resources.

There are three tasks a sensor node carries out that consume energy. These are:

- Sensing - listening for data to receive;
- Processing - preparing received data to be sent;
- Transmitting - sending processed data to its destination.

Certain operational characteristics of communication systems can lead to waste of available energy; major ones are explained below. Whilst such issues are not unique to WSNs, they are generally more of a concern because of the aforementioned limited power available to the battery-powered sensor nodes.

- **Idle Listening** - this refers to a node listening to receive traffic that is not sent; if nothing is sent, nodes will remain in idle mode most of the time. Many (Medium Access Control) MAC protocols, such as that of IEEE 802.11 [105] mandate listening before sending in an effort to avoid collisions occurring. This method however, is not appropriate for WSNs, not only because of the limited power available, but because the operating principles are different. In a traditional wireless network, it is necessary to provide equal access opportunity to users of the network, who are sending and receiving packets for their own applications. Conversely, in a WSN, there is usually only one

application, and all nodes on the network are co-operating with each other on a common task.

- **Collisions** occur when two or more nodes attempt to transmit data simultaneously. Not only does this increase latency in the network, but it also means that the corrupted packets need to be discarded and transmitted, which increases energy consumption.

- **Excessive listening** occurs when a node receives a frame that was addressed to another node. When such a condition occurs, the node will discard the packet, which, together with the re-transmission that will be necessitated, will waste energy.

As sensor nodes are usually battery-powered, available node energy is what determines the lifetime and ultimately usefulness of a WSN, and therefore optimizing energy consumption is a major area of WSN-related research [106] [93]. Much of this is focused on the development of MAC protocols [107], as the MAC layer optimizes the most energy consumption, of which recent examples include [108] and [109].

In many WSN deployments, such as those underwater [110], replacing batteries is often impractical, in some cases impossible, and the WSN is effectively rendered useless when the batteries are depleted. As such, efficient energy consumption, whilst important in any deployment, is a crucial consideration of designing any battery-powered WSN that is deployed in a location where energy cannot easily be replenished.

3.4.2 Bandwidth Limitations

A number of constraints are present in wireless networks as a result of available bandwidth being shared between all devices that are within radio range of each

other, since they all make use of the same transmission medium. In terms of this research this is an important consideration, since nodes are likely to be deployed in close proximity to each other, and as such, the greater the number of nodes, the lesser the bandwidth available to each. Node density, although a benefit, as previously discussed, (3.3.1) in terms of enabling multi-hop routing, may also be a drawback in terms of bandwidth availability, as relatively small amounts of bandwidth will be available for each node to utilize the greater number of nodes there are. This issue is compounded by the fact that sensor nodes generally only have rather small bandwidth amounts of bandwidth to utilize to begin with, due to the energy constraints that were discussed in 3.4.1. Therefore, whilst the bandwidth of most typical wireless local area networks (WLANs) can be measured in megabits-per-second (mbps), WSN bandwidth is generally measured in the order of kilobits-per-second (kbps). With this in mind, it is crucial to utilize available bandwidth as effectively as possible.

The most efficient method of transmission is to permit a node to transmit whenever it requires. However, on a shared medium this is not practically possible, as this would result in collisions occurring. As such, the design of MAC protocols [111] must take preventing interference into account, whilst ensuring that the available bandwidth is effectively utilized.

3.4.3 Security

Security is an important concern in any computer network, though generally more in those that use wireless communication, since no physical connection is required for an attacker to gain access. Whilst the attacks that a WSN is vulnerable to are much the same as any other wireless network, the problems are often exacerbated by the broader problem of energy limitations; the more complex a security protocol the more processing work a sensor node will need to do. As a result, it may be

necessary to make a compromise between security and energy efficiency; which takes priority will likely depend on the specific application of the WSN; if sensitive data is being collected (for example in the case of military deployments), it might require encryption to prevent it being read in the event it was compromised. Chen et.al provide a detailed discussion of WSN security in [112].

3.5 Wireless Sensors vs Traditional Methods

Monitoring of the coastal zone is generally achieved by means of a small number of expensive and high precision sensing devices, which collect relevant data which must then be manually downloaded and analysed, although some such devices can be combined with long-range communication networks, such as the Global System for Mobile Communications (GSM), which has the benefit of allowing locations to be monitored remotely [69]. This chapter has discussed in detail WSNs as a means to improve monitoring technologies. The drawbacks of current coastal monitoring methods are summarised below, followed by the ways in which WSNs can overcome these.

- Each device is generally only able to monitor one location (point) at a time, whilst in many cases it is desirable to monitor multiple points simultaneously in order to provide a more complete view of the site and associated coastal processes.

- Permanent deployments, whilst theoretically possible, are not realistic in most cases; data loggers are generally large in size and high in cost, and therefore permanent deployment on a beach would leave them vulnerable to potential damage or theft. As a result, use of data loggers remains a personnel-rich process; if new measurements need to be taken the site must be revisited.

- The above drawback is compounded by the fact that repeated visits to take measurements at a site may not always be possible. Beaches represent a highly dynamic system that is constantly reshaped by wind and waves. As a result, a point that was possible to measure previously may not be at a later time as a result of conditions such as higher tide levels, resulting in incomplete data collection.

- Beach monitoring using data loggers remains a largely manual process. Typically the researcher must be present on the site to operate equipment, and in the case of large beach profiles, this can be a highly time-consuming process, and, as previously mentioned, one that must be repeated in order to measure changes over time.

- There is a single point of failure. If a data logger fails measurements cannot be taken, and replacing them can be costly.

In comparison to traditional monitoring equipment, WSNs have a number of significant benefits that help eliminate or at least alleviate the above issues:

- Economical - current coastal monitoring technologies, whilst providing real-time data, typically require researchers to be present to operate the device and take measurements; future measurements will require future visits. A WSN provides substantial economic benefits by comparison. Firstly, they enable data to be accessed in real-time without repeated visits to the monitored site being necessary. Secondly, logistics are greatly reduced to deployment of the network and occasional maintenance.

- Safety - since WSNs can be permanently deployed, they are particularly advantageous for the monitoring of areas where repeated visits would be potentially unsafe for researchers.

- Access to more sites - WSNs can be deployed in locations that may not be reachable by researchers, for example underwater, thus enabling a better range of data to be collected and a more complete understanding of a process, such as erosion, to be established. Additionally, nodes that make up a WSN can be deployed across a number of different locations, enabling multiple points to be monitored simultaneously.

- WSNs are typically deployed in the form of a mesh topology, in which all nodes are able to communicate directly with each other, eliminating the single point of failure that exists with traditional technologies. Additionally, the multi-hop nature of this topology enables potentially unlimited communication range, as more sensor nodes can be added to the network as required.

3.6 ASTEC

Previous work also carried out by the University of Wales Trinity Saint David (UWTSD) (at the time Swansea Metropolitan University), in collaboration with Wireless Fibre Systems (WFS) Ltd and Vale Port Ltd, developed an underwater sensor network that deployed differential pressure sensors on the seabed [113], known commercially as Automated Sensing Technologies for Coastal Monitoring (ASTEC) [114]. Sensor nodes were fixed and measured the movement of sediment by determining the amount of sediment that was settling on top of them. Data was gathered at two hour intervals and transferred to the sink node on the surface once a day. The sink node would then transmit the collected data via the mobile phone network (GSM) to a computer for analysis [115]. Significantly, this project also demonstrated the potential of using electromagnetic (EM) communications underwater, differing from most underwater deployments which primarily use acoustic communication [116].

Although acoustics is a proven technology for underwater communications [117], its performance can be adversely affected by conditions such as turbidity and ambient noise, particular in shallow water close to the shore, where wave activity worsens their effects. This was a problem for deployments for monitoring depth of closure, which by necessity would have to operate in shallow waters (as discussed in Section 2.5, this typically ranges from 4 to 6 metres). Optical communication was considered as an alternative, but since it relies on the propagation of light it requires line of sight (LOS), and is only a realistic approach in very clear water over short distances [118]. As such, it was not considered further.

Considering the shallow water environment in which the WSN would be deployed, EM communications provide a number of benefits over both acoustics and optical communications [119]:

1. EM waves are easily able to smoothly cross through the air and water boundaries, unlike acoustics or optics, which opens additional transmission paths which can extend the communication range of the network. For example, communication could occur (a) completely through the water, (b) through the seabed, or (c) through the water, through the air, and through the water again [120]. This concept is illustrated in Figure 3.12.

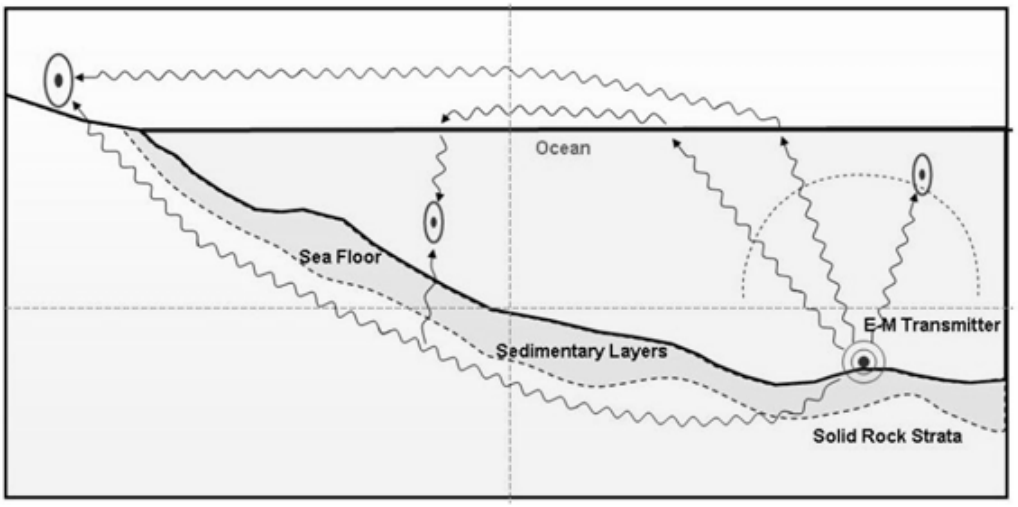

FIGURE 3.12: Paths of Transmission [120]

2. EM waves are able to tolerate turbulence caused by wave or human activity, unlike acoustics or optical waves.

3. EM waves are able to function in dirty water conditions.

4. EM waves offer significantly higher bandwidth than acoustic communications.

A multi-hop WSN was designed with a fixed topology; as is the case with most WSNs, the architecture had a multiple source single destination traffic pattern. Data was delivered in cycles, with all nodes being kept in sleep mode until they received a synchronization signal for communication of data. Once they had finished transmitting data, they switched back to sleep mode.

Although, as previously mentioned, EM signals in general have far higher bandwidth than acoustics, their transmission range through salt water is restricted due to the conductivity of the medium, resulting in significant attenuation. Therefore, a 3kHz frequency was utilised with a 100bps data rate [121]. This allowed a transmission radius of 40m; accordingly, this was set as the maximum distance between any two nodes.

Field trials were conducted of the developed system offshore at Tenby and also in Port Edgar Marina in Scotland. The physical layout of the network is shown in Figure 3.13. Measurements were acquired over a 24 hour period with data logging scheduled at 5, 15, 25, 35, 45 and 55 minutes past each hour and data upload occurring at 10, 20, 30, 40 and 50 minutes past each hour [122].

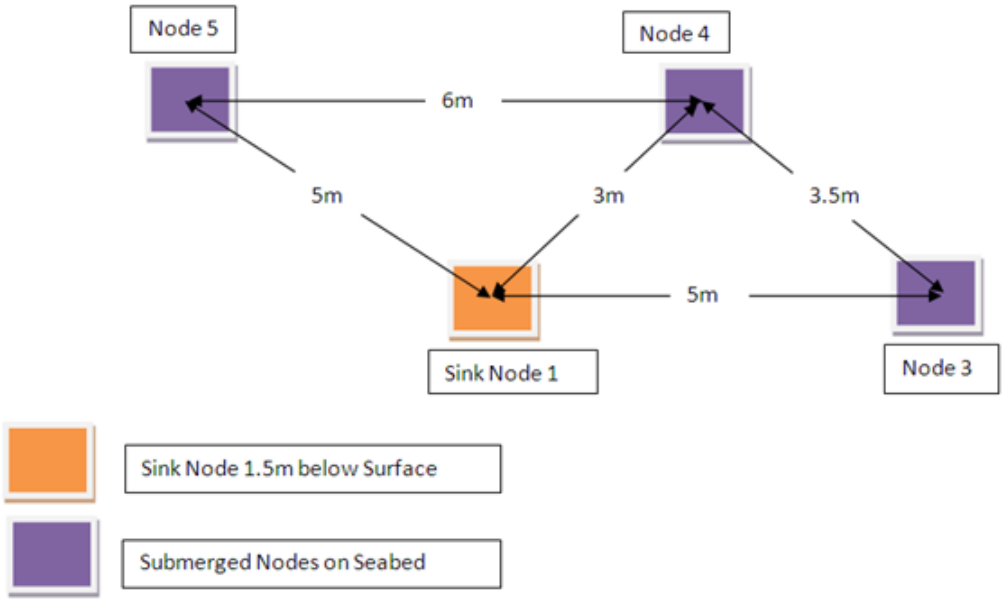

FIGURE 3.13: ASTEC Physical Layout] [122]

A remote sensor node from the ASTEC project is shown in Figure 3.14. These nodes were located on a seabed and communicated with the sink node which was located 1.5m below the surface and tethered to a buoy, from where it was then relayed to a remote computer for processing and analysis.

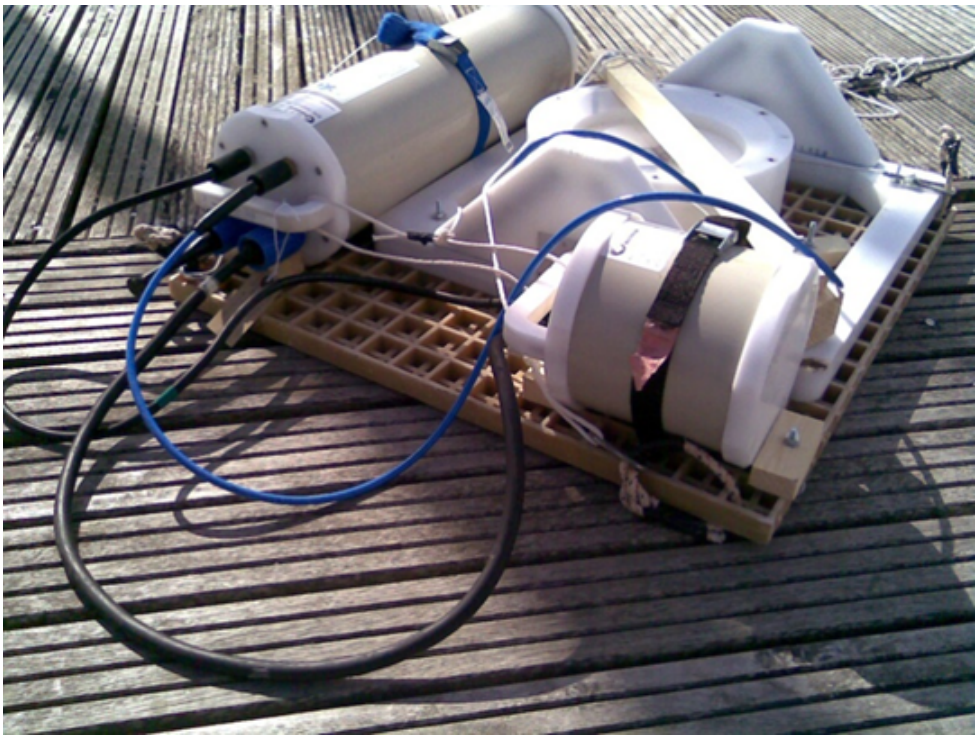

FIGURE 3.14: ASTEC Remote Node [122]

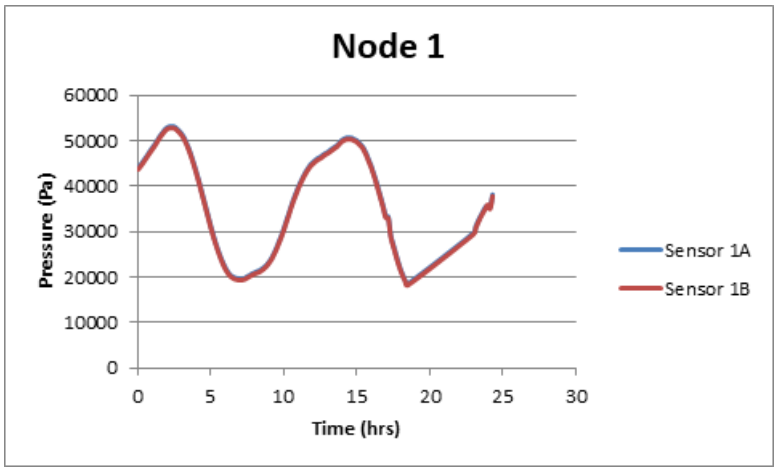

(a) Node 1

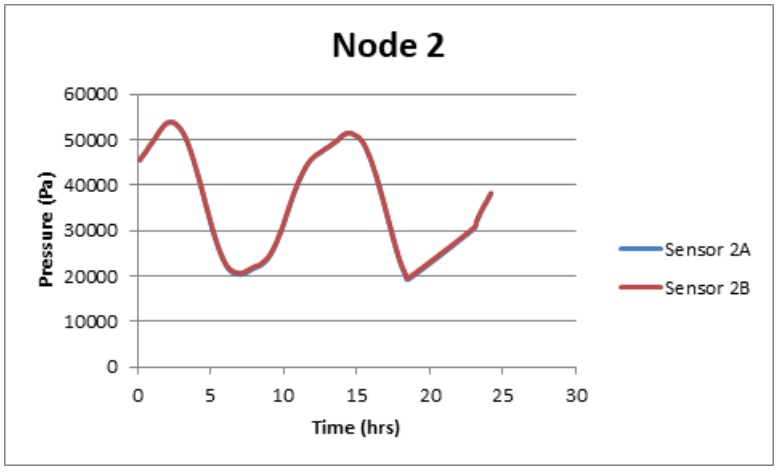

(b) Node 2

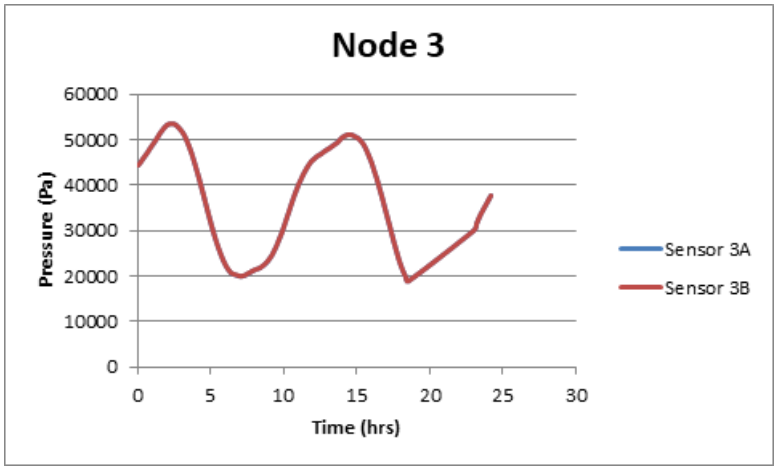

(c) Node 3

FIGURE 3.15: ASTEC Trial Results [122]

Sediment transport was determined based on the pressure difference. Based on the results shown for each sensor node in Figure 3.15, which demonstrate the collection of data for two tidal cycles during the 24 hour measurement period, the difference between the pressure sensor readings were calculated as shown in Figure 3.16. Based on these results, it was determined [122] that they represented the sensitivity of the system (in that the pressure differences were caused by noise fluctuations) rather than evidence of sediment transport. Unfortunately, no data from longer periods of measurement was available for comparison.

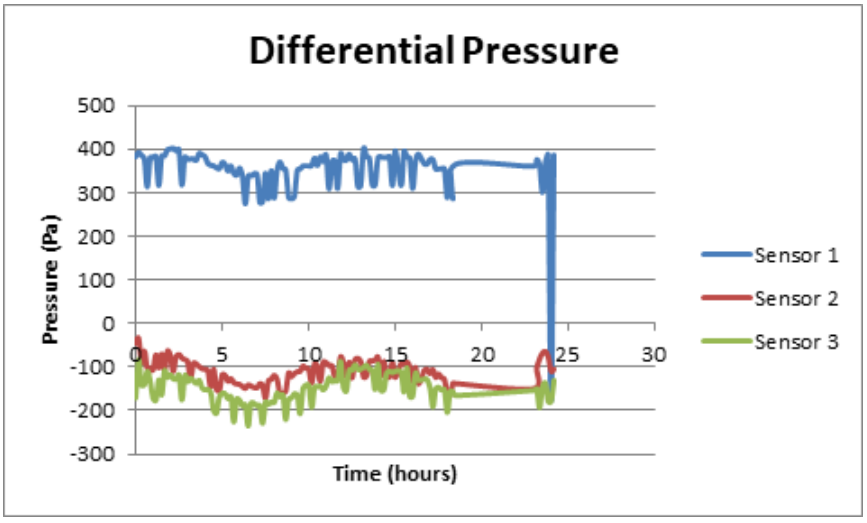

FIGURE 3.16: Differential Pressure [122]

As described throughout this section, The ASTEC project was successfully deployed and demonstrated proof-of-concept, however, little useful data could be gathered due to problems relating to energy consumption and associated issues with deployment and maintenance. These issues were not unique to the ASTEC project however; rather they were of a general nature that would likely impact any underwater WSN deployment. It was therefore considered worthwhile to investigate different deployment approaches. This led to a comparison being carried out between submerged and floating WSN deployments for the purpose of monitoring underwater sediment transport, which highlighted a number of advantages to using a floating deployment, which are discussed throughout the remainder of this

chapter, leading to the proposal of a new method of monitoring sediment transport using a floating WSN.

3.7 Comparisons - Underwater vs Floating WSNs

3.7.1 Cost

Sensor nodes in terrestrial WSNs are expected to become increasingly inexpensive. However, UWSNs require more complex transceivers that can function underwater as well as advanced hardware protection capable of withstanding the conditions of the underwater environment, such as pressure, extremely low temperatures and salinity levels. Additionally, the processing capabilities of sensor nodes may need to be more advanced; the underwater communication channel is likely to be intermittent meaning that it may be necessary for sensor nodes to perform data caching. This increases cost of the devices as well as their power requirements.

Floating WSNs, whilst naturally requiring their hardware to be protected against water, need this to a much lesser extent, due to the absence of extreme pressure levels on the surface. Additionally, since communication occurs on the surface it is not necessary for nodes to communicate underwater, reducing the complexity of transceivers and processing requirements of the sensor nodes, and therefore the overall deployment and maintenance costs.

3.7.2 Deployment and Maintenance

Deployment of a UWSN is likely to be an intensive process; the sensor nodes are likely to be heavy and bulky due to the necessary hardware protection. Additionally, in order to ensure more accurate pressure measurements, the angle of the sensor node on the seabed would need to be observed, likely requiring the use of

divers to ensure that the nodes are correctly positioned. However, the underwater environment can cause the node to move, which could potentially reduce the validity of the measurements. In terms of maintenance and reliability, once an UWSN is deployed it is virtually impossible to carry out any maintenance without retrieving the device from the seabed, meaning the device will be out of operation during this process. Finally, despite hardware protection, pressure levels at the bottom of the sea are such that water damage is still possible.

These problems are largely absent with floating WSN deployments, due to their lesser water protection requirements. Additionally, they can be retrieved easily for maintenance purposes, and the ability to recharge batteries using solar cells and/or small wind turbines improves their longevity.

3.7.3 Communication

The three possible underwater communication technologies, acoustics, RF, and optical, have all been proven to work underwater, but none of them can be classed as the one optimal medium for UWSNs. A WSN deployed for the same purpose of monitoring sediment transport is presented in [115]. Whilst demonstrating that RF communication is possible underwater, its use of very low frequencies resulted in a data rate of only 100 bps, which would not be sufficient for many UWSN applications, especially if the system needed to collect and transmit data on a regular basis.

A floating WSN does not need to communicate underwater; following data collection it can transmit readings to the sink node using wireless technologies such as ZigBee, enabling the data communication to avoid issues such as extreme bandwidth limitations and propagation delays.

3.7.4 Power Supply

Energy efficiency is a problem prevalent in all battery-operated WSNs. However, it worsens when the WSN is deployed in a location where batteries cannot be easily replaced or recharged; such is the case with UWSNs. Additionally, power requirements for underwater communications are greater, as more complex digital signal processing (DSP) has to be performed by the receivers in order to compensate for the channel impairments [123].

By communicating on the surface, floating WSNs not only reduce the communication power requirements, they also ease the process of replenishing sensor node battery power, either through replacements or by charging using small solar panels or wind turbines on the surface.

3.7.5 Localization

Localization refers to determining the location of the sensor node, which, for many applications is crucial in order for collected data to be meaningful, and can also be important for such tasks as routing and node tracking [124]. Localization is achieved with ease in terrestrial sensor networks due to the availability of the Global Positioning System (GPS). However, limited propagation of radio waves through water means that GPS will not work with UWSNs. Even if the sensor nodes are fixed in position it can be difficult to rely on location, as the harshness of the underwater environment means that can still be moved around. As a result, localization techniques for UWSNs is an active research topic; a recent review of several proposed solutions is provided in [125]. Floating WSNs do not suffer from this problem, since they communicate on the surface of the water they can work with GPS easily much like terrestrial WSNs.

3.7.6 Security

Security is an important concern in any computer network, though generally more in those that use wireless communication, since no physical connection is required for an attacker to gain access. Whilst attacks that a WSN is vulnerable to are much the same as any other wireless network, they are often exacerbated by broader problems of energy limitations; the more complex a security protocol the more processing work a sensor node will need to do. As a result, it may be necessary to make a compromise between security and energy efficiency, though which takes priority will likely depend on the specific application of the WSN; if sensitive data is being collected, it will require encryption to prevent it being read in the event it was compromised.

A floating deployment can make use of existing wireless networking protocols such as ZigBee and 6LoWPAN, which provides the facilities for carrying out secure communications [126]. Additionally, reduced power requirements and comparative ease of replacing and/or recharging batteries make more processing capability available to meet security requirements.

3.7.7 Comparison Summary

The comparison between underwater and floating WSN deployments is summarised in Table 3.2. Following a critical comparison of both approaches, it is suggested that the dominant means to date of deploying WSNs for monitoring sediment transport is inefficient both practically and technically. The remainder of this chapter therefore focuses upon the proposal of a new method with the view of overcoming the deficiencies identified.

Criteria	**Underwater Sensor Networks**	**Echosounding Sensor Networks**
Cost	- Complex node design - Require advanced hardware protection	Less complexity required in transceiver design and node processing
Deployment/ Maintenance	- Heavy and bulky due to hardware protection required - Difficult to maintain once deployed	- Relatively easy to deploy and retrieve for maintenance purposes
Medium	- No optimal communication medium	- No underwater communication necessary - Existing established technologies such as ZigBee and 6LoWPAN can be used
Power Supply	- Complex DSP resulting in higher power requirements - Difficult to replenish power	- Reduced communication power requirements - Easier to replace/recharge power supply
Localization	- No firmly established method	- GPS can be used to accurately establish the position of a sensor node
Security	- Increased power requirements result in less power available for security protocols	- Can take advantage of existing protocols that consider security such as ZigBee and 6LoWPAN

Table 3.2: Underwater vs Floating Sensor Networks

3.8 Chapter Summary

This chapter has discussed ultrasonic sensors and WSN technologies as a means to overcome limitations of existing coastal monitoring methods that were previously highlighted in Chapter 2: their inability to measure processes in the submerged portions of the coastal zone, and their need for largely manual operation. Combined, ultrasonic sensors and WSNs show promise in overcoming not only these main limitations, but also at a lower cost and with lower-risk operation. Accordingly, ultrasonic sensors and WSN technology will form the basis of a new method for monitoring underwater sediment transport, the development of which is presented in Chapter 4.

Chapter 4

Novel Method of Measuring Sediment Transport

4.1 Introduction

A review of literature (Chapters 2 and 3) identified that although extensive research has been carried out with respect to monitoring sediment transport, there are a number of significant research gaps, which are summarised as follows:

- There is currently no method of monitoring movement of sediments beneath the sea's surface. This results in a lack of important data for coastal engineers to utilise in the development of coastal management strategies.
- Certain characteristics of ultrasonics and WSN technology make them a very promising solution in terms of overcoming limitations identified with current monitoring methods. However, examples of the deployment of this approach are limited.
- Whilst there have been recent studies that investigate the use of WSNs for monitoring sediment transport these, much like current methods, have

been largely limited to monitoring the visible beach and do not consider underwater activity.

- Previous work undertaken by UWTSD (ASTEC) developed an underwater wireless sensor network (UWSN) to monitor sediment transport on the seabed. However, it was not able to collect significant amounts of useful data, due to problems relating to energy consumption as well as more general implications associated with underwater deployments.

- Floating echosounding deployments have the potential to overcome most problems that hindered the usefulness of the ASTEC deployment. A floating deployment would measure water depth, and by correlating this with tide level data the change in sediment levels could be measured. More research needs to be carried out to determine feasibility of this approach.

This thesis proposes a new novel method of monitoring sediment transport on the seabed by measuring water depth in correlation with tide level measurements. The development of a prototype system to test this method is accordingly the focus of this chapter.

Although this system is eventually intended for use in water, as resources were limited it was only possible to carry out tests in air for the purpose of this research, which was sufficient in terms of achieving proof of concept. Although testing in water would have been desirable to further validate the approach, the complexity, time and money that would be involved in terms of the equipment required was not considered justifiable. Therefore, in-air validation is achieved in this thesis, with recommended further stages being presented for extending this method to the underwater environment in Chapter 6.

4.2 Proposed Novel Method

Based on the comparisons carried out in the preceding sections of this chapter, this thesis proposes a new method of monitoring sediment transport by employing a combination of echosounding (ultrasonic distance measurement) and wireless sensor networks. This new method aims to reduce the complexity and limitations in underwater sensor networks previously discussed.

4.2.1 Overview

The expression for the proposed new method of monitoring sediment transport (T, measured in cm) is given below in Equation 4.1:

$$T = D - R \tag{4.1}$$

where:

- D (cm) = datum, the baseline against which change is measured
- R (cm) = sensor reading

This method would be deployed in the form of a sensor network that floats on the surface of the sea and uses echosounding to determine water depth. In common with most coastal monitoring programmes (as discussed in Section 2.4.2), the initial stage of applying this method involves the establishment of a datum, a baseline measurement against which future change can be measured. This should include correlation with wave statistics and bathymetric data in order to take wave motion and the seabed's topographical features into account.

Depth of closure (as discussed in Section 2.5) is the depth at which there is little or no motion of sediments and accordingly, it is a point at which there would be an accretion sediments due to their lack of motion. Therefore, a depth measurement taken at this point would be smaller than one taken where there sediments are still moving. This concept is illustrated in Figure 4.1. By comparing this reading with the earlier established baseline, it can be determined whether accretion or erosion is occurring.

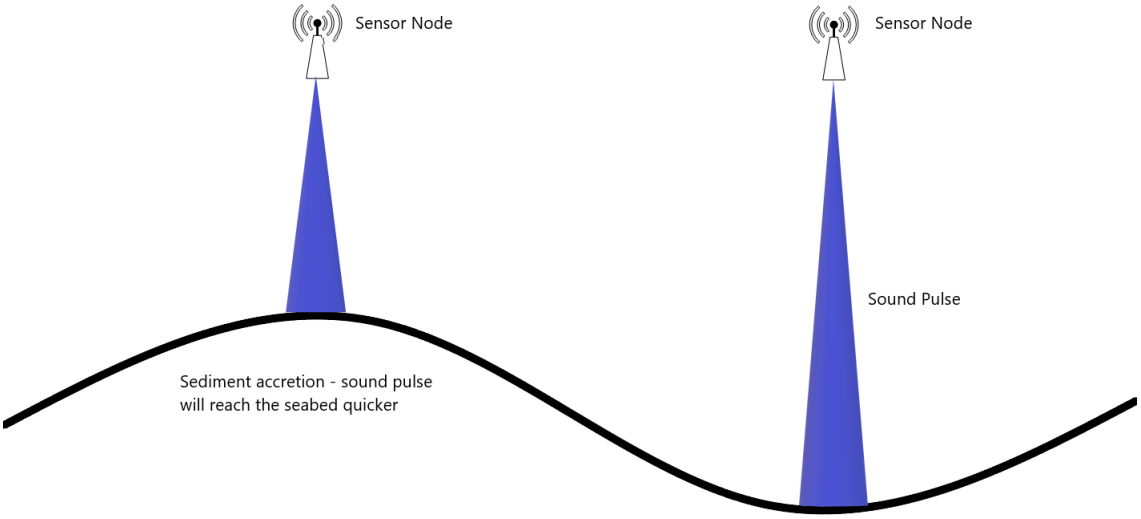

FIGURE 4.1: Identifying accretion or erosion of sediments

4.2.2 Advantages of new approach

In order to specify the advantages of this method, the research problems originally identified in Section 1.2 must be recalled:

- They are limited to the visible beach and do not have the ability to monitor beneath the sea's surface. This means that only a partial understanding of the relevant processes is achieved due to the absence of this important data.
- They require largely manual operation, and are therefore unable to gather data with the desired level of automation or regularity.

Considering these problems with existing methods, this new approach offers a number of advantages compared both to existing approaches as well as previous WSN-based approaches. The first limitation in current coastal monitoring methods is the inability to observe the motion of sediments underwater. This limitation would be eliminated with the use of ultrasonic distance measurement, which in combination with tide level measurements would determine movement of sediments by measuring depth. However, this on its own is not enough, as it would still not be capable of taking measurements regularly or automatically, which highlights the need for the features offered by WSN technology. As such, these two technologies form the basis of this new method, each of them solving one of the identified problems with existing approaches.

When this method is compared to previous WSN-based attempts for this application (the prime example of which is ASTEC, as discussed in Section 3.6), this new approach offers a number of further benefits:

- It does not need to communicate underwater, enabling the use of established wireless networking protocols such as ZigBee, and negating the need for the development of custom protocols for underwater communication.
- Deployed and maintenance of the system is far simpler as it would be deployed on the sea's surface rather than the seabed.
- Replenishing energy is possible through solar, wind, and osmotic means, extending the lifetime of the network and reducing the need to replace sensor nodes when batteries are depleted.

Considering the above benefits, the proposed new method has the potential to be both very effective and efficient compared to previous approaches. The remainder of this chapter will outline the development of a prototype system to demonstrate

the basic concept of this method. Following this, the experimental setup and results are presented in Chapter 5.

4.3 Development considerations

There are a number of considerations that must be made that must be taken into account when conceptualizing a WSN for coastal monitoring. These are discussed below, and throughout the rest of this chapter explanations are given as to how these criteria are met for the proposed system.

4.3.1 Low energy consumption

WSNs are most commonly battery powered and are often deployed in remote locations where charging or replacing batteries is unpractical. Therefore, energy consumption often the foremost concern in the development of a WSN, in order to utilise the limited energy available as efficiently as possible. The use of power efficient hardware and communication protocols is thus a crucial consideration.

4.3.2 Network topology

Free-space sensor networks were often deployed in the form of a star topology, where every sensor node is directly connected to a central hub. However, there are a number of limitations in this approach, both of which would hinder the application of this research. Specifically:

- Their physical range - this is limited by the fact that all sensor nodes need to be connected directly to the central hub.

- Their single point of failure - central hub failure leads to failure of the entire network.

Considering these limitations, use of a mesh/multi-hop topology (as discussed in Section 3.3.1) is a more realistic solution for sensor networks, particularly those that cover large geographical areas. Details of the network topology that was utilized for this research are discussed in Section 4.5.4.

4.3.3 Low cost

Since this research is about achieving proof of principle, costs of developing the sensor nodes had to be kept as low as possible. However, this is an important consideration for future real-world deployments of the system as well; since the system will eventually be deployed on the sea, maintenance costs can be much higher in comparison to a land-based sensor network. However, these can be minimised by ensuring:

- That the system is designed to operate autonomously, requiring minimal human intervention.
- That having low-cost sensor nodes remain a consideration throughout the design and development process. This will ensure that, in the event of a sensor node failure, it can be replaced with minimal financial implications.

4.3.4 Intervals between measurements

Due to the nature of coastlines, different regions may require more frequent monitoring than others. Therefore, frequent collection and transmission of data relating to regions where situations such as erosion and flooding are less of a concern (for

example because of the area being sparsely populated) may put unnecessary pressure on the system, wasting valuable energy. Conversely, leaving long intervals between measurements in a region with a high population that is at risk of erosion or flooding may render the monitoring ineffective. Results of previous studies must also be considered; an area where little recorded change has occurred would require less frequent monitoring than one where regular change has been observed. Accordingly, a system for monitoring the coastal environment should have the ability to remotely adjust the intervals of data collection.

4.4 Choice of Wireless Technology

Advances in wireless technology has resulted in the design and deployment of many different forms of wireless network, which are usually classified according to the area over which they can operate. For example, Wireless Local Area Networks (WLANs), based on Ethernet technology, are widely used to provide connectivity in a local environment. Low power wireless technologies were introduced to be used with power constrained devices such as battery powered sensing devices; these are known as Wireless Personal Area Networks (WPANs). Considering the requirements outlined in Section 4.3, ZigBee was selected to for this work.

Bluetooth was also investigated as a potential wireless technology. Bluetooth [127], despite its useful features such as low power consumption, was not considered suitable for this work due to two primary limitations. Firstly, a Bluetooth network (sometimes referred to as a Piconet) operates in the form of a master/slave topology. Each piconet has one master device and can support up to seven active slave devices; as such it is limited to point-to-point and point-to-multipoint connections. Secondly, only eight devices can be active in one Piconet at a time. Several piconets can be linked together to form a scatternet, as depicted in Figure 4.2. This enables devices to participate in more than one piconet; however, they

cannot participate in multiple piconets simultaneously, which limits the expansion capabilities of the network [128]. Consequently, it was not considered further.

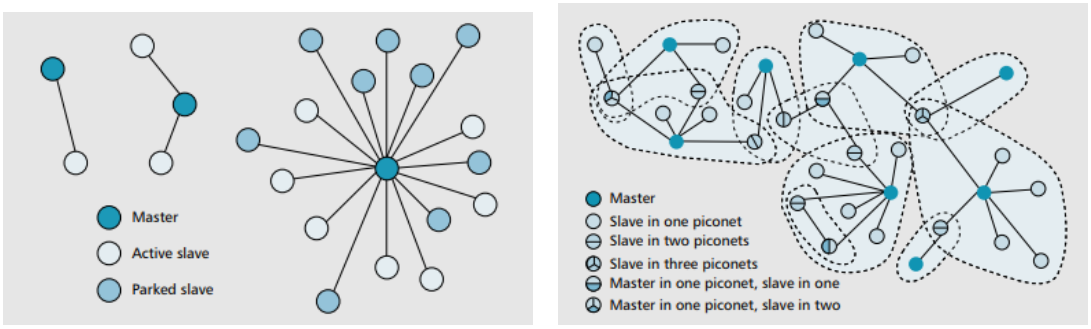

(a) Piconet (b) Scatternet

FIGURE 4.2: Bluetooth Topologies [127]

4.4.1 ZigBee

ZigBee is based on IEEE 802.15.4 and according to ZigBee specifications [129] is intended to reduce the complexity and expense associated with other WPAN technologies such as Bluetooth or other more general technologies such as Wi-Fi. The development of ZigBee is a collaboration between the IEEE 802.15.4 group and the ZigBee Alliance, although the two parties work on different aspects of the protocol, with the former focusing on the physical and medium access control (MAC layers), and the latter working on the development of the upper layers. Figure 4.3 shows the ZigBee protocol stack, as well how the development tasks are split between the two groups. ZigBee's key features are summarised in Table 4.1.

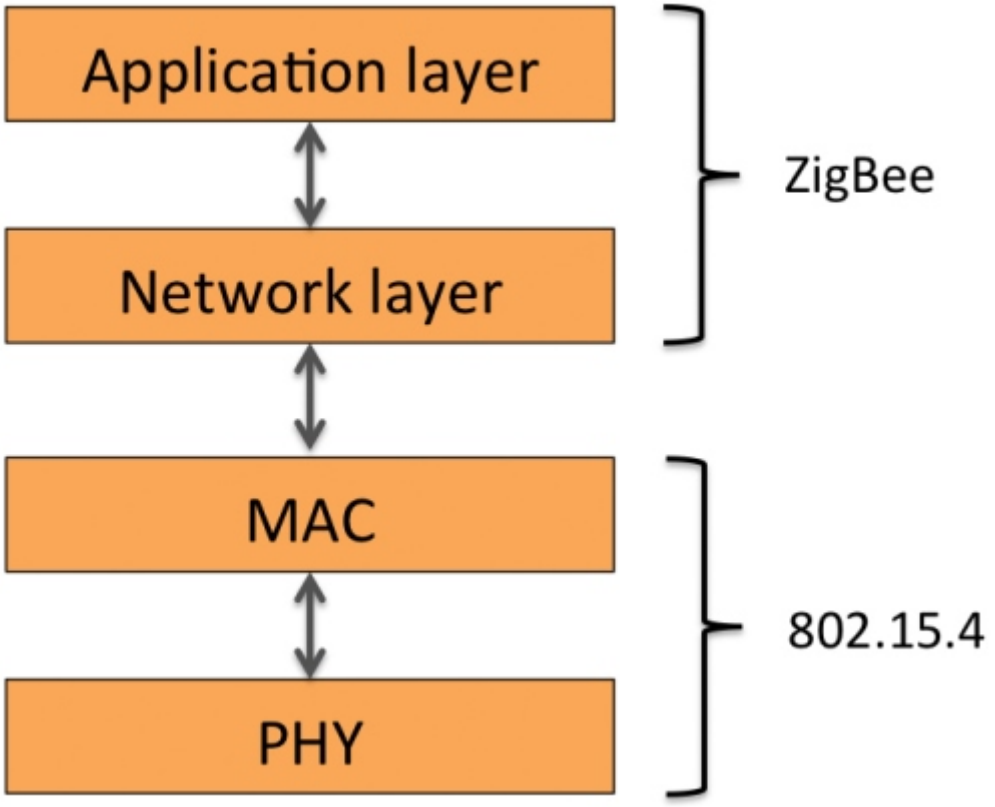

FIGURE 4.3: ZigBee Protocol Stack [130]

Frequency Band	2.4 GHz
Connection	Direct-Sequence Spread Spectrum
Transmission Power	0-20 dBm
Data Rate	250 Kbps
No. of Devices	65,000
Typical Range	10-100 metres

TABLE 4.1: Key features of the ZigBee protocol

Low power consumption results in transmission distances being limited to approximately 10-100 metres, dependant on power output and environmental conditions. However, its support for mesh topologies makes it possible to communicate over

long distances by relaying data across devices. It is most commonly used for applications that require low data rates and long battery life. It also features optional 128-bit encryption, which makes it a popular choice for applications that require secure communications in addition to the aforementioned features.

In a ZigBee network, a device can take one of three roles [131]:

- **Coordinator (ZC)**

  Co-ordinator is the first node to start up and is tasked with initialising the network, which includes selecting the frequency to use and the Personal Area Network (PAN) ID. All ZigBee networks need to have one co-ordinator node. To establish connections with routers and/or end devices, the co-ordinator node scans for channels that are not already in use by co-ordinator nodes in other networks. If no such channel can be found, the one with the lowest energy level will be selected.

- **Router (ZR)**

  Routers relay data to other nodes, and can also allow other nodes to join the network. These are not required in all ZigBee networks, for example one where all end devices are connected directly to the co-ordinator node in a star topology.

- **End Device (ZED)**

  End device is the simplest mode that can be configured; a node configured in this mode sends and receives messages but does not perform any other significant tasks in the network. Only devices configured as an end device can enter sleep mode.

4.5 Experimental Apparatus

This section discusses the equipment utilised for experimental aspects of this research, all of which was selected considering the factors discussed in Section 4.3. Electronic equipment utilised can be divided into two categories: that for collection and processing of data, and that for wireless transmission and receiving of data, as illustrated in Figure 4.4.

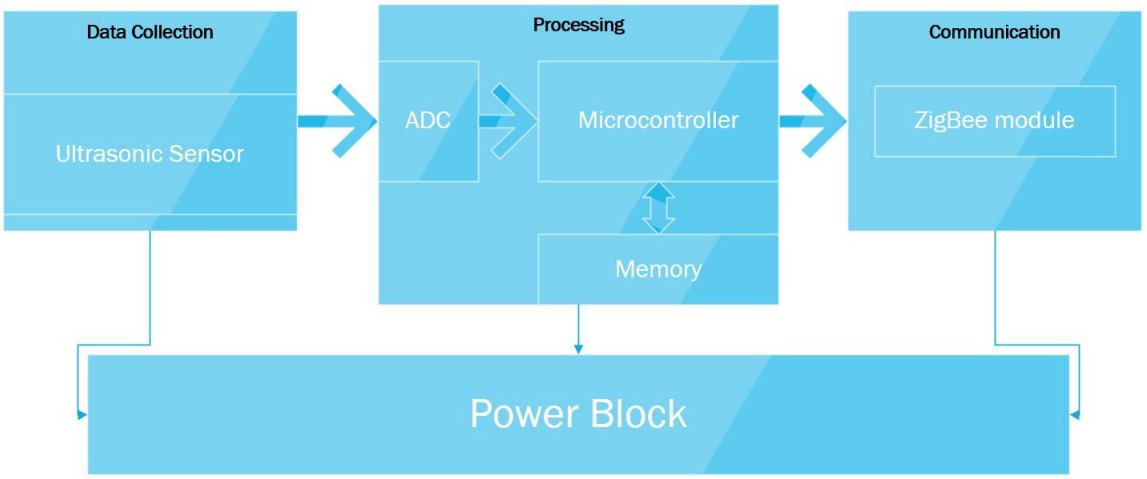

FIGURE 4.4: System Structure

4.5.1 Data Collection and Processing

4.5.1.1 Circuit board

For purposes of processing gathered data, and the communication of this data to its destination, a sensor node requires an electronic circuit. In the past this would in most cases have required the necessary circuitry to be developed from scratch; this has ceased to be the case today with the development of low cost general purpose circuit boards. In particular, single-board microcontrollers have become widely available. Since these devices provide all the basic circuitry that is needed for a control task, they are especially useful to application developers, since they minimize the need to develop custom hardware.

As was previously discussed in Section 4.3, the requirements of the sensor nodes used in this research are, as relates to the circuit board, low cost and low energy consumption. Considering these requirements, and following a careful investigation, an Arduino Uno circuit board was selected for this project, as shown in Figure 4.5. This board features a ATmega328 microcontroller, which is a low-power CMOS 8-bit microcontroller based on the AVR enhanced RISC architecture. By executing powerful instructions in a single clock cycle, the ATmega328 achieves throughputs close to 1MIPS per MHz, which allows power consumption versus processing speed to be optimised. [132].

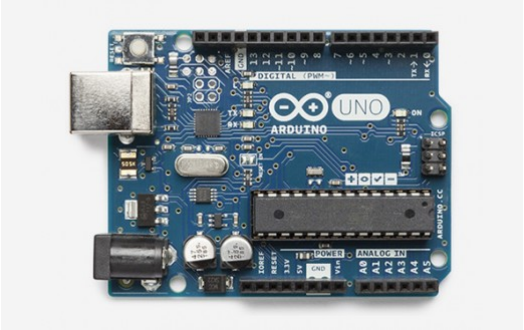

FIGURE 4.5: Arduino Uno Circuit Board

4.5.1.2 Ultrasonic sensor

Although the ultimate aim of this research is to develop a WSN capable of taking underwater measurements using acoustic pulses, the decision was taken to focus on air-based validation for this thesis. Since ultrasonic transducers for underwater operation require highly sophisticated and expensive electronics to operate, this was not considered justifiable considering this research was only proof-of-principle. Since low-cost ultrasonic transducers for use in air are widely available, this was the main consideration that led to in-air validation being the focus of this work. The ultrasonic sensor utilised is shown in Figure 4.6, and its specifications in Table 4.2.

An ultrasonic sensor with a low frequency (40Khz) was selected in order to minimize scattering effects. Although this has a drawback of reduced resolution, this is not considered to be a major hindrance in this case as the beam is only required to reflect off a surface (i.e. the top of the sediments), and not identify small characteristics. The specifications of the ultrasonic sensor utilised state that it has a blind zone (i.e. minimum distance) of 25cm. However, it should be noted that a restriction such as this is dependent on the speed of sound; the faster the speed of sound the larger the blind zone.

FIGURE 4.6: JSN-SR04T Ultrasonic Sensor

Parameter	**Specification**
Operating Voltage	DC 5V
Quiescent current	5mA
Total current work	30mA
Acoustic emission frequency	40khz
Farthest distance	4.5m
Minimum distance	0.25m

TABLE 4.2: Sensor Specifications

4.5.2 Communication

4.5.2.1 ZigBee Radio

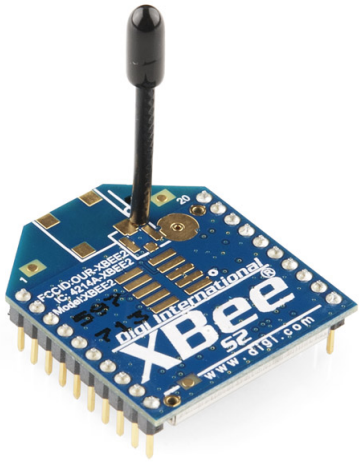

FIGURE 4.7: Xbee Radio

The radio module used for transmitting and receiving data was selected from the XBee family, a group of RF modules produced by Digi [133], and is shown in Figure 4.8. Its specifications are shown in Table 4.3.

Frequency band	2.4 GHz
Data rate	250kbps
Range	120m
Encryption	128-bit AES
Transmit power	1.25 mW (+1 dBm)
Receiver sensitivity	-95 dBm
Reliable communication	Achieved with re-transmission/acknowledgement
Configuration	Local or remotely

TABLE 4.3: XBee Radio Specifications

An Xbee Shield, as shown in Figure 4.8 is used for seamlessly interfacing the radio module with the circuit board. Power is taken from the 5V pin of the Arduino and regulated on-board to 3.3VDC before being supplied to the XBee.

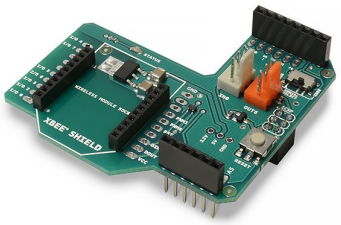

FIGURE 4.8: Xbee Shield

Radios can be configured in one of two modes: Application Transparent (AT) or Application Programming Interface (API). In AT mode, all serial data received by the radio module is queued for transmission, whilst data received is sent out of the serial interface. This mode has several limitations, chief among them that it is not possible to identify the source of received data and moreover, any data that is received will not include any transmission details, such as the reasons for success or failure. Therefore, although this is somewhat application dependant, AT mode is not of much use unless the application only calls for two way communication between XBee devices.

Conversely, API mode greatly improves on the above limitations [133], albeit resulting in increased complexity. Transmissions are structured in packets; as a result data received from sensors first needs to be encapsulated into packets, and then parsed to extract data from them once they are received at the destination. This has the benefit of being able to include data relating to the transmission, such as sender's address and reasons for success/failure, which is not possible with AT mode. The ability to diagnose problems with the network is therefore greatly

improved. API mode also allows nodes to be configured remotely, which was identified earlier in Section 4.3.4 as being a key requirement for this work.

Configuration of ZigBee Modules

Configuration of the radio modules involves many aspects and parameters and is therefore an important step in the development of a sensor network. Manufacturers generally provide their own software for the purpose of configuring hardware, which in this case is Digi's XCTU software, shown in Figure 4.9. XCTU contains many different versions of firmware, which can be programmed into the module via a USB or RS232 port.

Following configuration, the coordinator node initiates a scan in order to select a communication channel. It then broadcasts its address including a WPAN ID, which enables other nodes on the network to send a request to join the WPAN.

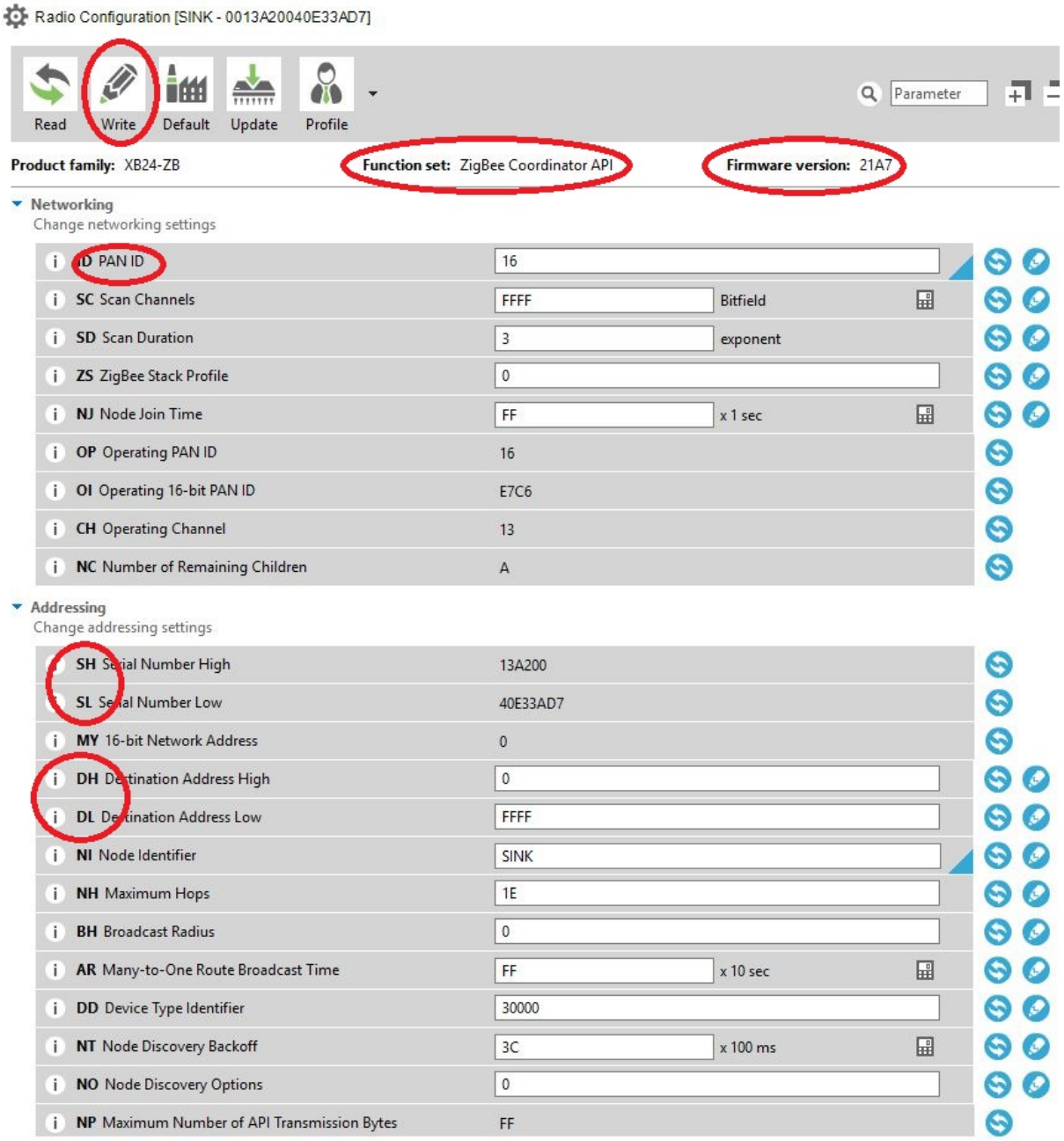

FIGURE 4.9: Digi XCTU Software

Configuration of Sink Node

The sink/master node was configured (Figure 4.9) with ZigBee Coordinator API firmware (version 21A7, the latest version at the time of writing). Configured parameters are explained below and summarised in Table 4.4. All other parameters were left at their default configuration.

Parameter	**Configuration**
WPAN ID	16
Node Join Time	FF
Destination High	0
Destination Low	0
Power Mode	Boost Mode Enabled
Power Level	Highest (4)
Encryption	Disabled

Table 4.4: Sink/Master Node Configuration

Configuration of Sensor Node

The sensor nodes were configured with ZigBee Router API firmware (version 22A7). Configuring sensor nodes as routers rather than end devices was necessary in order to fulfil two of the originally defined requirements in Section 4.3. Firstly, in enables them to operate in a mesh topology and relay data between nodes, which accommodates any future expansion in terms of node density. Secondly, as previously discussed in Section 4.5.2.1, the use of API mode allows the configurations of the nodes to be changed remotely whenever necessary.

The parameters that have been configured (both for the sink and sensor nodes) are explained below:

- The WPAN ID is a 16-bit number that is used to identify the network; in order for sensor nodes (end devices) to establish communication; they must be configured with the same WPAN ID as the co-ordinator node.
- ZigBee supports 64-bit destination addresses, which are divided into upper and lower destination, each 32 bits. For this experiment, both these values

were set to 0 for all sensor nodes so that the coordinator (sink) node is the default destination for transmission of collected data.

- The Node Identifier (ID) is a phrase/identifier used within the network to distinguish data based on the node it was sent from.

4.5.3 Sensor Node

Following selection and configuration of the sensor node components, they were assembled in an electronics enclosure as shown in Figure 4.10 in order to protect the components from dust and water. The ultrasonic sensor itself was threaded through a hole drilled in the bottom of the enclosure and sealed in place with silicone. The sensor node with the enclosure sealed is shown in Figure 4.11.

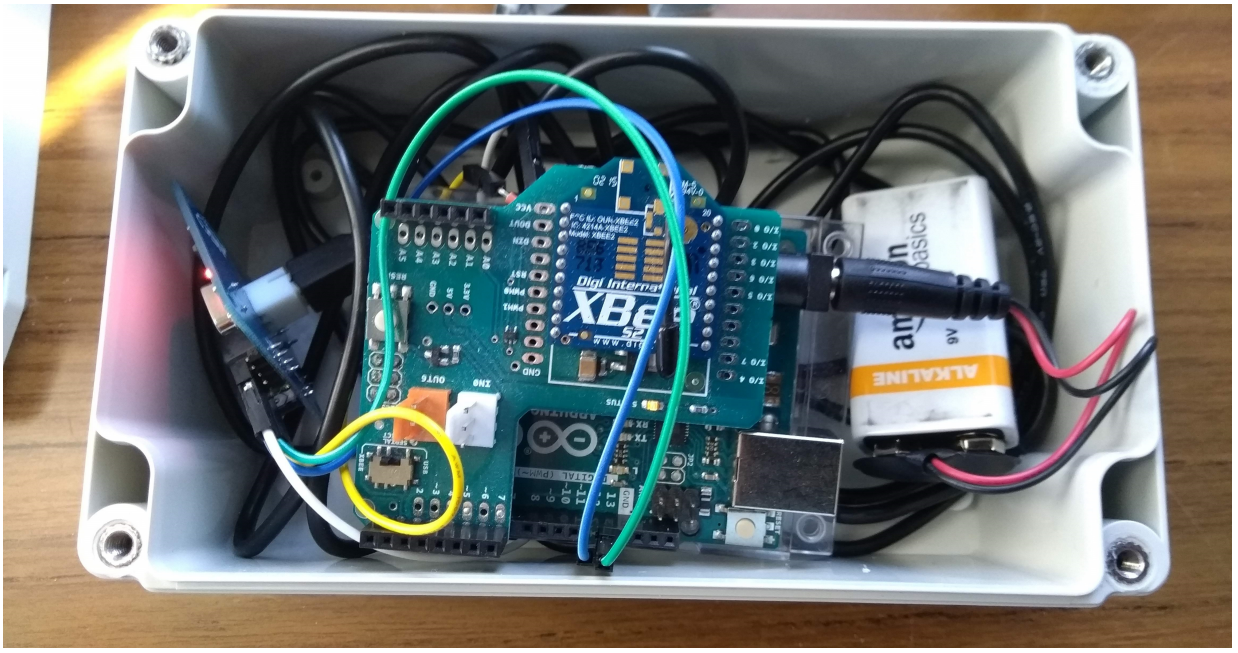

FIGURE 4.10: Sensor Node Components

FIGURE 4.11: Sealed Sensor Node

4.5.4 Network Architecture

The overall architecture of the network is in the form of a ZigBee-based mesh topology. Each sensor node is configured as a ZigBee router, whilst the sink node is configured as a ZigBee coordinator. API mode was utilised in order to enable remote configuration of sensor nodes.

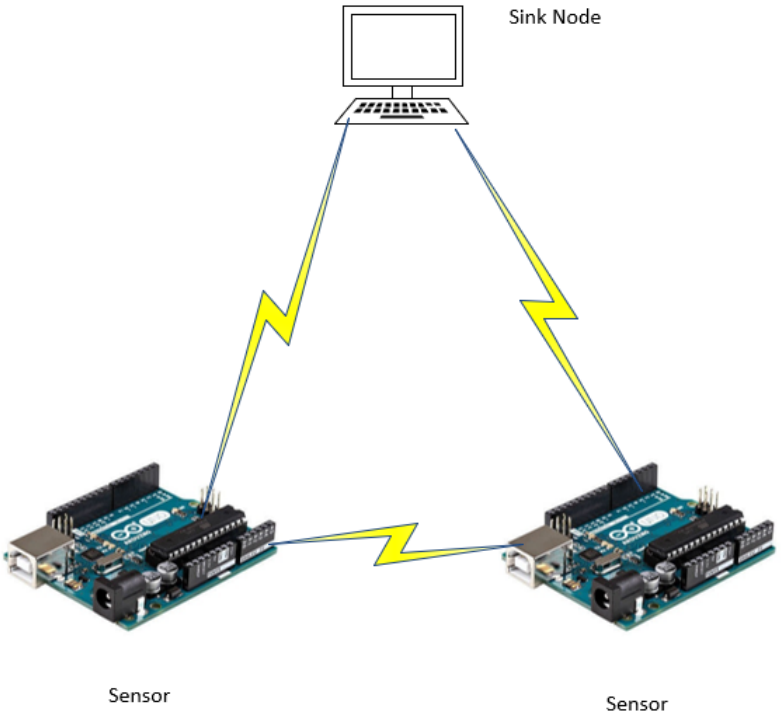

FIGURE 4.12: Network Diagram

4.6 Power consumption

As previously discussed in Chapter 3, power consumption efficiency of sensor nodes is critical in terms of how long they are able to operate for, and by extension their suitability for many applications. The energy resources available to sensor networks is typically very limited, and in many cases are impossible to replenish. Low power consumption was identified as one of the main development considerations earlier in this chapter (refer to Section 4.3.1). In order to effectively minimise the power consumption of the sensor nodes, it is necessary to establish an understanding of the power consumption of different components at different stages of sensor node activity. In this research, the typical cycle of operation can be divided into five stages: measurement, processing, transmitting, and receiving. These five stages are detailed in Table 4.5.

Operation	**Power consumption factors**
Sediment measurement	Sensor reading Sensor stabilisation time Processing speed
Data processing	Processing speed Voltage
Transmitting data	Transceiver operation (TX) Message length Bandwidth
Receiving data	Transceiver operation (RX) Message length Bandwidth Hops Synchronisation

TABLE 4.5: Factors affecting power consumption

When measuring sediment movement, the microcontroller unit initialises the sensors and records the readings taken via the Analogue to Digital Converter unit (ADC). During this stage the node's overall power consumption is primarily owed to the power usage by the ultrasonic sensors and the processing speed of the microcontroller. Consumption at the data processing stage is again primarily based on the microcontroller's processing speed, and this must therefore be optimised in order to achieve a lower rate of power consumption [134]. However, a balanced approach must be taken; on the one hand, higher processing speed will reduce duration, but on the other it will increase the microcontroller's power consumption, and vice versa.

The power consumption in both transmitting and receiving mode is primarily dependent on operation of the transceiver device and specifically, the length of time

that it is required to be powered on, which in turn depends on packet size, available bandwidth, transceiver start-up time, and the rate at which data is transferred between the microcontroller and transceiver. When transmitting data, processed data is transferred to the transceiver by the microcontroller, which then transmits the data packets. Similarly, when in receiving mode, the receiver is powered on by the microcontroller at a synchronised time and waits to receive data that has been transmitted by other nodes in the network, as stipulated by the routing protocol in operation, in this case ZigBee. The data is then processed and stored in the node's memory.

4.6.1 Theoretical battery capacity

The capacity of lithium batteries, which were used to power the WSN, is generally measured in milliamp hours (mAh). Accordingly, the same quantifier is used to measure the energy consumption of the WSN components. Considering the factors accounting for power consumption in Table 4.5, the components utilising the most power are:

- XBee module - 40 mAh (if never put in sleep mode)
- Ultrasonic sensor - 30 mAh

The power consumption of other components is negligible compared to the above two, therefore, they are the only ones used in the calculation of power consumption. Calculating node lifetime has been carried out under the assumption that the battery has a capacity of 500 mAh, a typical capacity for a 9V battery which is what was utilised. The total power consumption of the node (P) can be calculated as shown in Equation 4.2:

$$P = P_{radio} + P_{sensor} = 40mAh + 30mAh = 70mAh \tag{4.2}$$

Given this value, life time in hours (LT) of the node assuming a 500 mAh battery capacity is calculated in Equation 4.3:

$$LT = \frac{Capacity}{Total} = \frac{500mAh}{70mAh} = 7.14hrs \tag{4.3}$$

This gives a node lifetime of just 7.14 hours, which is an unacceptably low value. However, by applying the same equation to batteries with greater capacities more promising results are obtained, as documented in Table 4.6.

Battery	**Capacity (typical)**	**Node Lifetime**
D	13000	185 hrs
C	6000	85.71 hrs
AA	2400	34.28 hrs
AAA	1000	14.28 hrs

Table 4.6: Node Lifetime with Standard Batteries

If, for example, a D battery was used, node lifetime would be 185 hours, or just over a week. Though far better, this would still have implications for a deployed WSN where access to replace batteries is impractical. Since the final version of this WSN is expected to be deployed for months at a time it will be necessary to continually replenish energy to ensure continual operation. Therefore, methods of energy harvesting [135], such as solar, wind, or osmotic, is an important area of future research.

4.7 System Software

This section describes the software utilised to operate the WSN and collect and process the data, which can broadly be divided into two parts: software that runs on the sensor node and software responsible for processing the data gathered by the sensor node.

4.7.1 Sensor node

Software that runs on the sensor node is tasked with collecting data via the ultrasonic sensors and then transmitting them to the sink node. This software was written using the C programming language, with Arduino's integrated development environment (IDE) being used to compile the developed code and load it into the sensor node's flash memory. The Arduino IDE is shown in Figure 4.13.

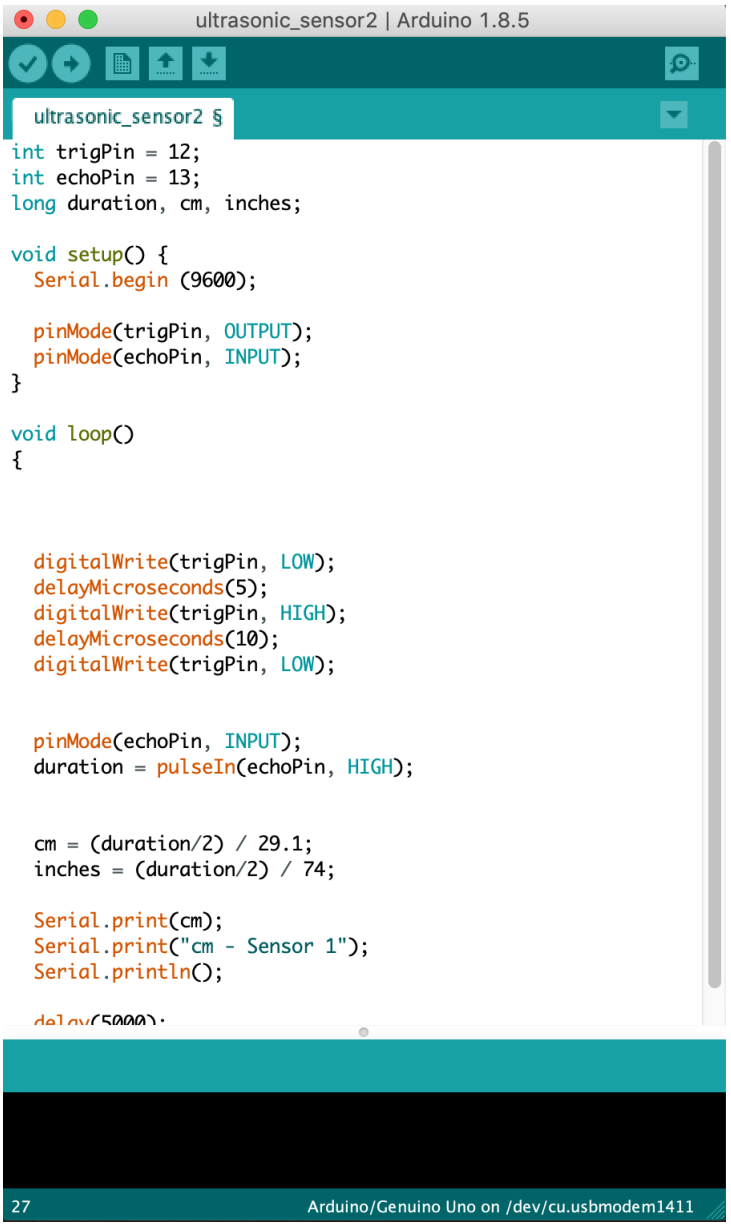

FIGURE 4.13: Arduino Studio development environment

4.7.2 Processing

The sink node consisted of an XBee radio connected to a laptop computer via the USB port. Initial collection of raw data was carried out using the XCTU software in a terminal session. This enabled real-time viewing of not just the readings reported by the sensors, but also the details of each packet that was received, as shown in Figure 4.14.

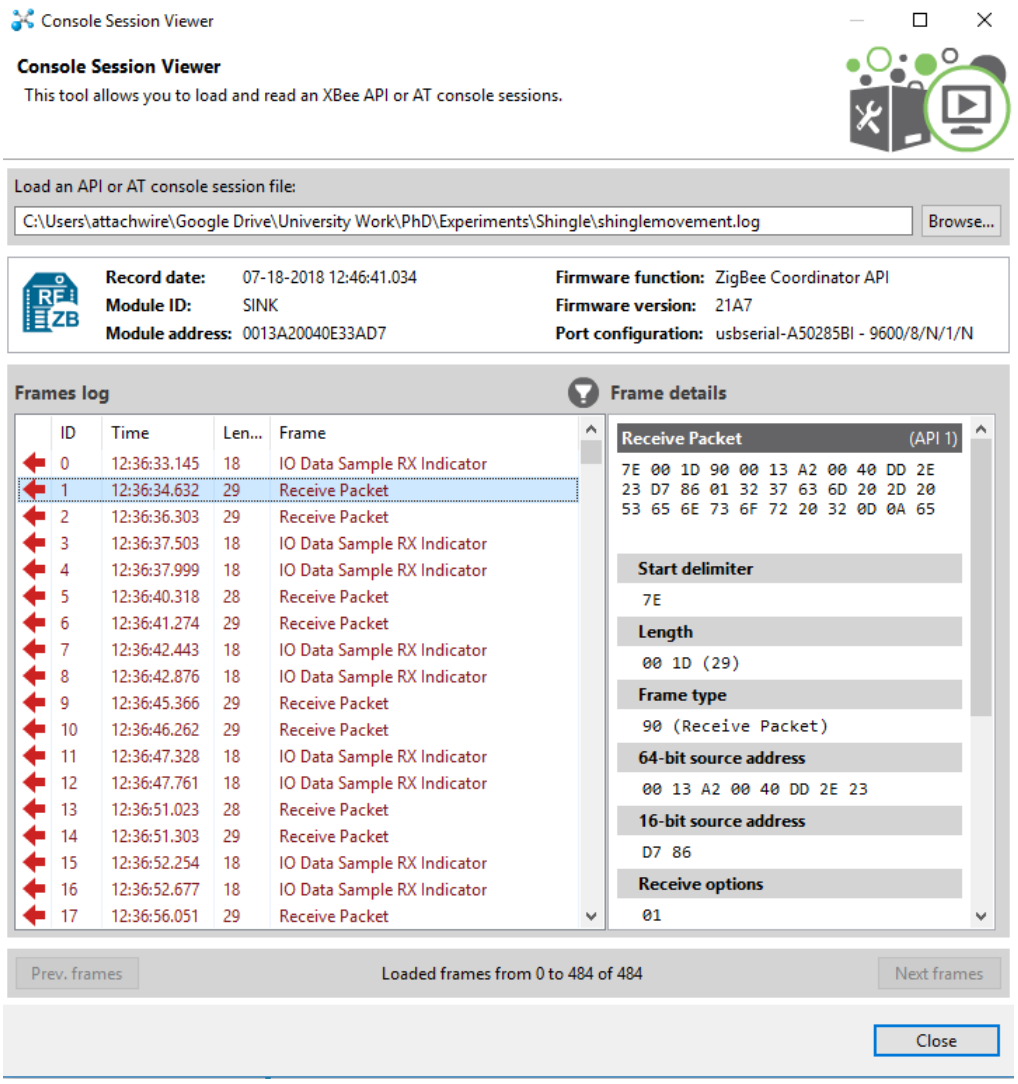

FIGURE 4.14: XCTU Terminal and Packet Information

Following the completion of each experiment, the terminal log file was saved and imported into Microsoft Excel, which was used to parse the data packets and extract data gathered by the sensors for analysis. These results are presented and discussed in Chapter 5.

4.8 Chapter Summary

Following presentation of the new method of monitoring sediment transport in Section 4.2, this chapter has presented and discussed the equipment (and its configuration) that was utilised in order to create a prototype system in order to test the new method. Chapter 5 outlines procedures followed in order to evaluate the prototype system, and also presents and discusses the experimental results.

Chapter 5

Experimental Procedure and Results

5.1 Experimental Procedure

An implementation of the designed system was carried out in a laboratory environment in order to investigate its performance, and specifically to evaluate any variations that occurred with different experimental scenarios. Three types of sediments were used to compare the performance of the system, as described throughout the rest of this chapter. All experiments were carried out using a glass fish tank (45.5 x 103.5 x 53 cm), in order to maintain a controlled and contained environment. Two sensor nodes were utilised, one securely fastened at each end of the tank, so that the depth, and by extension the movement of sediments from one end of the tank to the other, could be measured. The experimental setup is shown in Figure 5.1.

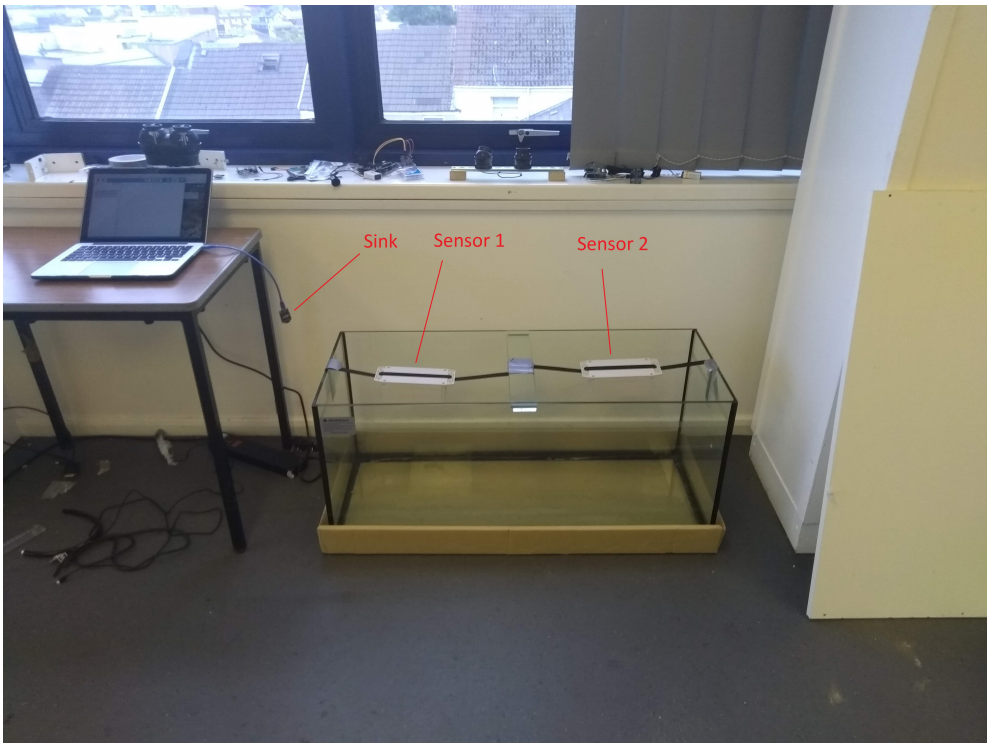

FIGURE 5.1: Experimental setup

The sensors determined depth measurements according to the pulse-echo equation that was previously discussed in Section 3.1.1, and is reproduced below:

$$d = vt/2 \tag{5.1}$$

The speed of sound in air is dependant primarily upon temperature and is independent of the frequency or magnitude of the wave. At 20 degrees Celsius the speed is typically given as 343 metres per second (m/s). Room temperature was therefore maintained at 20 °C, and the temperature verified prior to conducting each experiment to ensure consistent experimental conditions.

Each experiment, with the exception of the initial tank measurements, lasted approximately fifteen minutes and was divided into two stages:

- Establishing the datum, 5 minutes.

- Measuring sediment movement over ten minutes, with sediments manually moved at two minute intervals.

The true depth between the sensors and the top of the sediment was measured with a tape measure prior to starting the datum measurement, and after each movement of sediments (i.e. every two minutes). These were then compared with sensor readings in order to evaluate their accuracy.

Sensors were programmed to collect depth measurements every five seconds, and in order to avoid potential crosstalk, were configured to take measurements at different times. This resulted in 60 readings from each sensor (120 total) for initial tank measurements and each datum measurement, and 120 readings from each sensor during the ten minute collection of data whilst moving sediment (240 total, 24 for each two minute period per sensor). The mean of each dataset was calculated from these values and used to assess accuracy of the measurements (compared to the actual measured values) as well as to compile data to measure the movement of sediment. Standard deviation and standard error values were also calculated in order to evaluate precision of measurement.

5.2 Format of Results

Raw data from all experiments that were carried out can be found in Appendices 2-4. All results are given in centimetres (cm), unless otherwise stated. Each datum measurement and two minute movement interval are shown in the form of line graphs. Considering the depth of the tank that was utilised, the range of measurements that were obtained, and to ensure consistent visualisation of data, the scale on all line graphs is 20-35cm.

Results of each measurement interval are then summarised in Table form, the columns of which are structured as follows: Reading Average, Actual Average,

Datum, and Change. Change is calculated using Equation 4.1, which was introduced in Section 4.2 and is reproduced below for reference. Accordingly, a negative value in the Change column indicates erosion, whilst a positive value indicates accretion of sediments. The summarised results are visualised in the form of colour-coded bar-charts.

$$T = D - R \tag{5.2}$$

Percentage accuracy of each period of measurement is calculated for each sensor, which is averaged to provide an overall accuracy for both sensors. Standard deviation and standard error values are calculated in order to assess the precision of each sensor within a given period of measurement.

Following the presentation and description of results in Sections 5.3 and 5.4 , they are then discussed in Section 5.5, in order to assess performance of the WSN across different types of sediment.

5.3 Initial tank measurements

Initial measurements were undertaken with an empty tank, both in order to verify correct operation of the sensors, and also to establish a depth which can be compared with subsequent measurements in order to measure the amounts of sediment in the tank. This experiment was carried out over a five minute period with a reading being taken every five seconds. Results are shown in Figures 5.2 and 5.3.

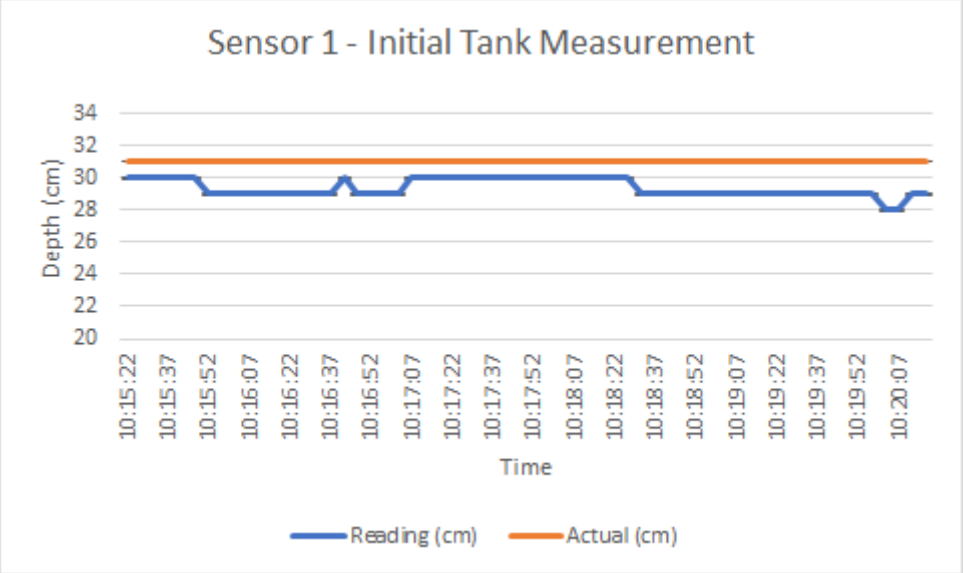

FIGURE 5.2: Initial Tank Measurement - Sensor 1

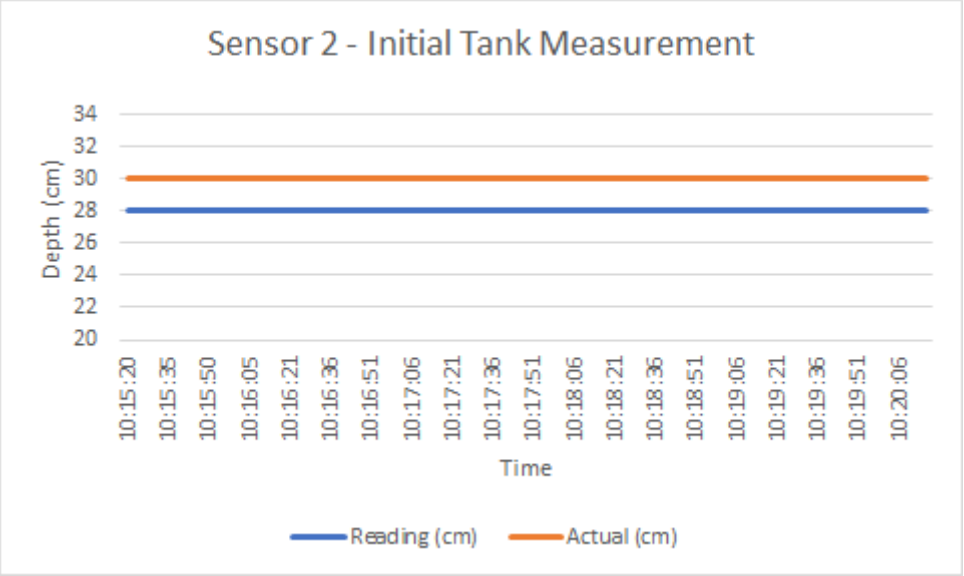

FIGURE 5.3: Initial Tank Measurement - Sensor 2

Sensor 1 (S1) reported an average of 29.36 cm against an actual depth of 31 cm, a difference of -5.26%, whilst Sensor 2 (S2) reported an average of 28 cm against an actual depth of 30 cm, differing by -9.67%.

Although accuracy of S2 was poorer, the reading was repeated consistently over the five minutes, thus achieving a better rate of precision, whilst S1's readings were more varied, giving a standard error of 0.07.

S1 measured the depth with 94.73% accuracy, while S2's accuracy was 90.32%, giving an overall accuracy between the two sensors of 92.52%.

5.4 Measurement of sediment movement

Movement of sediments was measured according to the procedure outlined in Section 5.1. Three types of sediment were evaluated: sand, shingle and a mix of both. These were selected not only for conformity with typical sediments found in the coastal environment (as previously discussed earlier in Chapter 2 and specifically Figure 2.2), but also to test the developed system across materials of differing hardness and particle size, since these characteristics (among others) will affect how the ultrasonic pulse transmitted by the sensor interacts with the material, as previously discussed in Section 3.1.1.

5.4.1 Sand

The setup for the measurement of sand movement is shown in Figure 5.4. Approximately 25kg of sand was obtained and used to fill the tank for this experiment.

FIGURE 5.4: Setup with sand

5.4.1.1 Datum measurement

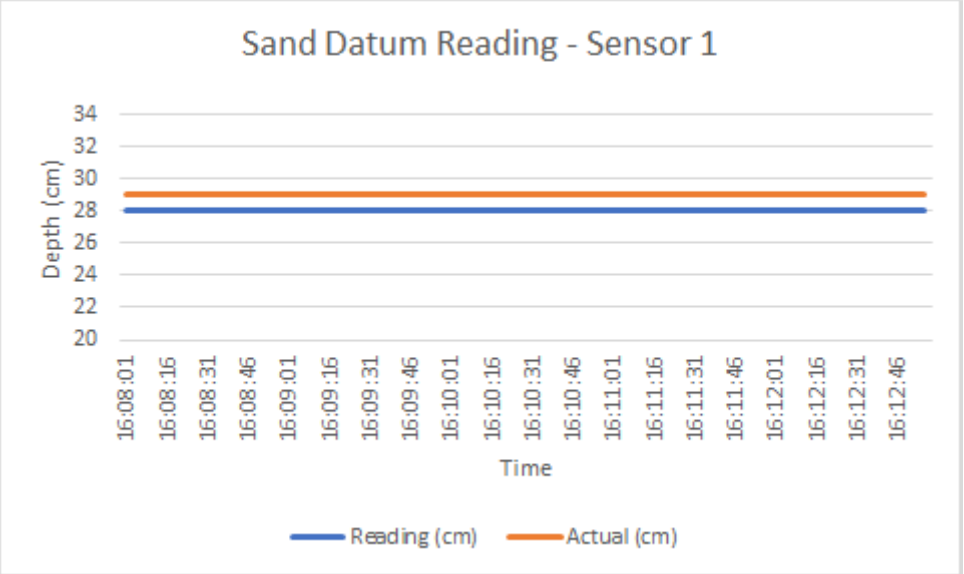

FIGURE 5.5: Sand Baseline - Sensor 1

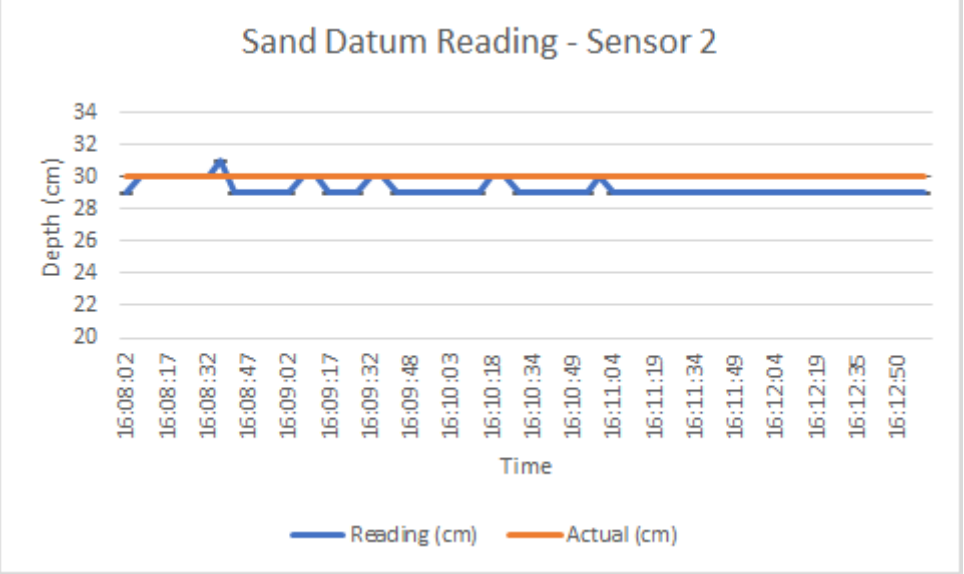

FIGURE 5.6: Sand Baseline - Sensor 2

Actual depth for the datum was measured as 29 cm under S1 and 30 cm under S2. The datum was then established over five minutes with S1 reporting an average of 28 cm (96.55% accuracy) and S2 reporting an average of 29.25 cm (97.5% accuracy), giving an overall accuracy of 97.02%. S1 did not show any variance in precision whilst measurements from S2 showed a 0.06 standard error.

5.4.1.2 Movement

Following the establishment of the datum measurement, the measurement of sand movement was carried out over a ten minute period, with sand being moved at two minute intervals. The results for each two minute interval for both sensors are shown in Figures 5.7 to 5.16, and are then summarised and discussed.

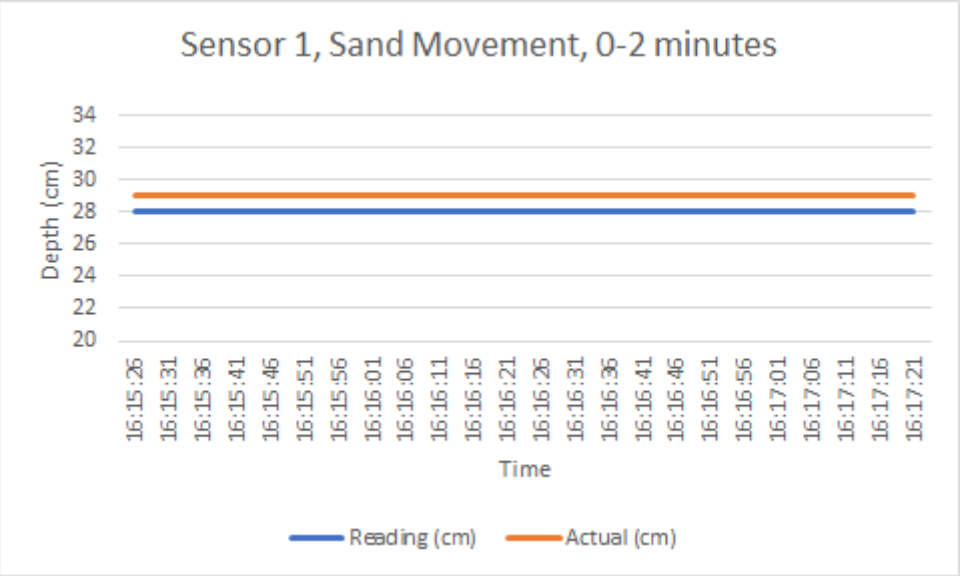

FIGURE 5.7: Sensor 1, Sand Movement, 0-2 minutes

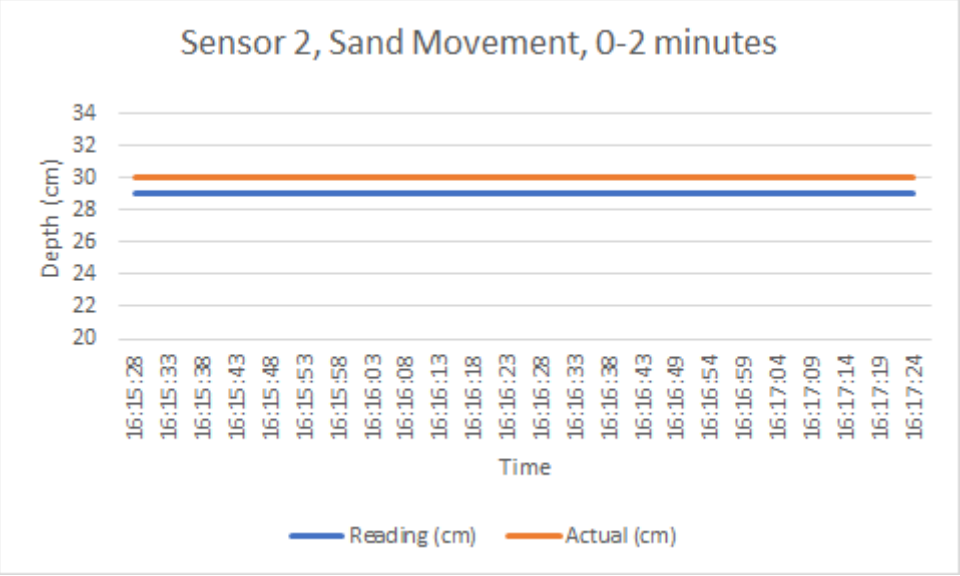

FIGURE 5.8: Sensor 2, Sand Movement, 0-2 minutes

Figures 5.7 and 5.8 show sand movement data for the 0-2 minute interval. Readings for both sensors were 1cm less than the actual depth, thus achieving accuracies of 96.55% and 96.66% respectively. Both sensors also recorded measurements with a perfect level of precision, with standard deviation and hence standard error calculated as zero.

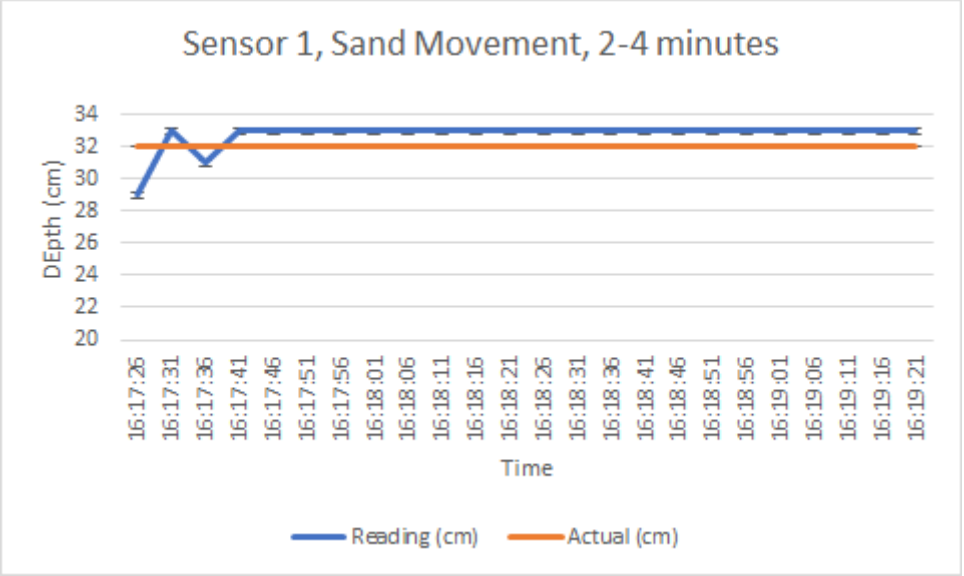

FIGURE 5.9: Sensor 1, Sand Movement, 2-4 minutes

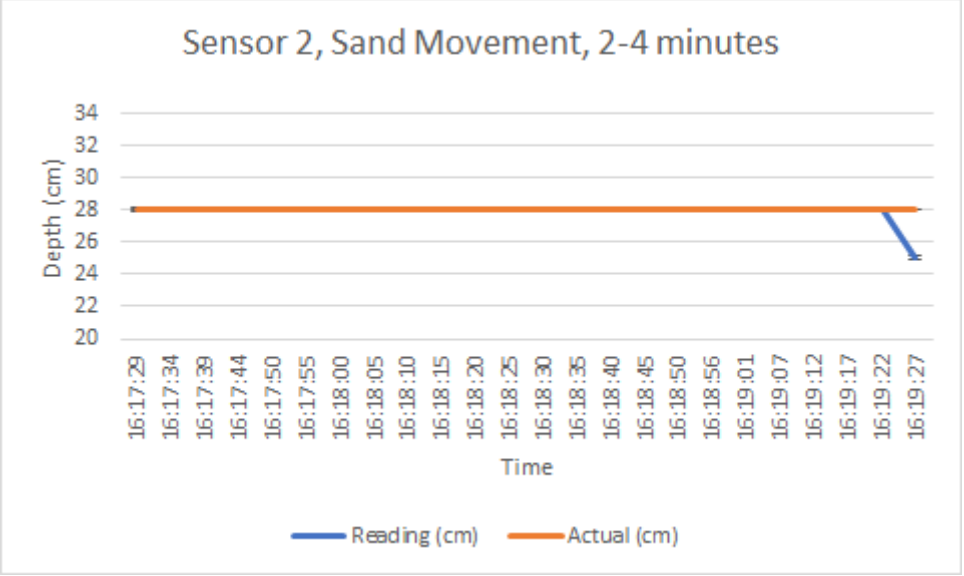

FIGURE 5.10: Sensor 2, Sand Movement, 2-4 minutes

Figures 5.9 and 5.10 show sand movement data for the 2-4 minute interval. Sensor 1 reported an average reading of 32.75cm against an actual depth of 32cm, showing a change of -3.75cm compared to the datum and an accuracy level of 97.65%. Sensor 2 gave an average reading of 27.87cm against an actual measurement of 28cm, indicating an accretion of sediments to the value of 2.12cm when compared to the 30cm datum. Sensor 2 thus achieved an accuracy of 99.55%. However, precision was poorer than the 0-2 minute interval, with the standard error calculated as 0.18 (Sensor 1) and 0.12 (Sensor 2).

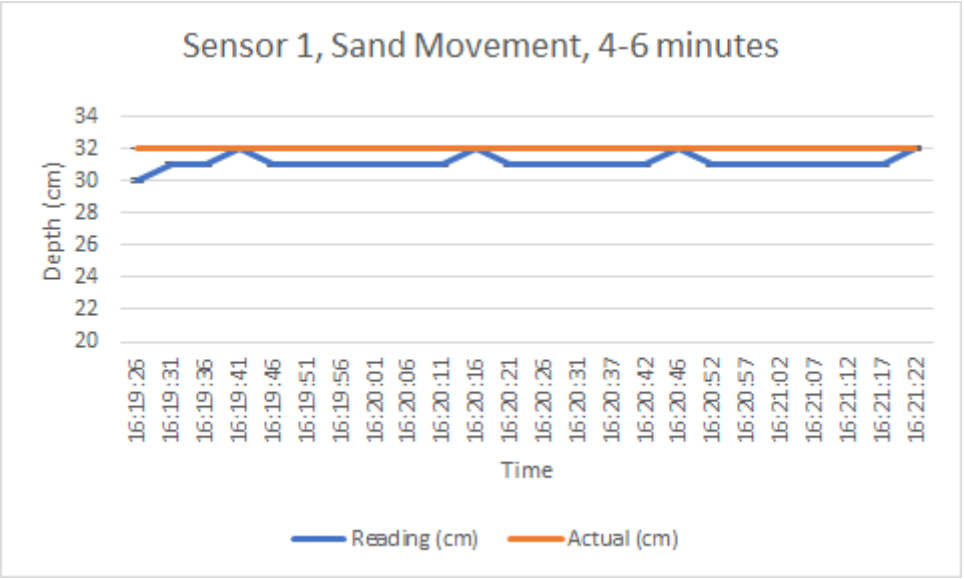

FIGURE 5.11: Sensor 1, Sand Movement, 4-6 minutes

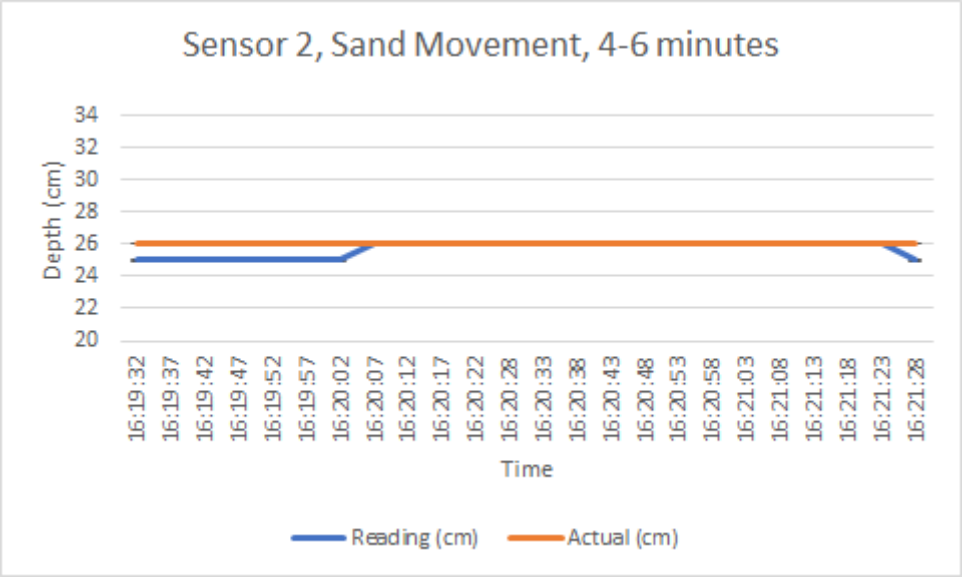

FIGURE 5.12: Sensor 2, Sand Movement, 4-6 minutes

Figures 5.11 and 5.12 show sand movement data for the 4-6 minute interval. Sensor 1 reported an average reading of 31.12cm, slightly below the actual value of 32cm, with an accuracy of 97.26% and standard error of 0.09. Similarly, the average reading from Sensor 2 (25.66cm) was slightly below the actual measurement of 26cm. However it should be noted that, as can be observed in Figure 5.12, that Sensor 2 did achieve 100% accuracy for the majority of the two minute interval,

despite the overall average being slightly below (98.71%). The standard error for Sensor 2 was also calculated as 0.09.

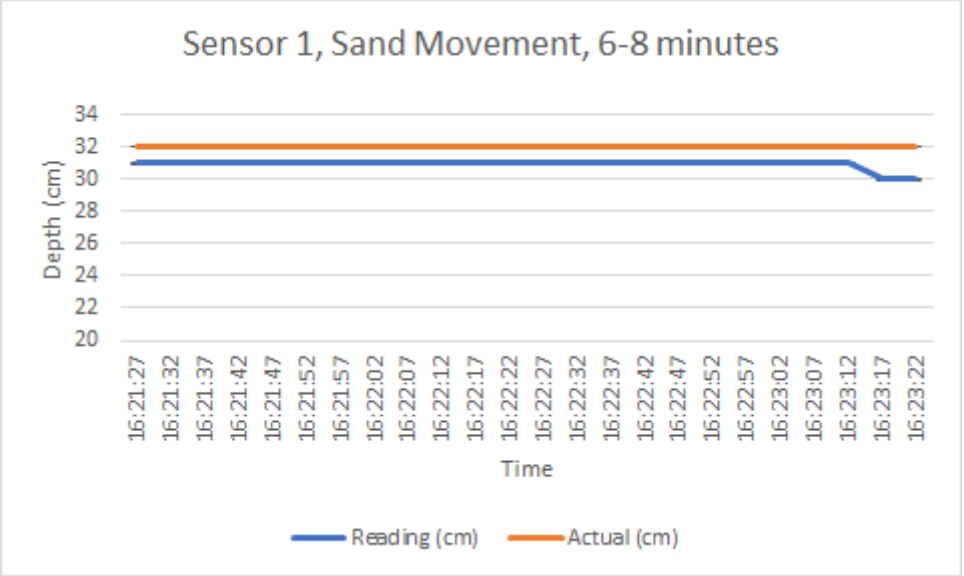

FIGURE 5.13: Sensor 1, Sand Movement, 6-8 minutes

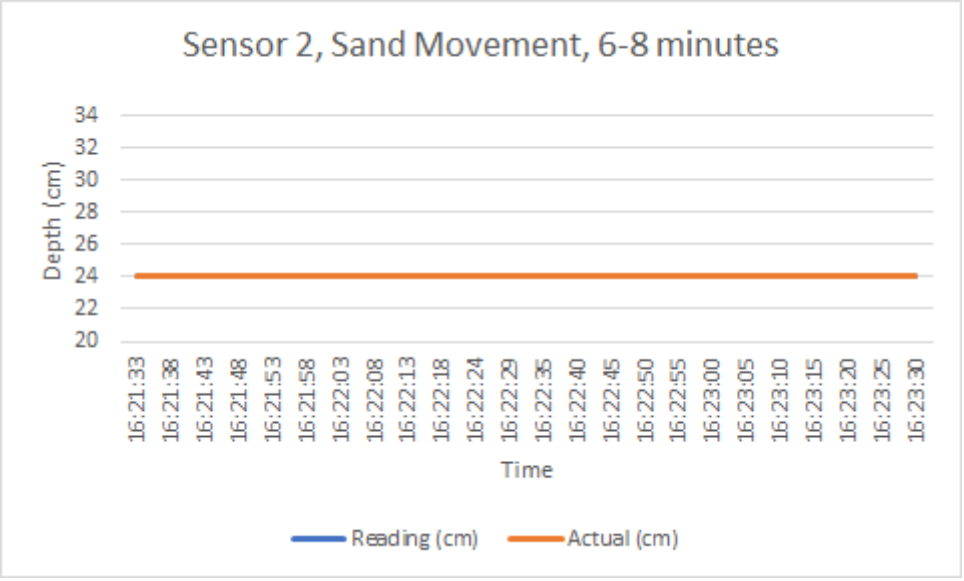

FIGURE 5.14: Sensor 2, Sand Movement, 6-8 minutes

Figures 5.13 and 5.14 show sand movement data for the 6-8 minute interval. Sensor 1 reported an average of 30.91cm against an actual measurement of 32cm, thereby achieving 96.61% accuracy and a standard error of 0.05. Notably, Sensor 2 achieved 100% accuracy and a standard error of 0, the only instance of perfect accuracy and precision in all the experiments. It is also worth noting that the actual distance in this instance was within the advertised blind zone of the sensor, but as can be observed it did not impact the sensor's accuracy or precision. However, it can be seen later in results for the 8-10 minute interval that moving further within the blind zone did adversely affect the measurements.

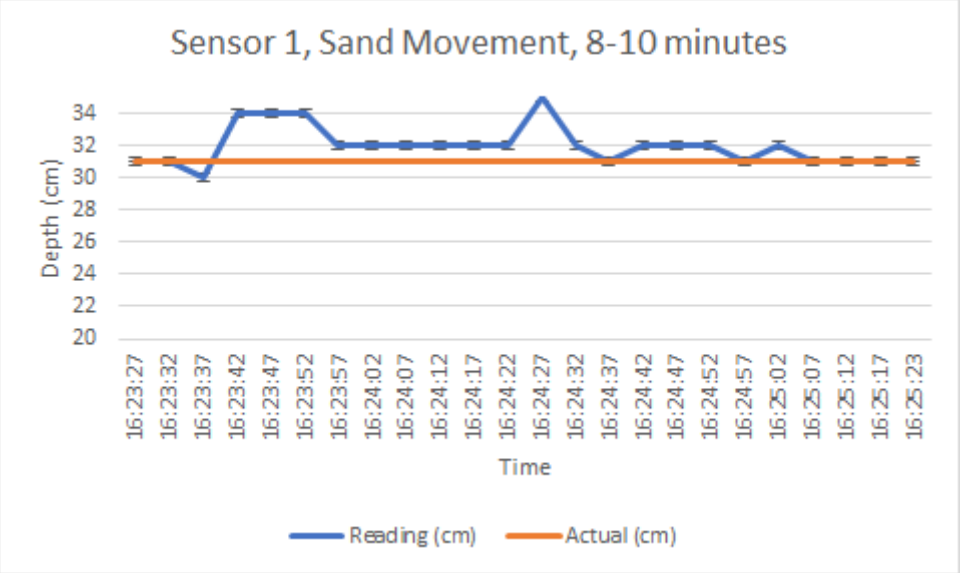

FIGURE 5.15: Sensor 1, Sand Movement, 8-10 minutes

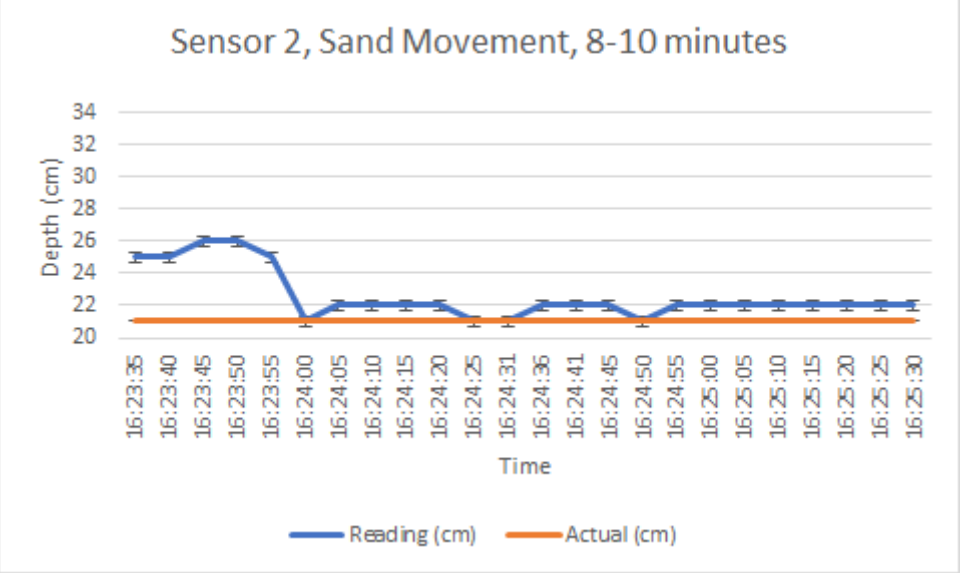

FIGURE 5.16: Sensor 2, Sand Movement, 8-10 minutes

Figures 5.15 and 5.16 show sand movement data for the 8-10 minute interval. The average measurement of Sensor 1 was recorded as 31.95cm against an actual value of 31cm, whilst the same for Sensor 2 was 22.54cm against 21cm. Therefore, this is the only interval in which the average measurement of both sensors was above the actual values. Additionally, this interval saw the poorest level of accuracy out of all the sand movement measurements, with Sensor 2 achieving an accuracy value

of 92.65%. This can in part be attributed to the actual distance being significantly within the sensor's advertised blind zone.

Tables 5.1 and 5.2 show the overall results for each of the above two minute intervals of measurement. These are displayed in graphical form in Figures 5.17 and 5.18 and then discussed.

S1	**Reading Avg.**	**Actual Avg.**	**Datum**	**Change**
0 min	28	29	29	1
2 min	32.75	32	29	-3.75
4 min	31.125	32	29	-2.125
6 min	30.9166667	32	29	-1.9166667
8 min	31.95833333	31	29	-2.95833333

TABLE 5.1: Sand Measurements - Sensor Node 1

S2	**Reading Avg.**	**Actual Avg.**	**Datum**	**Change**
0 min	29	30	30	1
2 min	27.875	28	30	2.125
4 min	25.6666667	26	30	4.33333333
6 min	24	24	30	6
8 min	22.54166667	21	30	7.45833333

TABLE 5.2: Sand Measurements - Sensor Node 2

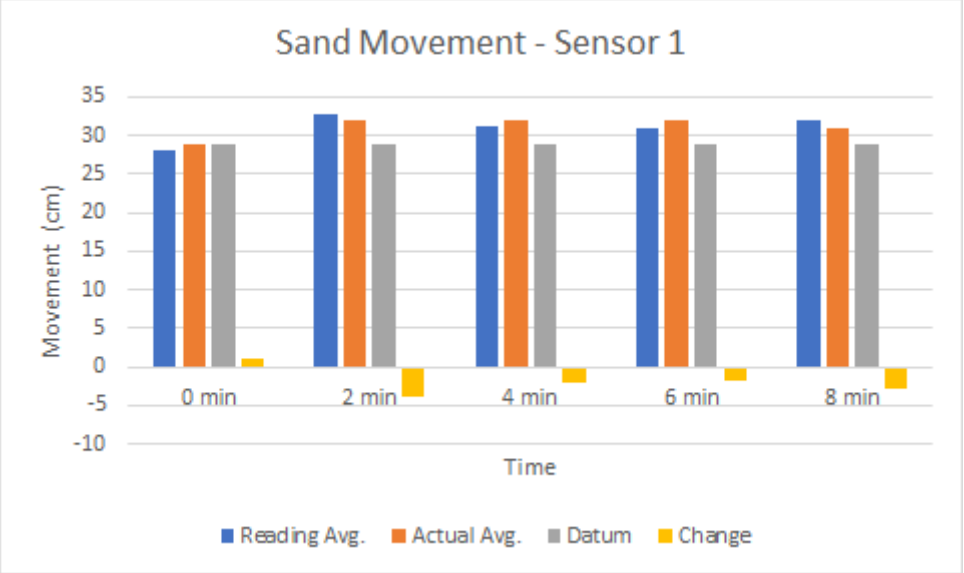

FIGURE 5.17: Sand Movement - Sensor 1

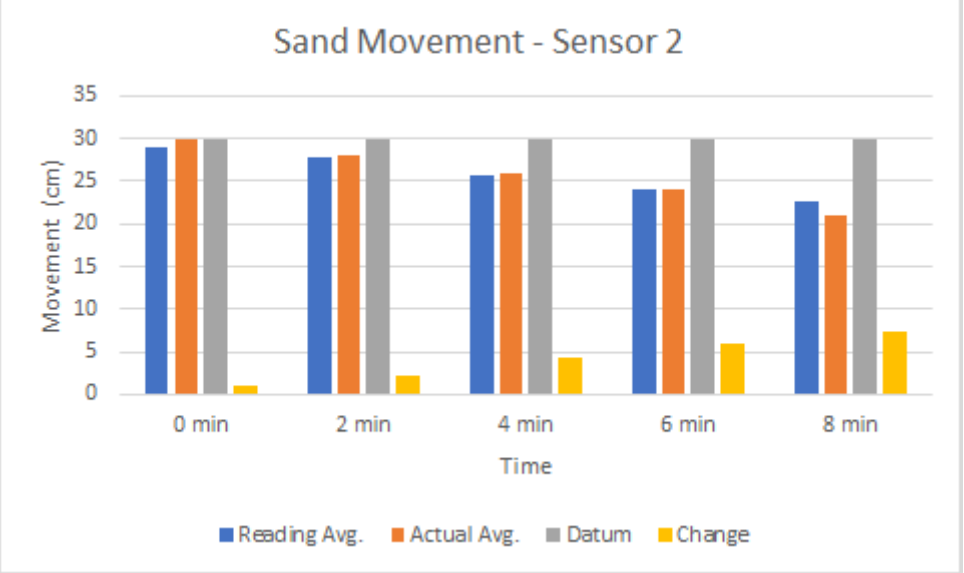

FIGURE 5.18: Sand Movement - Sensor 2

Patterns of sediment movement can be seen in Figures 5.17 and 5.18, in particular the latter, by observing the **Change** bar, which gradually increases over the ten minutes, indicating accretion rather than erosion. Conversely, measurements from S1 from 2 minutes onwards, when measured against the datum are consistently negative, indicating erosion. This shows the pattern of movement from the left side to the right side of the tank.

Sensor 1	**Accuracy (%)**	**Std. Deviation**	**Std. Error**
0 mins	96.55	0	0
2 mins	97.65	0.896854406	0.183069639
4 mins	97.26	0.448427203	0.09153482
6 mins	96.61	0.282329851	0.05763034
8 mins	96.90	1.197067673	0.244350416
Sensor 2	**Accuracy (%)**	**Std. Deviation**	**Std. Error**
0 mins	96.66	0	0
2 mins	99.55	0.61237244	0.125
4 mins	98.71	0.48154341	0.09829464
6 mins	100	0	0
8 mins	92.65	1.55979839	0.31839251

Table 5.3: Sand Movement - Performance Statistics

From the statistics provided in Table 5.3, overall accuracy of S1 was 96.99%, whilst S2 achieved 97.51% over the ten minutes. This is shown in Figures 5.19 and 5.20. Therefore, an overall accuracy rate of 97.25% for measurement of sand movement is achieved, a slight improvement (0.23%) on the accuracy of the datum measurement. The standard error of the measurements was averaged at 0.11, which was the highest level of precision obtained out of the three experiments conducted. Additionally, sand was the material with which most measurement intervals showed a standard error of 0, three in total.

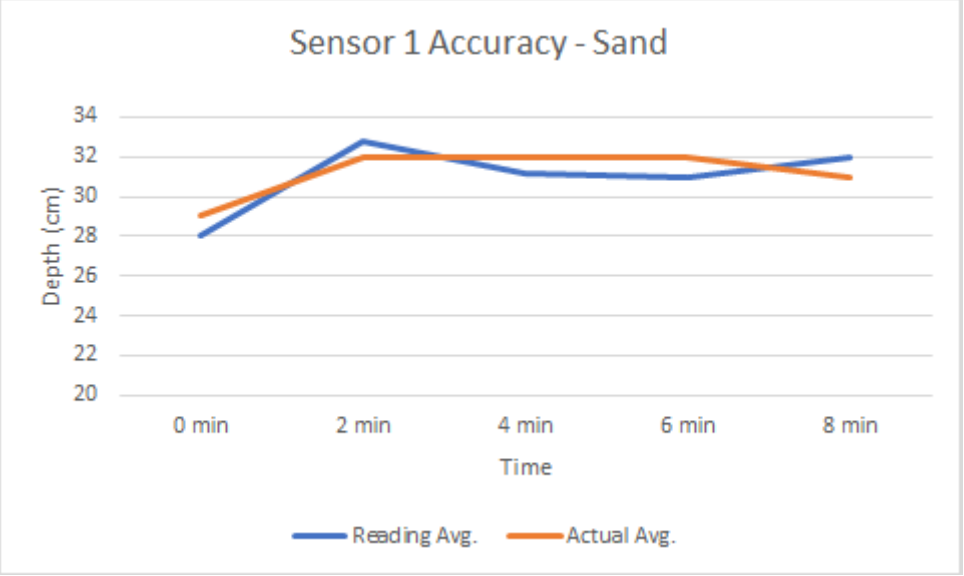

FIGURE 5.19: Sensor 1 Accuracy - Sand

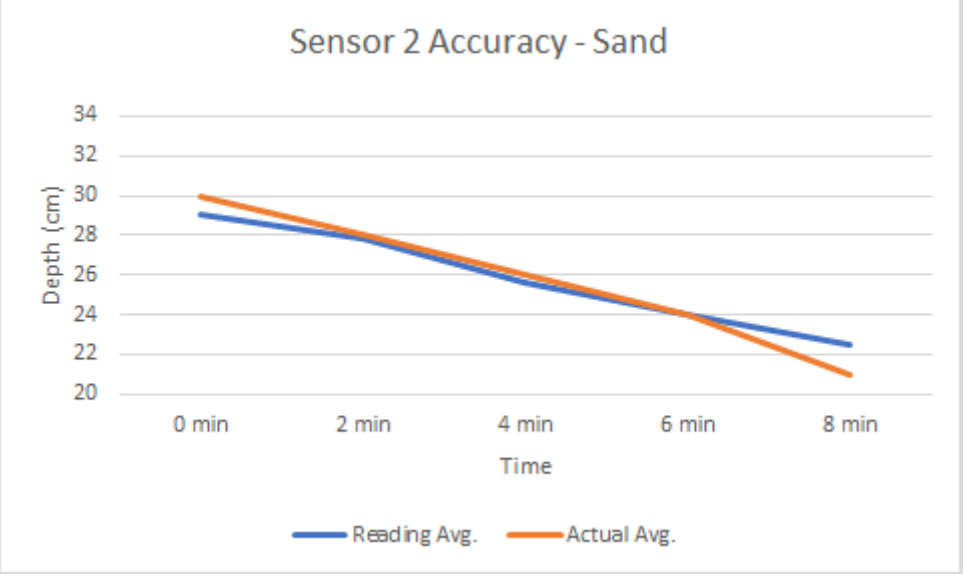

FIGURE 5.20: Sensor 2 Accuracy - Sand

5.4.2 Shingle

The experimental setup for measuring shingle movement is shown in Figure 5.21. Around 30kg of sediment was obtained, with particle sizes of between 1 and 100 millimetres (mm), which is consistent with sizes at which sediment is considered shingle as previously shown in Figure 2.2.

FIGURE 5.21: Setup with shingle

5.4.2.1 Datum measurement

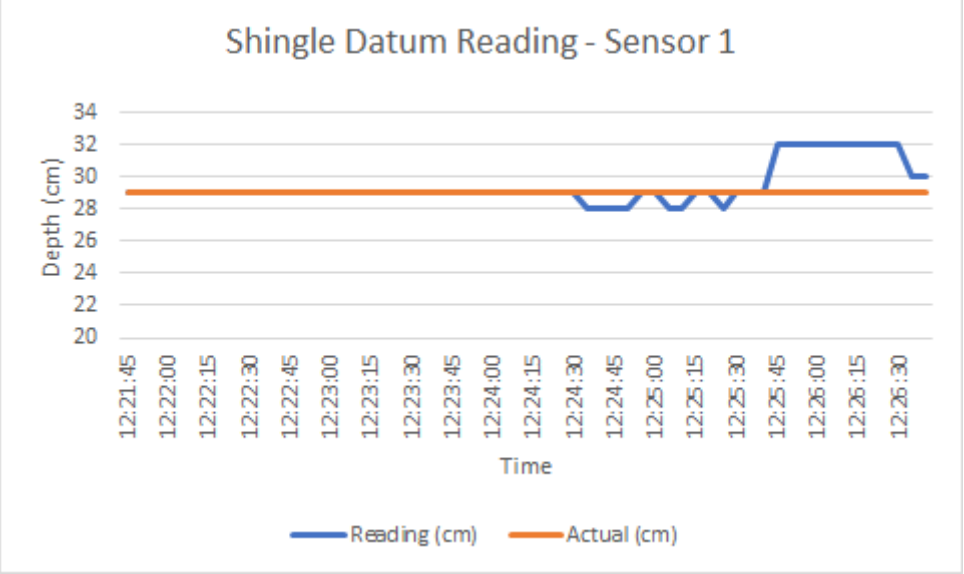

FIGURE 5.22: Shingle Datum - Sensor 1

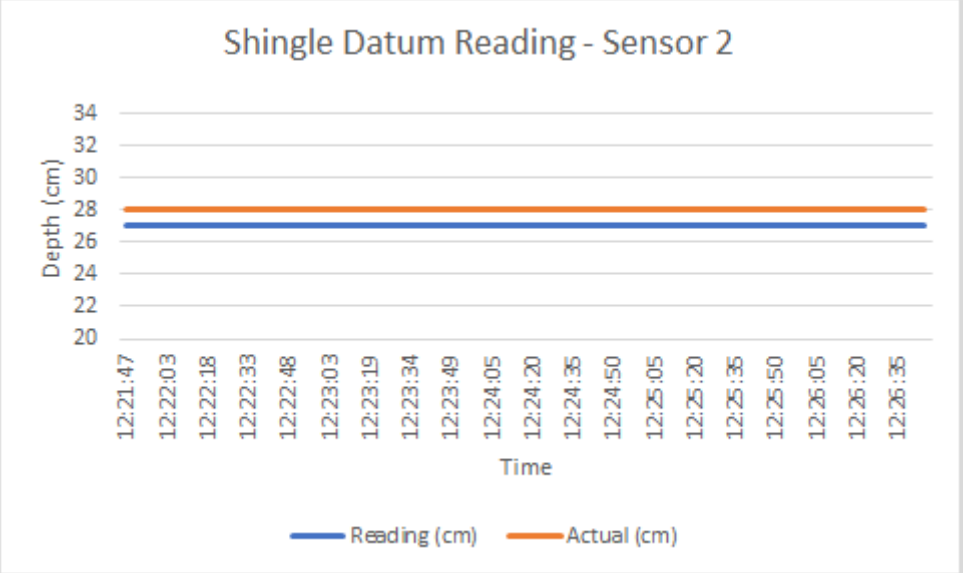

FIGURE 5.23: Shingle Datum - Sensor 2

As shown in Figures 5.22 and 5.23, actual depth of the tank containing shingle was measured at 29cm under S1 and 28cm under S2. S1's averaged reading was 29.41cm over the five minutes, with a standard error of 0.15, thus overestimating the depth in this case. S2 on the other hand, reported a precise reading of 27cm with no variability in precision. Therefore, measurement of the shingle datum achieved an accuracy of 97.49%.

5.4.2.2 Movement

Figures 5.24 to 5.33 show the results reported by each sensor over a period of ten minutes with sediment being moved at two minute intervals.

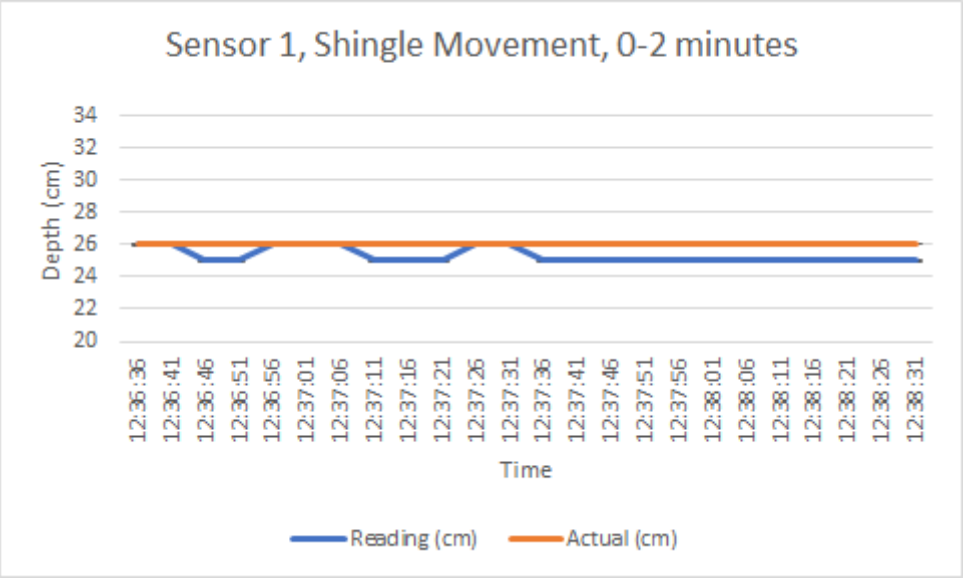

FIGURE 5.24: Sensor 1, Shingle Movement, 0-2 minutes

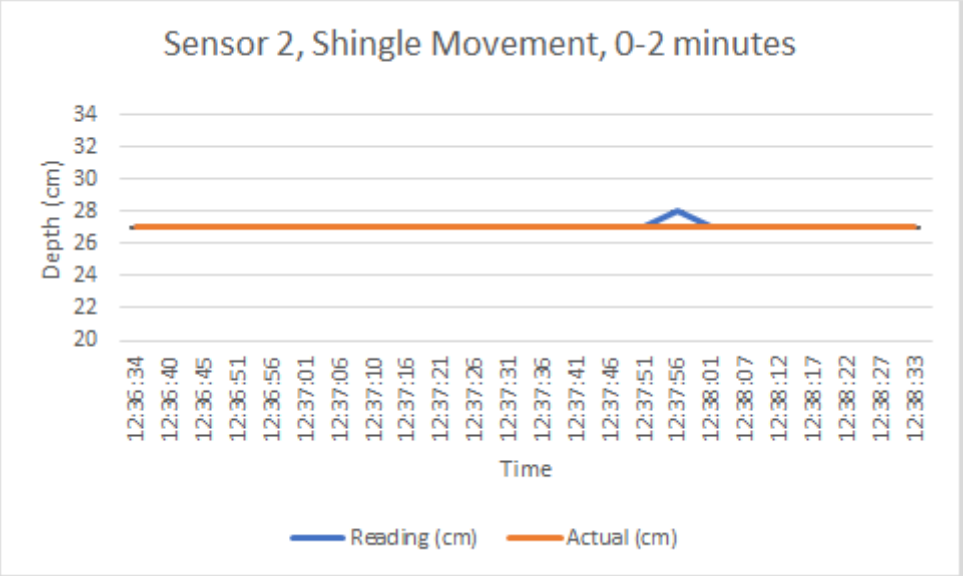

FIGURE 5.25: Sensor 2, Shingle Movement, 0-2 minutes

Figures 5.24 and 5.25 show shingle movement data for the 0-2 minute interval. Sensor 1 recorded an average measurement of 25.29cm against the actual value

of 26cm (97.27% accuracy), indicating an accretion of sediments to the value of 3.70cm. Sensor 2 achieved better accuracy, with the recorded average of 27.04cm against an actual value of 27cm, an accuracy rate of 99.84%. Standard error values were calculated as 0.09 for Sensor 1 and 0.04 for Sensor 2.

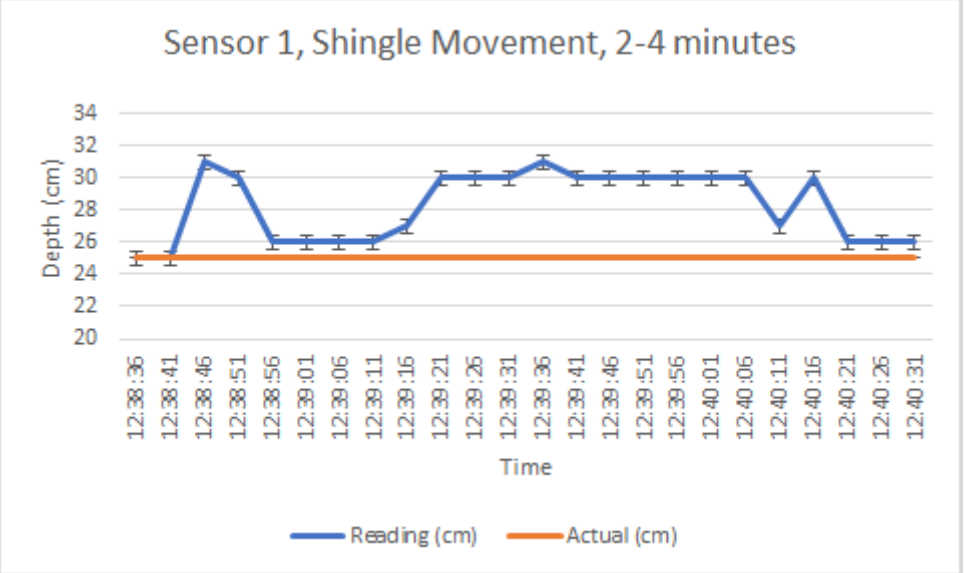

FIGURE 5.26: Sensor 1, Shingle Movement, 2-4 minutes

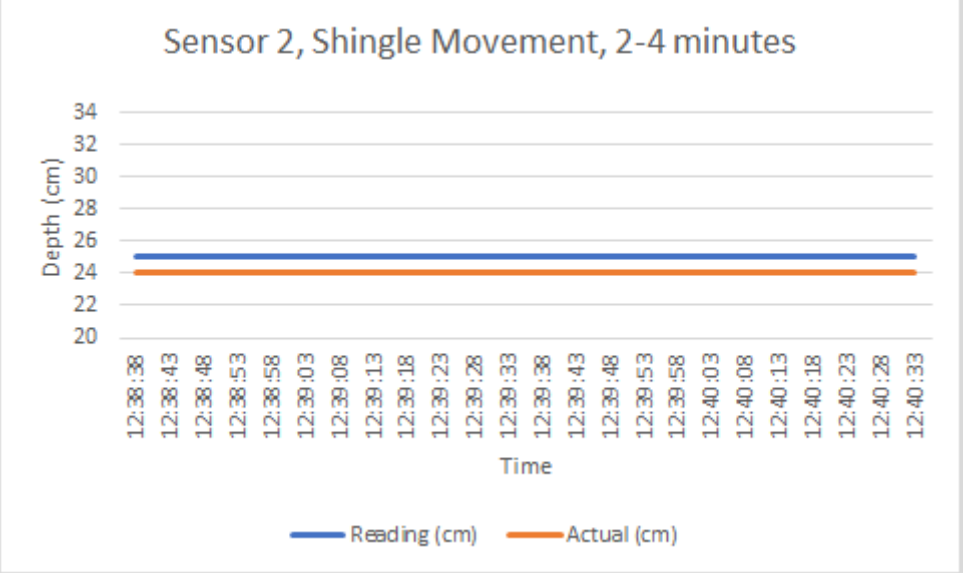

FIGURE 5.27: Sensor 2, Shingle Movement, 2-4 minutes

Figures 5.26 and 5.27 show shingle movement data for the 2-4 minute interval. Significantly, this measurement interval showed the worst accuracy rate of any of

the experiments, with Sensor 1 reporting an average reading of 28.25cm against an actual value of 25cm, an accuracy of 87%, thus the only instance in which accuracy dropped below 90%. It was also the worst rate of precision, with a standard error of 0.44. Sensor 2 performed better, reporting an average measurement of 25cm against an actual value of 24cm (95.83%), and doing so with perfect precision.

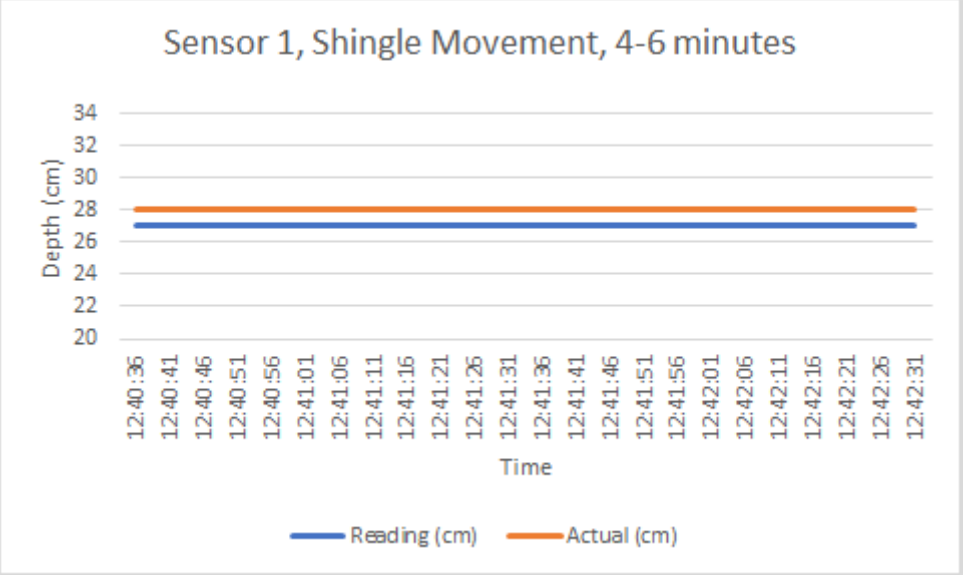

FIGURE 5.28: Sensor 1, Shingle Movement, 4-6 minutes

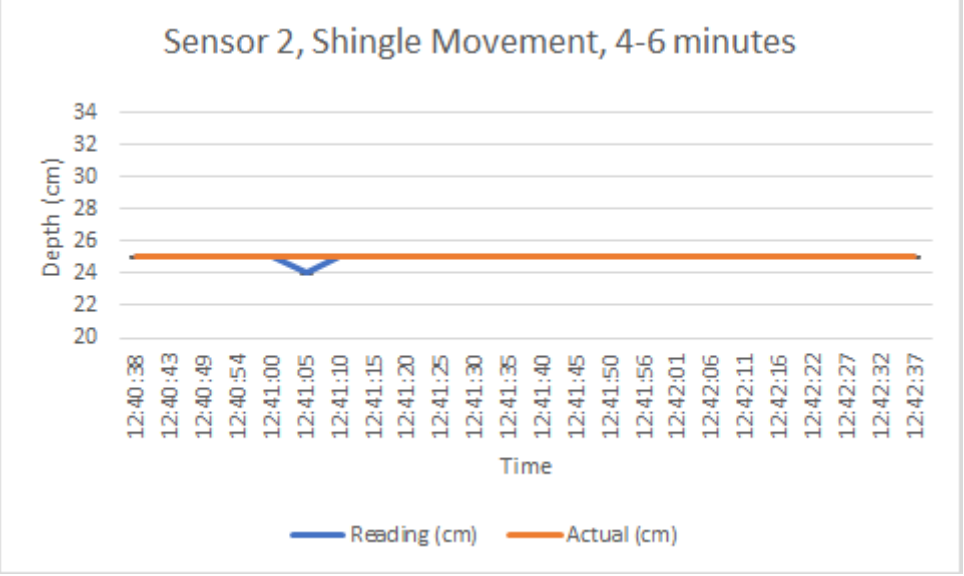

FIGURE 5.29: Sensor 2, Shingle Movement, 4-6 minutes

Figures 5.28 and 5.29 show shingle movement data for the 4-6 minute interval. Sensor 1 achieved an accuracy of 96.42%, recording an average of 27cm against a 28cm actual value with perfect precision. Sensor 2 performed similarly, recording an average depth of 24.95cm. The actual depth was 24cm, and the accuracy was therefore 96%. Sensor 2 also came close to achieving perfect precision, save for a brief spike at approximately 12:41:05, which is most likely attributable to minor movement of the sensor node. The standard error was therefore 0.04.

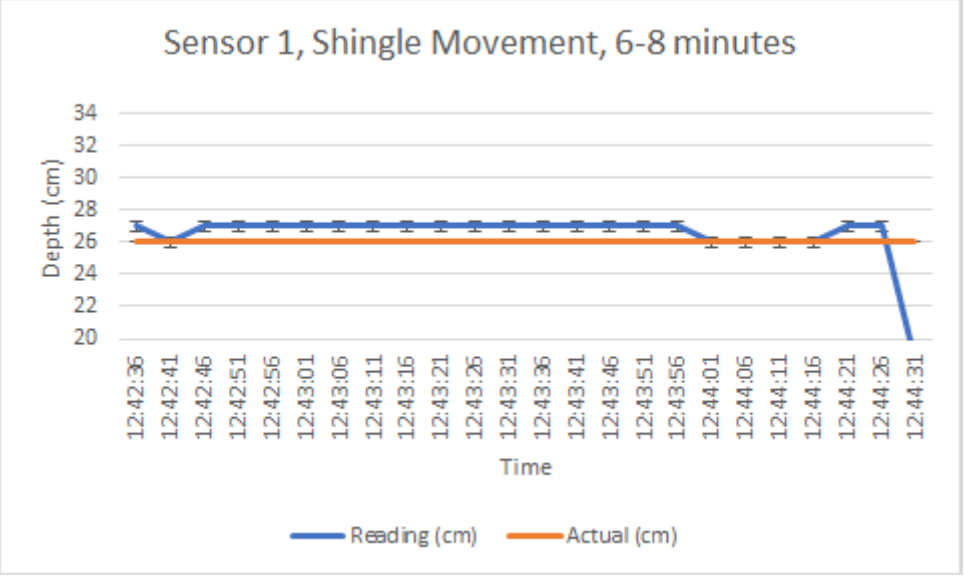

FIGURE 5.30: Sensor 1, Shingle Movement, 6-8 minutes

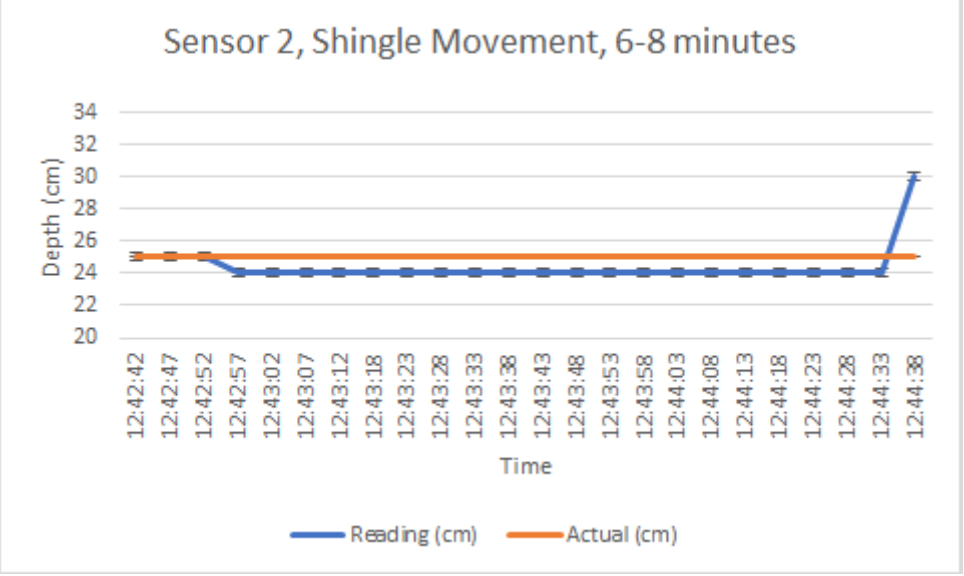

FIGURE 5.31: Sensor 2, Shingle Movement, 6-8 minutes

Figures 5.30 and 5.31 show shingle movement data for the 6-8 minute interval. For this measurement, Sensor 1 recorded an average depth of 26.45cm against an actual measurement of 26cm, with accuracy of 98.23%. The standard error was calculated at 0.33. Sensor 2 reported an average depth of 24.37cm, slightly below the actual value of 25cm, thus achieving 97.5% accuracy and better precision than Sensor 1, with a standard error value of 0.25.

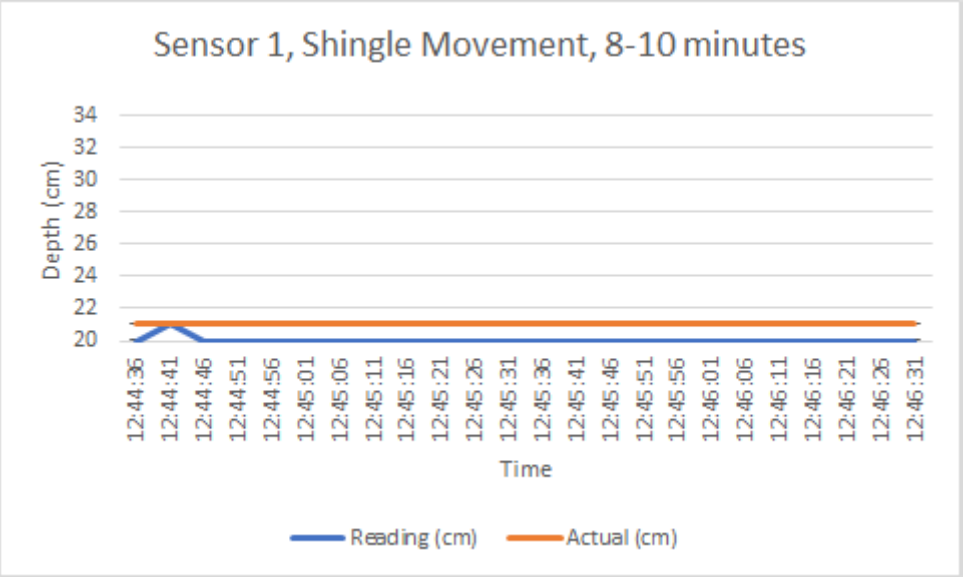

FIGURE 5.32: Sensor 1, Shingle Movement, 8-10 minutes

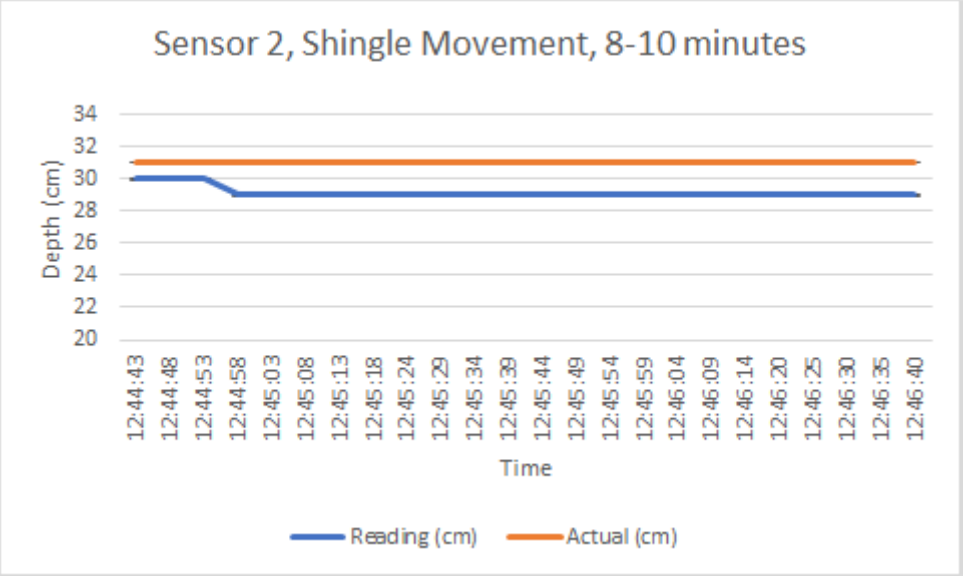

FIGURE 5.33: Sensor 2, Shingle Movement, 8-10 minutes

Figures 5.32 and 5.33 show shingle movement data for the 8-10 minute interval. Sensor 1 recorded an average depth of 20.04cm, 95.4% accuracy when compared to the actual value of 21cm. Sensor 2 was less accurate, with an average reading of 29.12cm compared to a 31cm actual measurement, 93.95% accuracy. Standard error values were calculated as 0.04 and 0.06 for Sensor 1 and 2 respectively.

Tables 5.4 and 5.5 show the overall results for each of the above two minute intervals of measurement. These are displayed in graphical form in Figures 5.34 and 5.35 and then discussed.

S1	**Reading Avg.**	**Actual Avg.**	**Datum**	**Change**
0 min	25.2916667	26	29	3.70833333
2 min	28.25	25	29	0.75
4 min	27	28	29	2
6 min	26.4583333	26	29	2.54166667
8 min	20.04166667	21	29	8.95833333

Table 5.4: Shingle Measurements - Sensor Node 1

S2	**Reading Avg.**	**Actual Avg.**	**Datum**	**Change**
0 min	27.0416667	27	27	-0.0416667
2 min	25	24	27	2
4 min	24.9583333	24	27	2.04166667
6 min	24.375	25	27	2.625
8 min	29.125	31	27	-2.125

Table 5.5: Shingle Measurements - Sensor Node 2

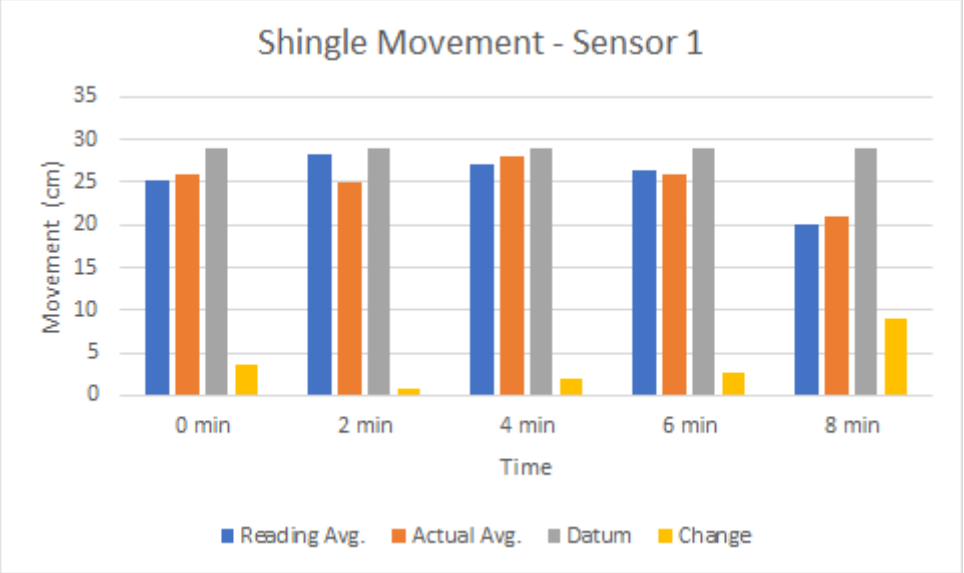

FIGURE 5.34: Shingle Movement - Sensor 1

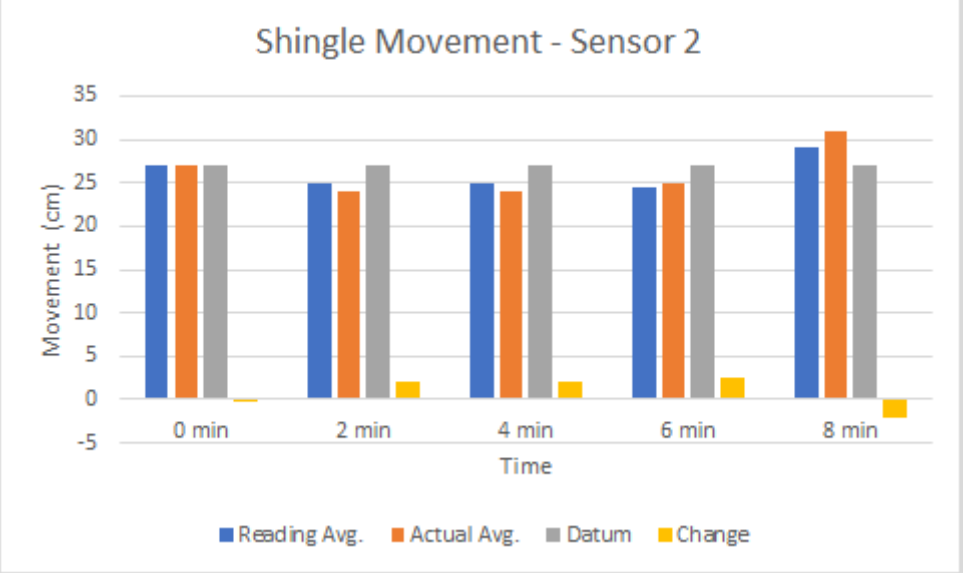

FIGURE 5.35: Shingle Movement - Sensor 2

Figures 5.34 and 5.35 show overall shingle movement over a ten minute measurement period, based on the data in Tables 5.4 and 5.5. Although patterns of accretion or erosion is not as clear as with the sand movement measurements; it can be observed from the **Change** bars for S1 in addition to the numerical data in Table 5.4 that all readings are less than the datum measurement, which was not

consistently true with S2, particularly during the period of 8-10 minutes. Therefore, although there is not a consistent pattern of erosion or accretion, it could be determined that accretion was more likely underneath Sensor 1.

Sensor 1	**Accuracy (%)**	**Std. Deviation**	**Std. Error**
0 mins	97.27	0.464305621	0.094775988
2 mins	87	2.171955641	0.443348589
4 mins	96.42	0	0
6 mins	98.23	1.64129235	0.335027398
8 mins	95.4	0.204124145	0.041666667
Sensor 2	**Accuracy (%)**	**Std. Deviation**	**Std. Error**
0 mins	99.84	0.20412415	0.04166667
2 mins	95.83	0	0
4 mins	96	0.20412415	0.04166667
6 mins	97.5	1.24455335	0.25404339
8 mins	93.95	0.33783196	0.06895966

Table 5.6: Shingle Movement - Performance Statistics

As shown in Table 5.6 and visualised in graph form in Figures 5.53 and 5.54, S1 performed with 94.87% accuracy whilst S2 achieved 96.62%. This gives an overall accuracy of 95.75% for measurements of shingle movement, a 1.74% difference (negative) compared to the datum accuracy, and a 1.5% difference (also negative) compared to overall accuracy for sand movement. In terms of precision, results gathered were observed to be less precise than sand, with an overall standard error of 0.13 compared to 0.11 for sand. This was expected given the increased scattering of sound waves that occurs when they interact with coarse-grained materials (as discussed in Chapter 3).

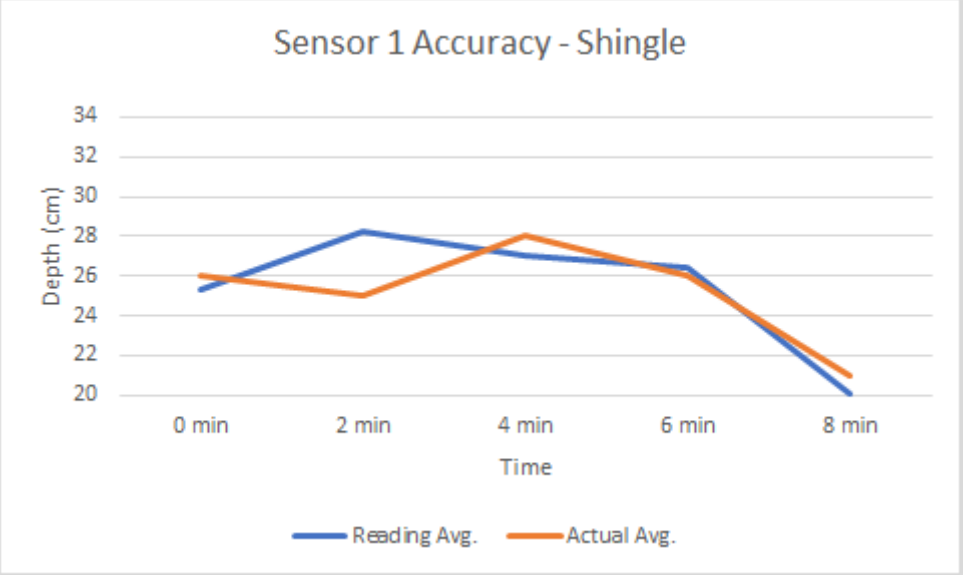

FIGURE 5.36: Sensor 1 Accuracy - Shingle

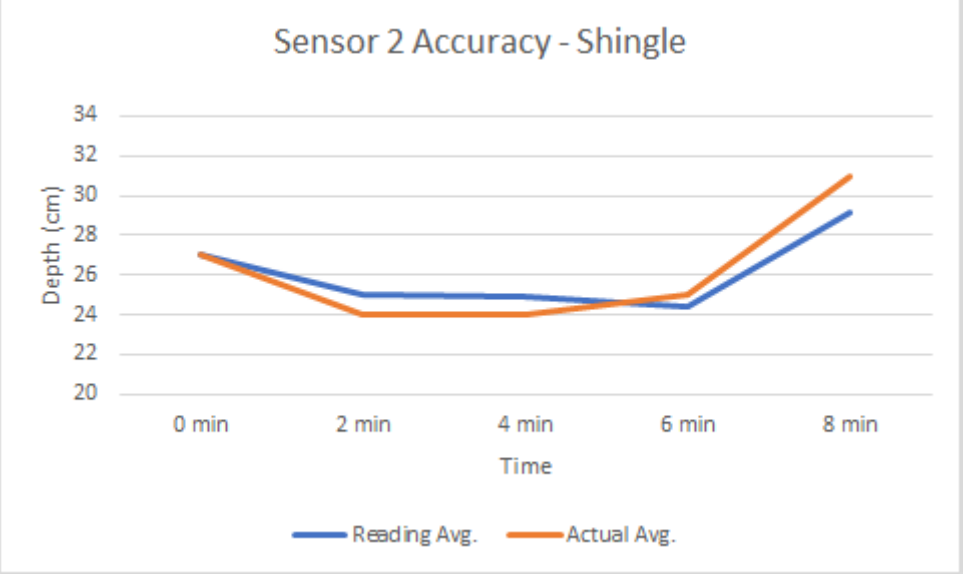

FIGURE 5.37: Sensor 2 Accuracy - Shingle

5.4.3 Mixed sediments

For this experiment, sediments used in the previous two experiments were mixed in order to introduce inhomogeneity and observe any effects this had on measurements. The experimental setup with mixed sediments is shown in Figure 5.38.

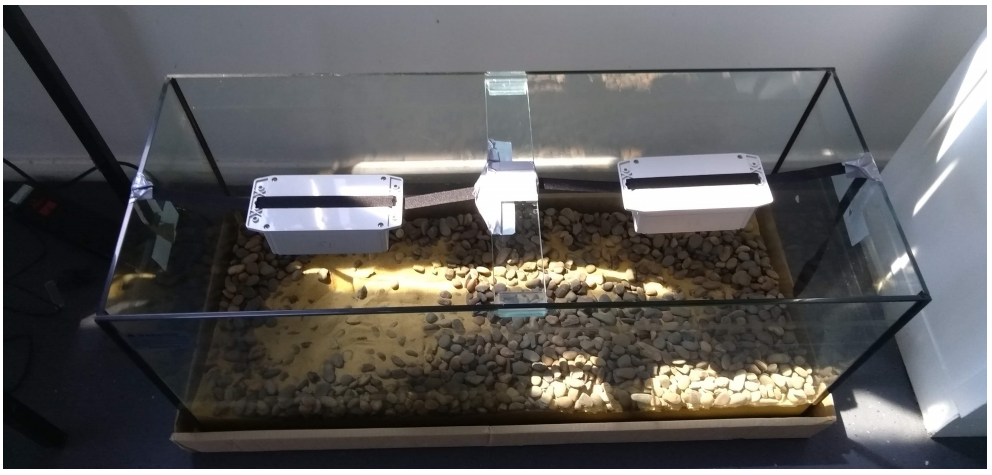

FIGURE 5.38: Setup with mixed sediments

5.4.3.1 Datum measurement

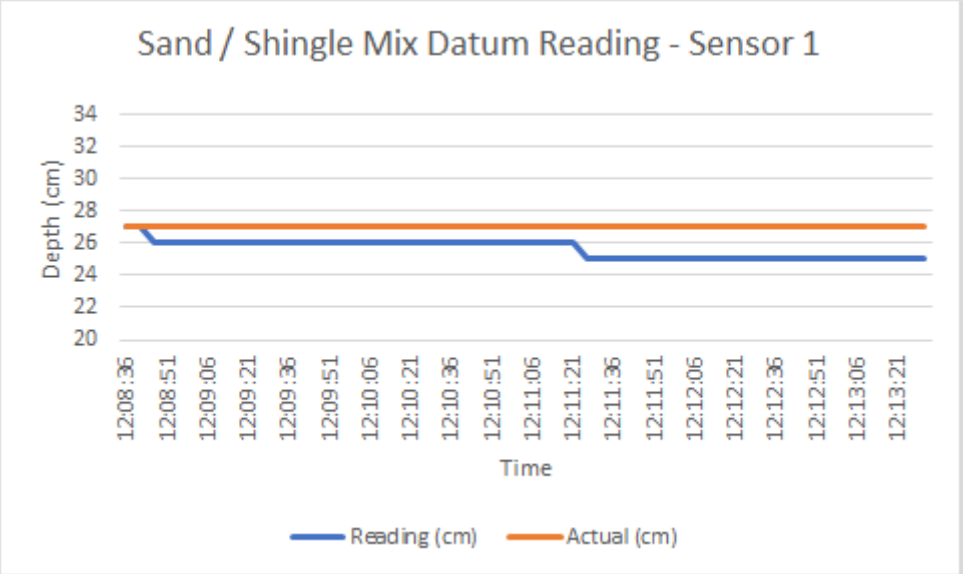

FIGURE 5.39: Sand/Shingle Datum Measurement - Sensor 1

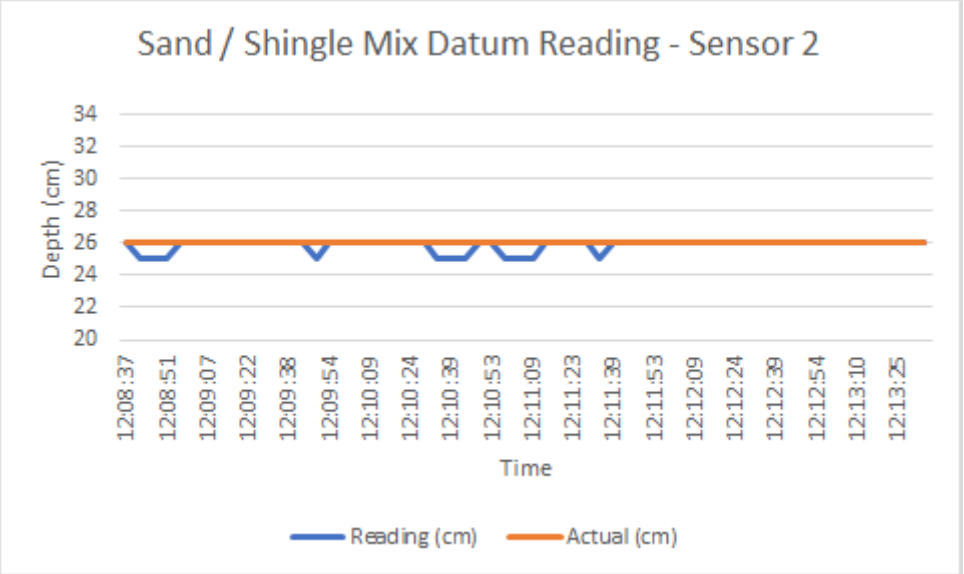

FIGURE 5.40: Sand/Shingle Mix Datum Measurement - Sensor 2

Actual depth for datum measurement with mixed sand/shingle was measured as 27cm for S1 and 26cm for S2. Despite a 3.84% difference in two actual depth values, differences in sensor measurements were much smaller at 0.78%, although S2's measurement was far more accurate. S1 measured an averaged 25.61cm and S2 25.81cm, thus achieving an accuracy of 94.85% and 99.28% respectively, with

an overall accuracy of 97.06%. Standard error values were calculated at 0.07 for S1 and 0.05 for S2.

5.4.3.2 Movement

Measurements of sediment movement at two minute intervals for each sensor are given in Figures 5.41 through 5.50, and then discussed.

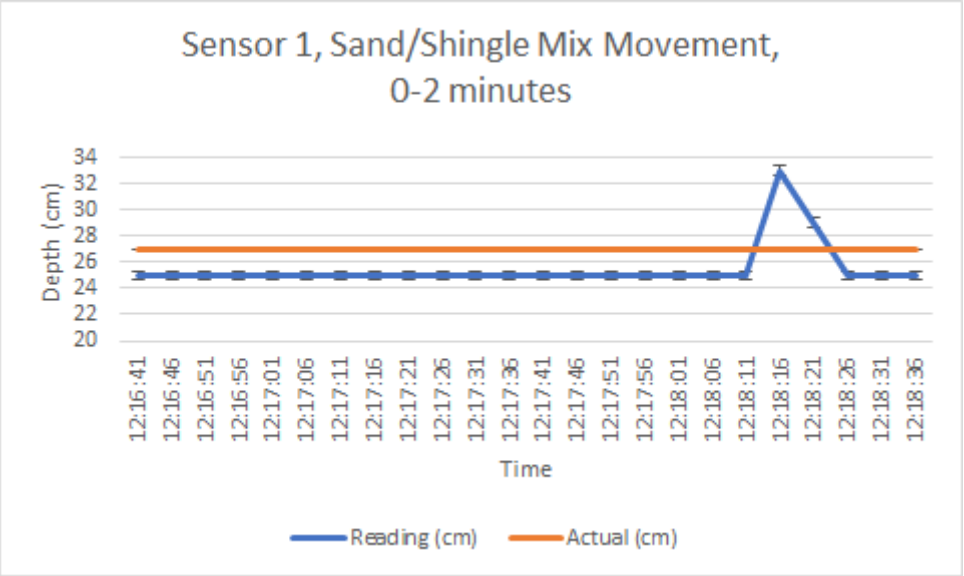

FIGURE 5.41: Sensor 1, Sand/Shingle Mix Movement, 0-2 minutes

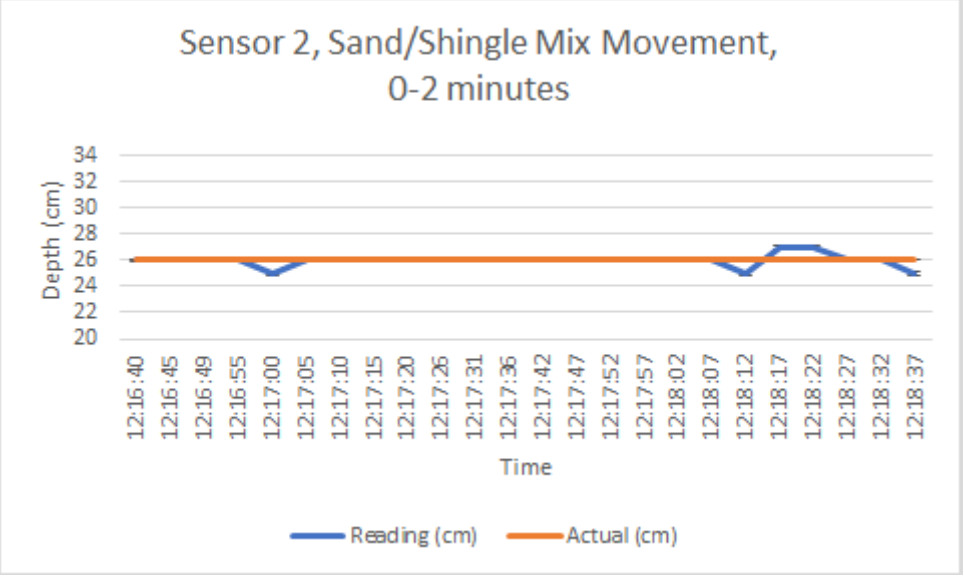

FIGURE 5.42: Sensor 2, Sand/Shingle Mix Movement, 0-2 minutes

Figures 5.41 and 5.42 show movement of mixed sediments for the 0-2 minute interval. The average reading of Sensor 1 was recorded as 25.5cm, 1.5cm less than the actual value of 27cm, or 94.44% accuracy. Sensor 2 achieved 99.83% accuracy, reporting an average reading of 25.95cm against a 26cm actual measurement. Standard error values were calculated as 0.36 for Sensor 1 and 0.09 for Sensor 2.

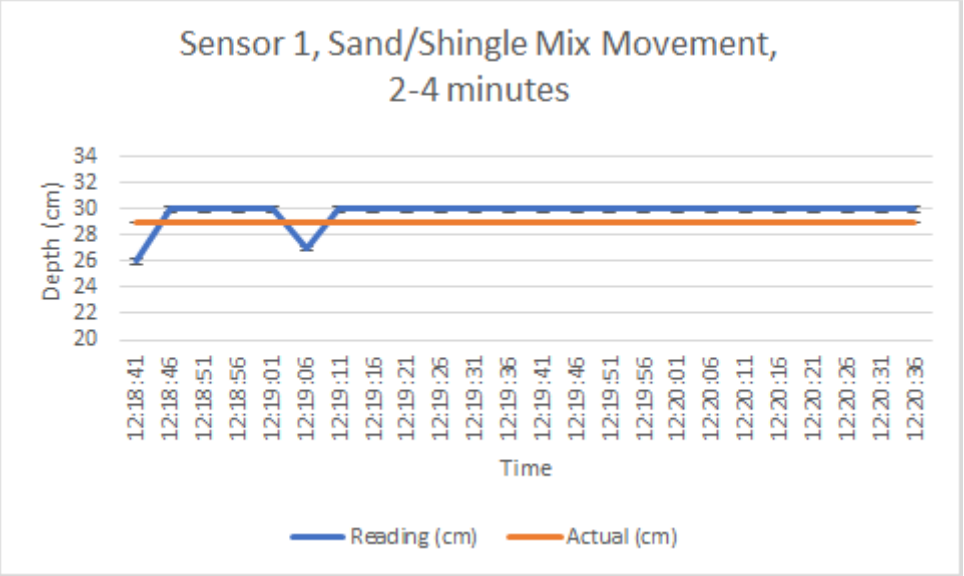

FIGURE 5.43: Sensor 1, Sand/Shingle Mix Movement, 2-4 minutes

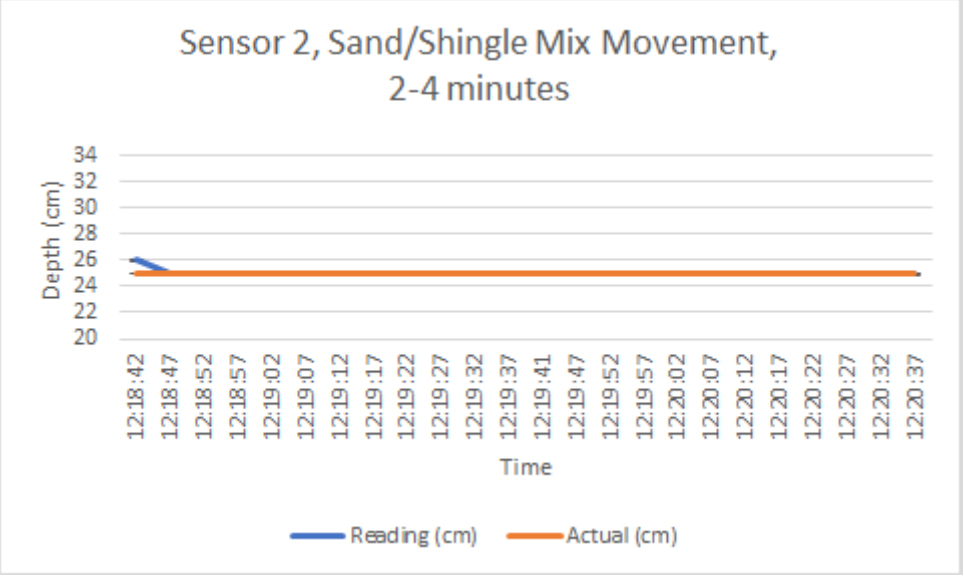

FIGURE 5.44: Sensor 2, Sand/Shingle Mix Movement, 2-4 minutes

Figures 5.43 and 5.44 show movement of mixed sediments for the 2-4 minute interval. Average readings of 29.70cm (actual value 29cm) and 25.04cm (actual value 25cm) were recorded by Sensor 1 and Sensor 2, respectively, accuracies of 97.55% and 99.83%. Sensor 2 achieved near perfect precision and the most consistent measurement when measuring mixed sediments, with a 0.04 standard error, compared to 0.20 for Sensor 1.

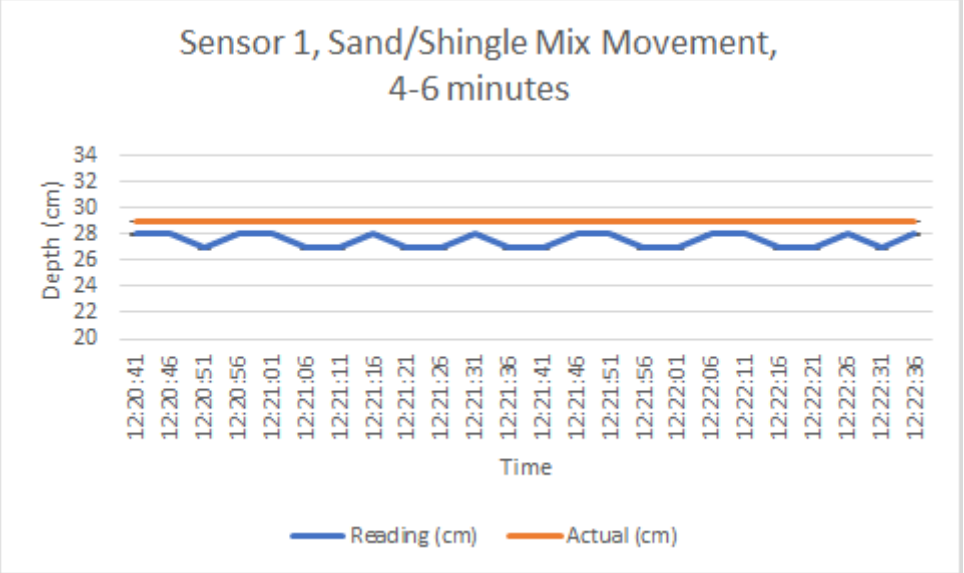

FIGURE 5.45: Sensor 1, Sand/Shingle Mix Movement, 4-6 minutes

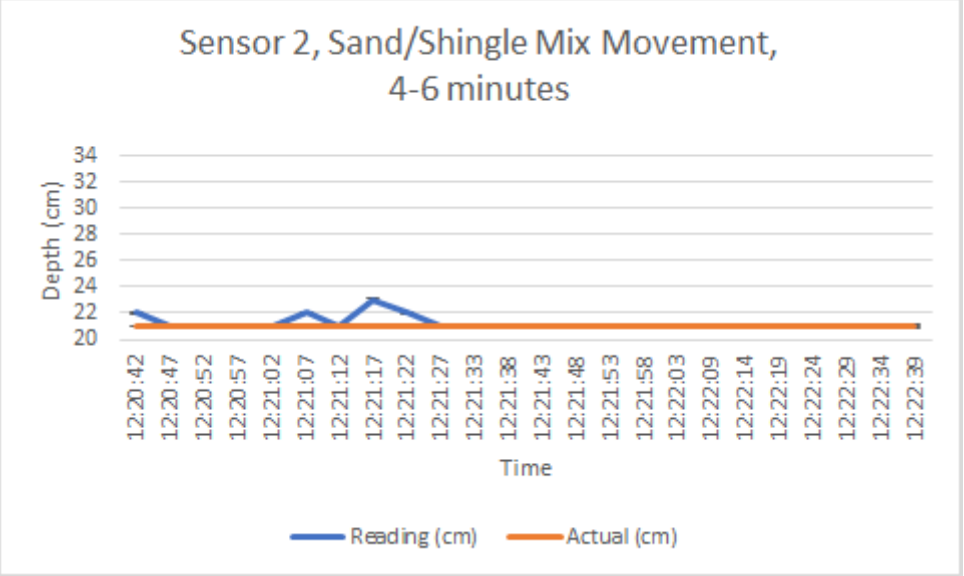

FIGURE 5.46: Sensor 2, Sand/Shingle Mix Movement, 4-6 minutes

Figures 5.45 and 5.46 show movement of mixed sediments for the 4-6 minute interval. Sensor 1 achieved an accuracy of 94.82% with a standard error of 0.10, reporting an average depth of 27.5cm against an actual value of 29cm. Sensor 2 achieved the same level of precision but a higher accuracy of 99%, giving an average reading of 21.20cm, slightly above the actual value of 21cm.

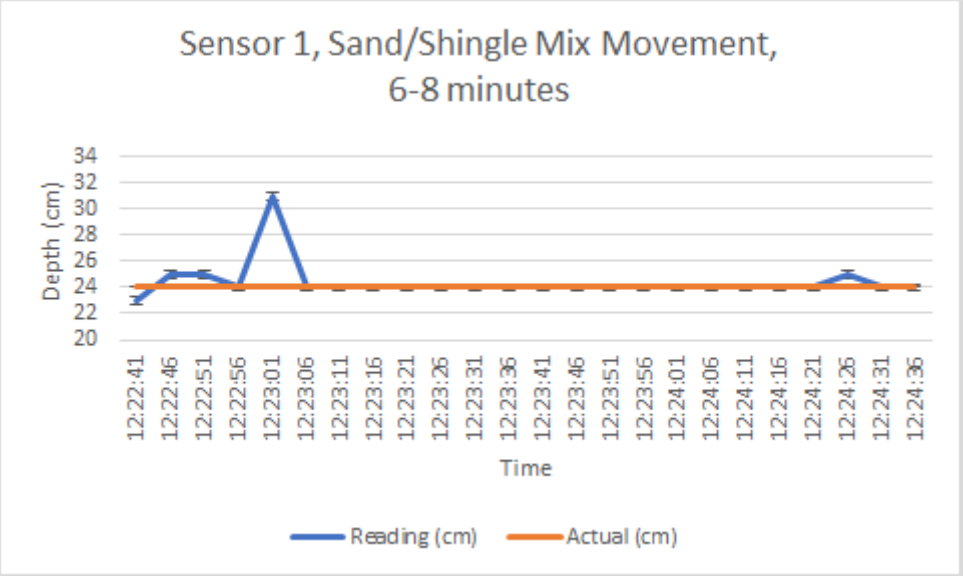

FIGURE 5.47: Sensor 1, Sand/Shingle Mix Movement, 6-8 minutes

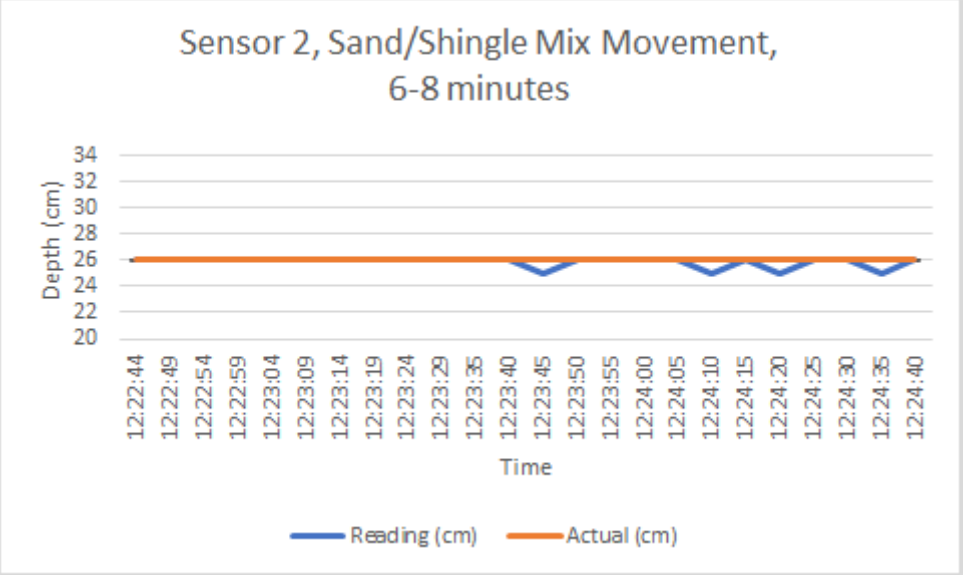

FIGURE 5.48: Sensor 2, Sand/Shingle Mix Movement, 6-8 minutes

Figures 5.47 and 5.48 show movement of mixed sediments for the 6-8 minute interval. Sensor 1 achieved 98.43% accuracy and a 0.29 standard error, measuring an average depth of 24.37cm, slightly above the actual value which was 24cm. Sensor 2 achieved 99.35% accuracy (an average measurement of 25.83cm against an actual value of 26cm) and 0.07 standard error, thus achieving better precision.

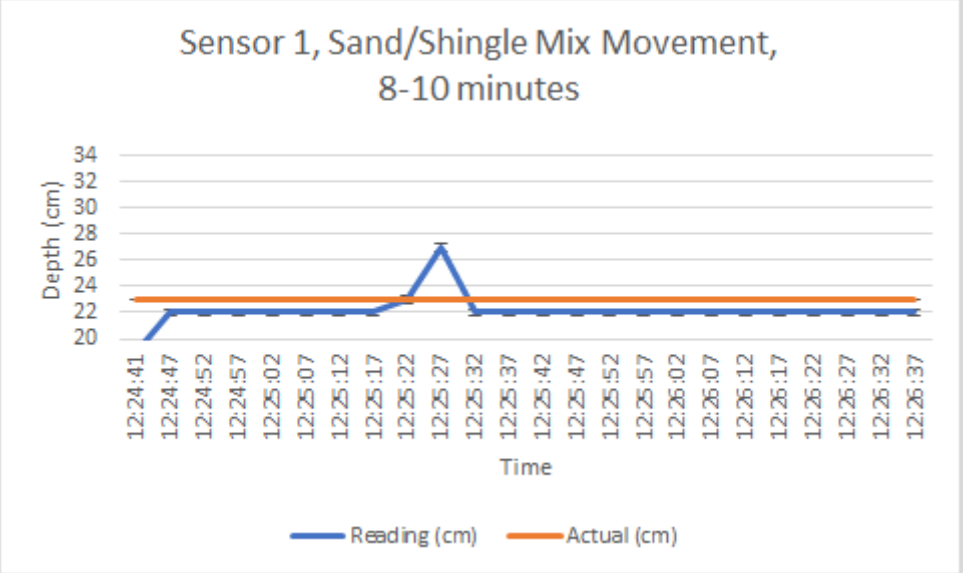

FIGURE 5.49: Sensor 1, Sand/Shingle Mix Movement, 8-10 minutes

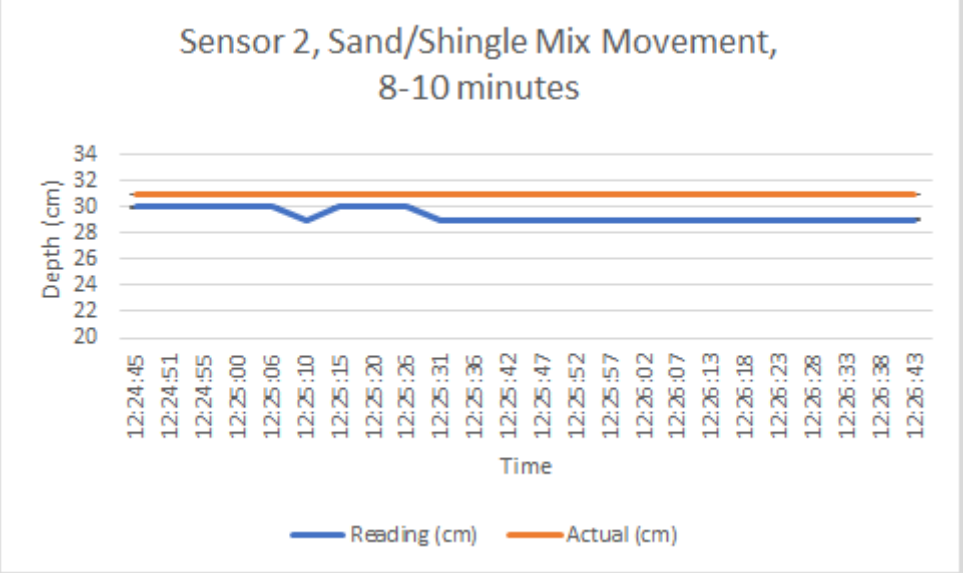

FIGURE 5.50: Sensor 2, Sand/Shingle Mix Movement, 8-10 minutes

Figures 5.49 and 5.50 show movement of mixed sediments for the 8-10 minute interval. The measurements recorded by Sensor 1 were 96.19% accurate with a standard error of 0.25. Average depth was recorded by the sensor as 22.12cm; the actual depth was 23. Sensor 2 recorded an average depth of 29.33cm compared to the actual value of 31cm, thus achieving an accuracy of 94.62% with the standard error being calculated as 0.09.

Tables 5.7 and 5.8 show the overall results for each of the above two minute intervals of measurement. These are displayed in graphical form in Figures 5.51 and 5.52 and then discussed.

S1	**Reading Avg.**	**Actual Avg.**	**Datum**	**Change**
0 min	25.5	27	27	1.5
2 min	29.7083333	29	27	-2.7083333
4 min	27.5	29	27	-0.5
6 min	24.375	24	27	2.625
8 min	22.125	23	27	4.875

TABLE 5.7: Sand/Shingle Mix Movement - Sensor 1

S2	**Reading Avg.**	**Actual Avg.**	**Datum**	**Change**
0 min	25.9583333	26	26	0.04166667
2 min	25.0416667	25	26	0.95833333
4 min	21.2083333	21	26	4.79166667
6 min	25.8333333	26	26	0.16666667
8 min	29.33333333	31	26	-3.33333333

TABLE 5.8: Sand/Shingle Mix Movement - Sensor 2

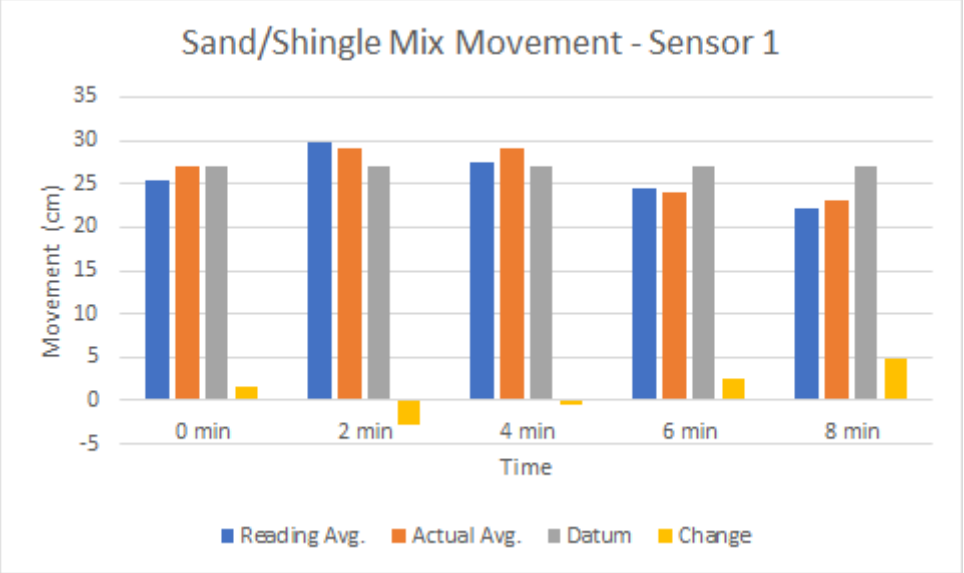

FIGURE 5.51: Sand/Shingle Mix Movement - Sensor 1

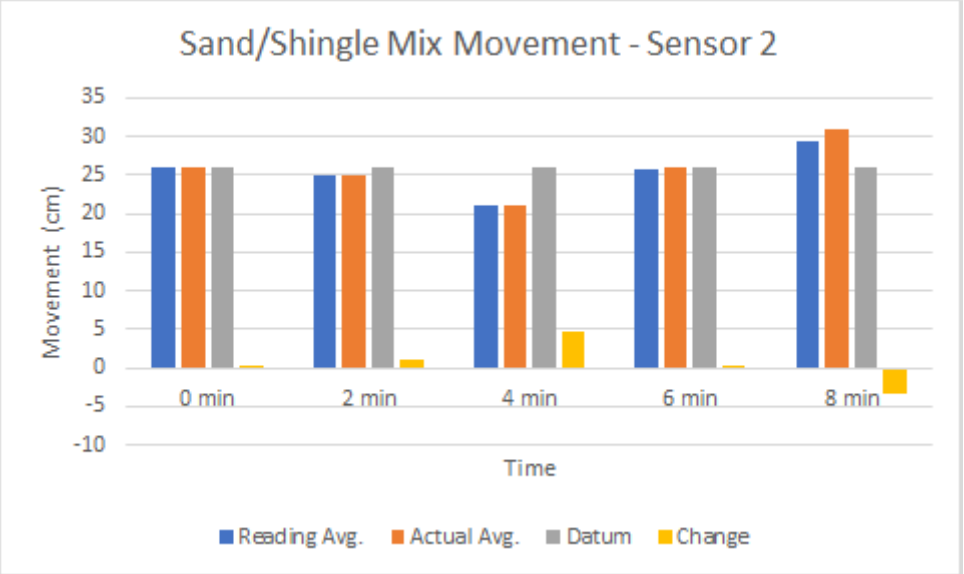

FIGURE 5.52: Sand/Shingle Mix Movement - Sensor 2

Sensor 1	**Accuracy (%)**	**Std. Deviation**	**Std. Error**
0 mins	94.44	1.793708813	0.366139278
2 mins	97.55	0.999093792	0.203939166
4 mins	94.82	0.510753918	0.104257207
6 mins	98.43	1.468880082	0.299833891
8 mins	96.19	1.226961606	0.250452489
Sensor 2	**Accuracy (%)**	**Std. Deviation**	**Std. Error**
0 mins	99.83	0.46430562	0.09477599
2 mins	99.83	0.20412415	0.04166667
4 mins	99	0.50897738	0.10389457
6 mins	99.35	0.38069349	0.07770873
8 mins	94.62	0.48154341	0.09829464

Table 5.9: Sand/Shingle Mix - Performance Statistics

S1 achieved an accuracy rate of 96.29%, compared to 98.53% for S2. These two values give an overall accuracy of 97.41% for sand/shingle mix, highest of the three sediments tested, and a 0.35% improvement on the datum measurement. Compared to the previous two sediment mixes, there was little improvement over the accuracy for sand at 0.16%, whilst the improvement over shingle was comparatively more significant at 1.66%. However, standard error was calculated as 0.16, showing the poorest precision of the three experiments that were conducted.

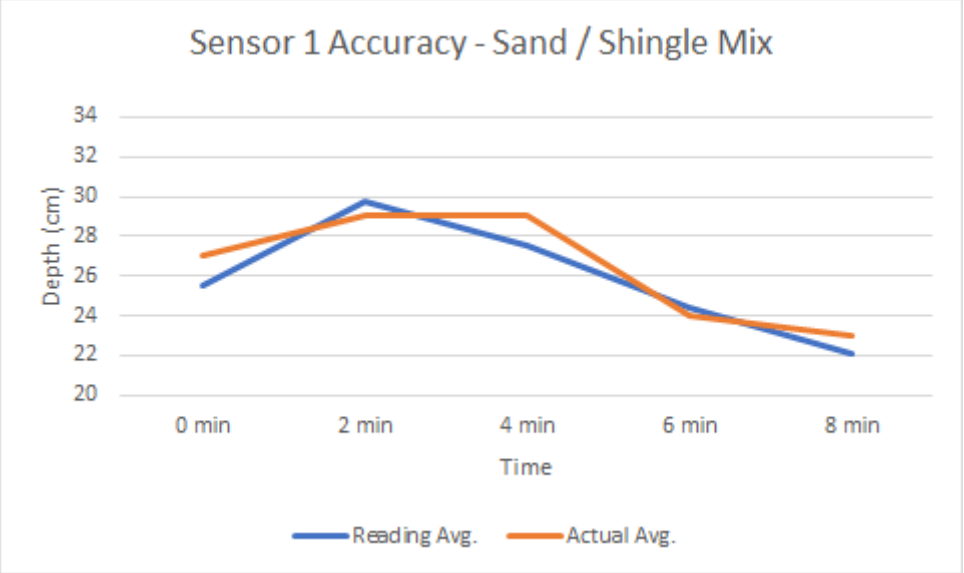

FIGURE 5.53: Sensor 1 Accuracy - Sand/Shingle Mix

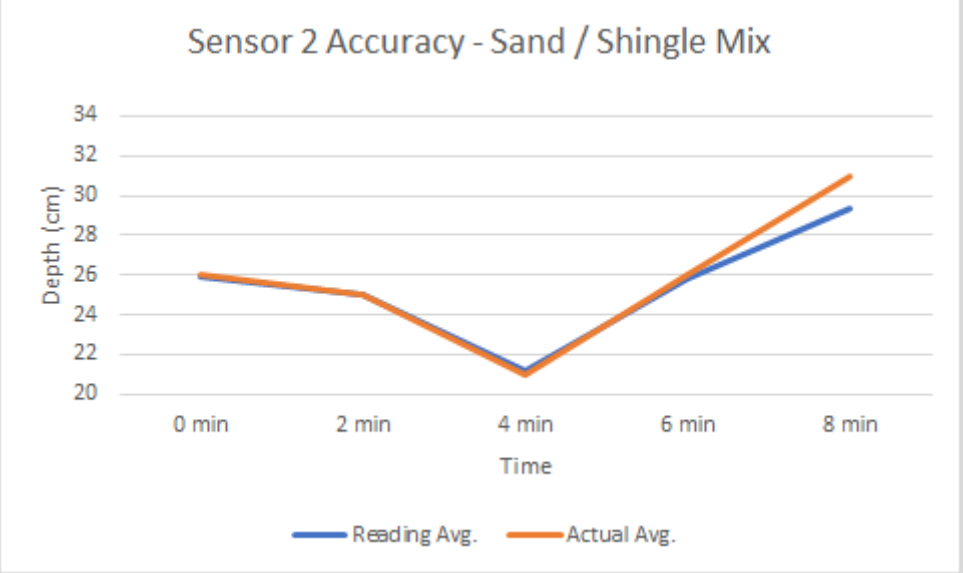

FIGURE 5.54: Sensor 2 Accuracy - Sand/Shingle Mix

5.5 Evaluation

This section provides an overall evaluation of results presented throughout the preceding sections of this chapter. After conducting all three experiments, it was clear that the developed prototype was able to measure sediment movement with high levels of accuracy; upwards of 95% in all cases. However, accuracy and precision varied between the different sediment mixes that were tested, and reasons will be considered throughout this section. Additionally, accuracy and precision values for datum and movement measurements are compared, with reasons for differences assessed.

5.5.1 Datum Accuracy and Precision

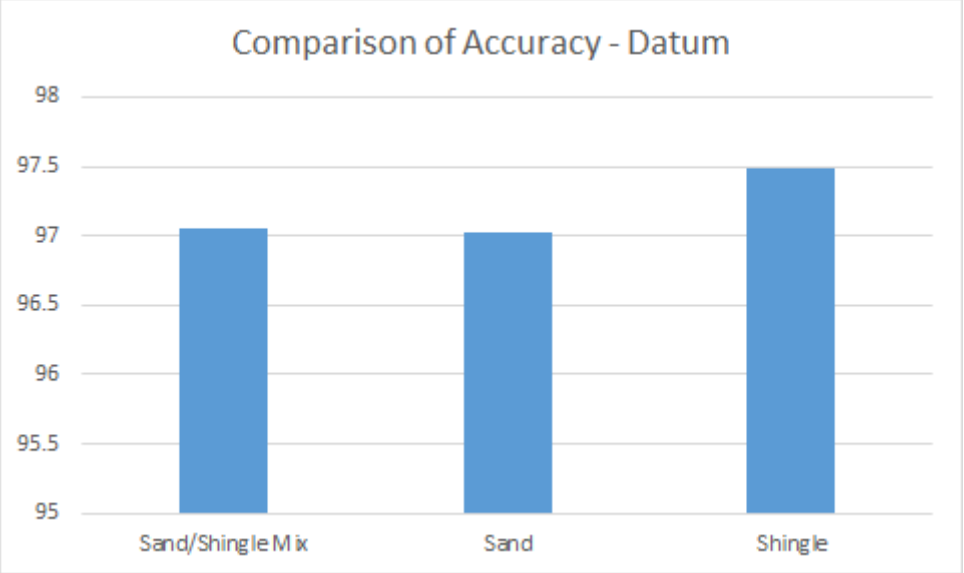

FIGURE 5.55: Datum Measurements - Comparison of Overall % Accuracy

Figure 5.55 shows overall accuracy of the datum measurement for each sediment mix. As can be observed, shingle achieved the most accurate overall measurement at 97.49%, although there was little difference between the three, with the shingle accuracy only being a marginal improvement over sand at 97.02% and the mix of sand and shingle at 97.06%.

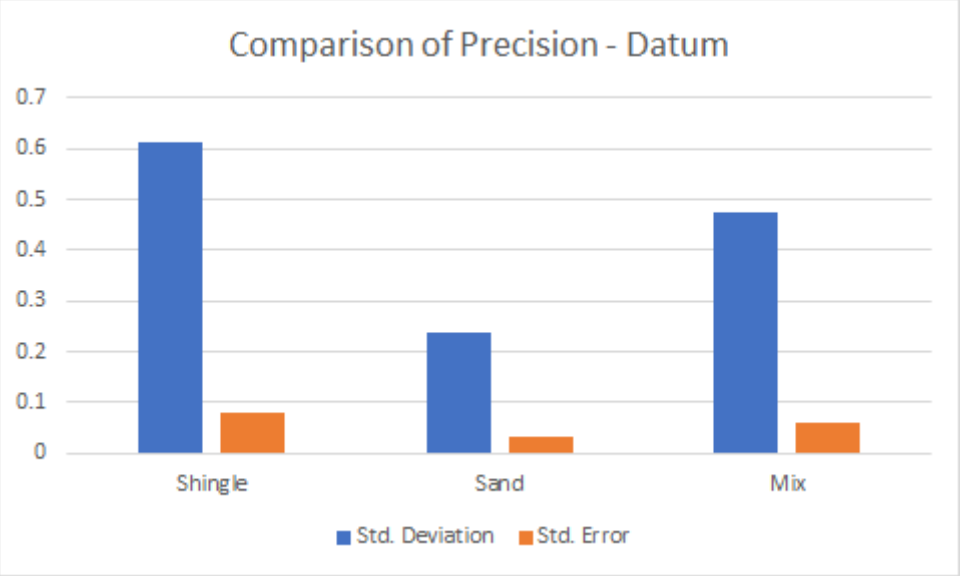

FIGURE 5.56: Datum Measurements - Comparison of Overall Precision

As shown in Figure 5.56, the most precise reading was obtained from sand datum measurements, with a standard deviation of 0.23, compared to 0.47 for sand/shingle mix and 0.61 for shingle, giving standard error values of 0.03, 0.06, and 0.07 respectively. This can be attributed to sand being a finer grained sediment which results in a reduced scattering of the sound wave. However, being a softer material compared to shingle, the reflection coefficient is lessened, leading to a poorer accuracy. This explains what can be observed by comparing Figures 5.55 and 5.56, which show that sand measurements achieved the worst accuracy but the best precision. The link between accuracy and precision is discussed later in this chapter in Section 5.5.3.

5.5.2 Movement Accuracy and Precision

After evaluating the accuracy and precision of datum measurements, a similar assessment was made for measurements of sediment movement.

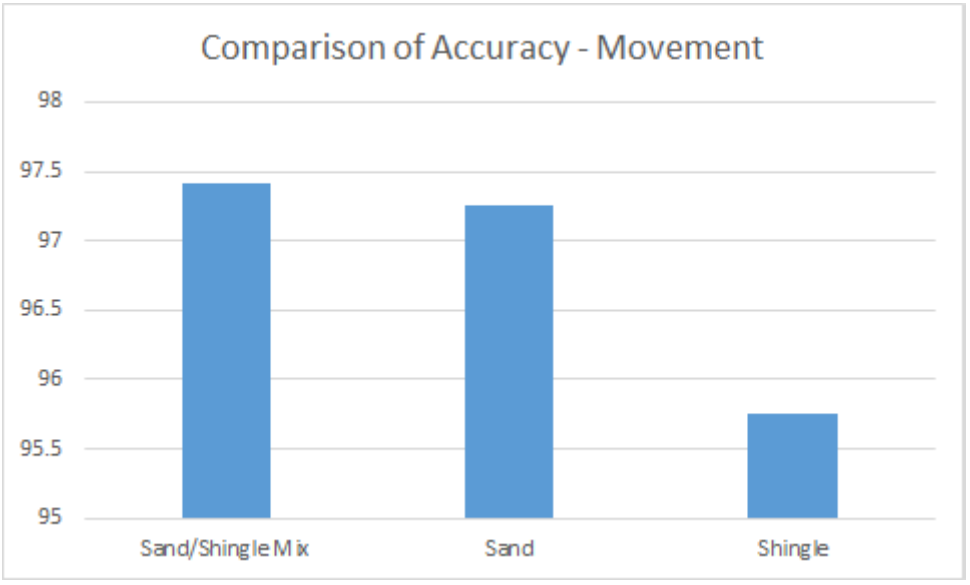

FIGURE 5.57: Sediment Movement - Comparison of Overall % Accuracy

Levels of accuracy for measuring movement of all three sediment mixes are shown in Figure 5.57, with sand/shingle mix showing the highest accuracy at 97.41%, followed by sand at 97.25% and shingle at 95.75%. The two former sediment mixes show little variance from the levels of accuracy observed for the datum (an improvement of 0.35% and 0.23% respectively). Shingle, on the other hand, differed from its datum accuracy by 1.74%, which, although a small variance, is significant compared to the other two. Reasons for this are discussed in Section 5.5.3.

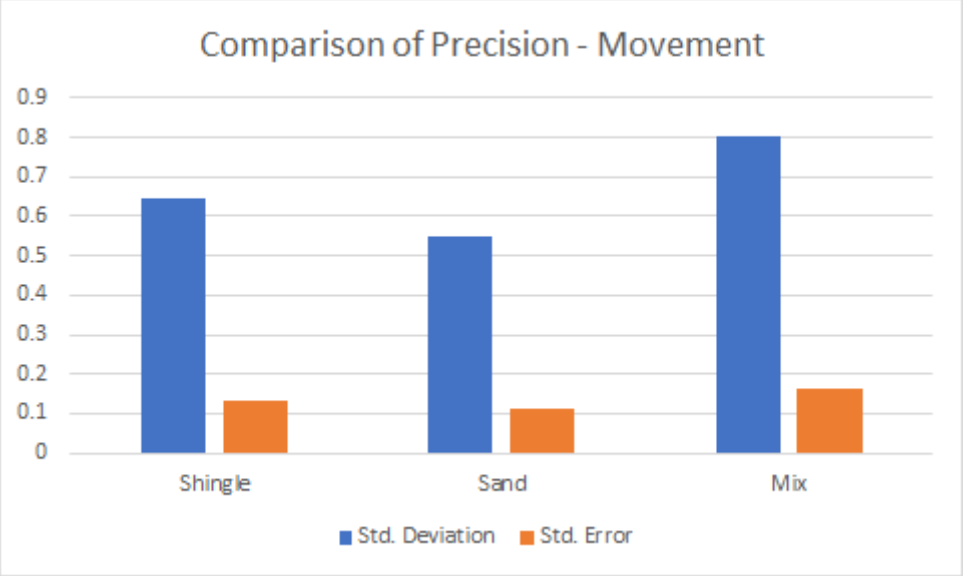

FIGURE 5.58: Sediment Movement - Comparison of Overall Precision

The levels of precision obtained for measuring sediment movement are shown in Figure 5.58. In all cases precision for movement was lower than precision for datum measurements; this was expected given the increased variability in distance (and hence a more varied signal strength, in addition to the effects of attenuation) between the sensors and sediments.

5.5.3 Overall Accuracy and Precision

In some cases there was a clear correlation between high accuracy and high precision; most notably the fact that the most accurate value (100%) correlated with the lowest standard error (0) and the least accurate (87%) correlated with the highest (0.44). However, they were not mutually inclusive; indeed, a standard error of 0 was achieved on four other occasions, none of which also achieved 100% accuracy. Furthermore, when the overall accuracy and precision were compared for each sediment mix, the opposite was observed, with the highest accuracy correlating with the lowest precision.

This is primarily attributable to attenuation, which as discussed in Section 3.1.2 is a combined effect consisting of scattering and absorption of a sound wave. In general, softer materials absorb sound better than harder, impenetrable materials which reflect it better. On this basis, purely considering absorption of the sound wave, it would be expected that softer sediments such as sand would not show as high an accuracy as a more dense sediment like shingle with better reflective properties. However, the effect of scattering is less likely to affect measurement of sand since it is a smooth, fine grained material. Shingle on the other hand, is more coarse, and is thus more likely to cause scattering of the sound wave. Consequently, shingle is expected to show a lower level of precision compared to sand, an expectation the results in Section 5.5.2 were in agreement with.

Expectations that shingle would show better accuracy than sand were confirmed in the case of datum measurements, but not movement measurements, where it showed the worst accuracy. In addition to the affects of scattering, since the sediment was moving at regular intervals and not remaining stationary, it is likely that the increased variability in distance between the sensors and sediment will negatively impact precision, since sound waves diminish with distance. The highest accuracy and lowest precision in terms of movement measurements was attained by a mix of sand and shingle, due to the combined effect of a sediment that has properties allowing good absorption and one that has properties allowing good reflection.

5.6 Chapter Summary

The experiment documented in this chapter aimed to discover the basic validity of the method originally given in Equation 4.1, and this chapter has presented the results of a lab-based experiment undertaken for this purpose.

The prototype developed in Chapter 4 was used to measure sediment movement in a glass tank using ultrasonic distance sensors. Three experiments were conducted, each with a different mix of sediment. Results were promising, achieving an accuracy of 95% or above in all cases. Overall, this chapter represents successful implementation of the prototype system, as well as in-air validation of the novel method of monitoring sediment transport that is the basis of this thesis.

Chapter 6

Conclusions and Future Work

6.1 Introduction

In previous chapters of this thesis a novel method of monitoring sediment transport using ultrasonic sensors and wireless networking technology was designed, built and evaluated in a lab environment. This chapter will summarise the thesis, with a particular focus on the contributions of the research carried out. Additionally, some challenges that were faced are discussed and finally, recommendations are outlined for potential future work.

6.2 Conclusions

The work presented in this thesis was derived to help coastal engineers better assess the coastal environment and associated processes, and consequently contribute to more effective shoreline management strategies being developed and implemented. Coastlines around the world are at increasing risk of erosion, largely as a result of sea level rise caused by a rise in global temperatures. At the same time, they are more densely populated than the hinterlands, and said population levels are

expected to increase in the future. Because of this, it is very important to be able to monitor transport of sediments in the coastal zone in order to assess shoreline change and ascertain any potential risks that may be faced as a result. Current methods of monitoring, whilst achieving high-accuracy and high-precision, are generally time consuming and most significantly are limited to monitoring the visible beach and cannot monitor sediment transport processes that occur underwater.

These limitations drive the need for the work that was undertaken in this thesis, which has introduced a novel method of monitoring sediment transport, utilising a combination of ultrasonic distance measurement and wireless sensor network technology. This method measures movement of sediments by using distance measurements to determine whether accretion or erosion is occurring, by comparing readings against a previously established datum measurement. In-air validation of this method has been achieved in this thesis, with recommendations made for future development presented in Section 6.4.

In conclusion, a novel method has been presented and its capability of monitoring the movement of sediments has been observed, with performance of the system verified by comparing the results with actual measured values. It was shown that the developed prototype was able to monitor sediment movement with high levels of both accuracy (97.25% for sand, 95.75% for shingle, and 97.41% for mixed sediments) and precision (average standard error was calculated below 0.2 for all experiments) were achieved in all cases. These results confirm the ability of this approach to accurately monitor sediment movements. Since depth measurement using sound pulses is well established, this method can easily be further developed for real-world deployments in the coastal environment, with some key considerations for future development are given later in this chapter.

6.3 Challenges

- At the outset of this research is was intended that all the stages shown in Table 6.1 would be completed as part of this PhD. As the candidature progressed it became clear that this was beyond the scope of a single PhD and that it would need to be divided into smaller more workable stages. This was the point at which it was decided to focus on just one stage of the overall research project. It was also an important lesson in terms of avoiding a PhD becoming too broad by trying to achieve too much, and ensuring that the work is focused so that the contributions are clear.

- As there was limited previous research that has been conducted for this specific application, there was little previous work upon which this research could be built. Although in some sense this allowed more flexibility in terms of deciding the approaches to take, having a more substantial body of previous work to refer to would have allowed greater confidence when making these decisions.

- This thesis combined the two disciplines of computer science and coastal engineering, the latter of which was a new field to the researcher whose background was in computer science. This resulted in the challenge of balancing a discipline which was very familiar, and another which was relatively unknown to the researcher. However, despite the challenges, it also created interest in how these two different disciplines could be brought together and demonstrated the importance, and appeal, of interdisciplinary research work. Ultimately, as long as there is an interest in one of the disciplines, then enthusiasm for both is possible, since the interest in seeing how that discipline can be applied to others is always there.

6.4 Recommendations for future work

There remain many opportunities for this research to be extended; indeed, as first mentioned in Chapter 1, the work in this thesis represents the first stage of a project that is divided into several stages, as shown in Table 6.1.

Stage 1	**Stage 2**	**Stage 3**	**Stage 4**	**Stage 5**	**Stage 6**
Initial prototype and in-air testing	Prototype for water testing	Wave tank tests	Sea trials	Final deployment	Development of predictive computational model

TABLE 6.1: Research Stages

This thesis has successfully achieved the first stage of this research project. Specific recommendations for future work are outlined below; with their contribution to each stage specified.

6.4.1 Mobile deployments (Stages 3,4,5)

The system presented in this thesis is in the form of a static WSN, which is not a realistic scenario for most real-world applications, where significant movement of sensor nodes is likely. This highlights requirements for future research into a system capable of mobility, where the sensor nodes are able to move but still be able to communicate so that data can be communicated back to the sink node. This would greatly improve flexibility of the system in terms of deployment and operation. However, it would also lead to increased cost as it would require the design of complex networking protocols in order to maintain communication.

6.4.2 Energy efficiency and harvesting (Stages 2-5)

Energy efficiency is one of the most important issues in the design, development and operation of WSNs, in particular when they are deployed in locations where

replenishing the energy is impractical. In terms of future deployments of this system on the ocean, this will be a particularly important consideration, especially since propagation of sound pulses through water requires much more energy than through air. However, it must also be noted that the final system would be expected to function continually for months at a time with minimal or no human intervention. Therefore, in addition to utilising the available energy as efficiently as possible, it is also essential to harvest energy (from sources such as wind, solar and, since this system would be sea-based, osmotic), to ensure that the WSN is able to remain in operation and gather data for as long as possible. Accordingly, approaches to energy harvesting and efficient use of that energy can be a major, and essential, area of future research.

6.4.3 Field trials (Stages 3-5)

In this research, the experiments were carried out in a lab environment, where sediment transport was measured in a water tank. Deploying the system on the ocean would introduce many more variables that would need to be considered, the most obvious of which include weather, water depth, location, and type of water. However, it is recommended that laboratory testing on a larger scale, in a purpose-built wave tank, is carried out prior to field testing, in order to allow more realistic testing but in a controlled environment.

6.4.4 Wave Motion (Stages 3-4)

Measuring underwater sediment transport by observing difference in water depth measurements is a simple principle if the sensors are deployed on water with a smooth surface and there is minimal movement of the sensors. In practice, this is more complex, since on the ocean sensors will continually be rising and falling with

the tides. Therefore, a key area of future work is to devise a method to account for the movement of sensor nodes due to wave motion.

6.4.5 Neural networks (Stage 6)

Methods of predicting coastal processes were discussed in Chapter 2, with empirical predictions being the most common, largely due to them being a cost-effective option. However, they have often been found to be inaccurate in comparison to field measurements. Furthermore, if the formulae are devised based on actual field measurement data, it is difficult to achieve generic application of them outside a specific local site.

Neural networks differ from conventional algorithms in that they, much like humans do, learn by example, whereas a conventional algorithm solves a problem by following a set of instructions that were programmed into it. Thus, conventional algorithms can only solve problems for which a solution is already known. Neural networks, on the other hand, cannot be programmed to perform specific tasks but instead are "trained" using datasets that characterize the problem at hand, which, when done correctly enable them to predict future patterns in the data. This makes them particularly useful for solving problems that do not have a clear algorithmic solution.

A model that can accurately predict the movement of sediments has the potential to be of use in a number of areas across several disciplines. In addition to the problems it can help address in predicting coastal evolution, it could also be useful for researchers in the fields of archaeology and landscape history for the purpose of predicting future changes based on historical data.

This area of future study need not necessarily be separate from the area of applying WSN technologies to coastal monitoring; indeed, the two could potentially compliment each other. A neural network model that is regularly trained using data collected by a WSN could then be used to predict future sand movement based on previously collected data to aid in predicting events such as climate change, pollution and coastal erosion.

References

[1] B.H. Ketchum. *The Water's Edge: Critical Problems of the Coastal Zone*. MIT Press, 1972. ISBN 9780262610162.

[2] B. Neumann, A.T. Vafeidis, J. Zimmermann, and R.J. Nicholls. Future Coastal Population Growth and Exposure to Sea-Level Rise and Coastal Flooding - A Global Assessment. *PLOS ONE*, 2015. ISSN 1932-6203. doi: 10.1371/journal.pone.0118571.

[3] J.B. Shukla, Maitri Verma, and A.K. Misra. Effect of global warming on sea level rise: A modeling study. *Ecological Complexity*, 32:99–110, dec 2017. ISSN 1476945X. doi: 10.1016/j.ecocom.2017.10.007.

[4] J.A. Church, P.U. Clark, A Cazenave, J.M. Gregory, S Jevrejeva, A Levermann, M.A. Merrifield, G.A. Milne, R.S. Nerem, P.D. Nunn, A.J. Payne, W.T. Pfeffer, D Stammer, and A.S. Unnikrishnan. Sea Level Change. In *Climate Change 2013 - The Physical Science Basis*, pages 1137–1216. Cambridge University Press. doi: 10.1017/CBO9781107415324.026.

[5] Robert M. DeConto and David Pollard. Contribution of Antarctica to past and future sea-level rise. *Nature*, 531(7596):591–597, mar 2016. ISSN 0028-0836. doi: 10.1038/nature17145.

[6] Mohammad Hanif Hamden and Ami Hassan Md Din. A review of advancement of hydrographic surveying towards ellipsoidal referenced surveying technique. *IOP Conference Series: Earth and Environmental Science*, 169, jul 2018. ISSN 1755-1315. doi: 10.1088/1755-1315/169/1/012019.

[7] CRC Press. *Wireless Sensor Networks: Current Status and Future Trends*. CRC Press, 2016. ISBN 9781466506084.

[8] A.T. Williams, Nelson Rangel-Buitrago, Enzo Pranzini, and Giorgio Anfuso. The management of coastal erosion. *Ocean & Coastal Management*, 156:4–20, apr 2018. ISSN 09645691. doi: 10.1016/j.ocecoaman.2017.03.022.

[9] J.R Houston. The economic value of beaches - a 2013 update. *Shore & Beach*, 81(1):3–10, 2013.

[10] Bank of Greece. Summary of the annual report 2005. 2005.

[11] Allan T. Williams and Ricardo A. Alvarez. *Vulnerability Assessment as a Tool for Hazard Mitigation*, pages 303–313. Springer Netherlands, Dordrecht, 2003. ISBN 978-94-010-0205-9. doi: 10.1007/978-94-010-0205-9_32.

[12] A. Sydow. *Environmental Systems - Volume I*. 2010. ISBN 9781848262102.

[13] D.A. DellaSala. Oceans and Global Change: One Blue Planet. In *Encyclopedia of the Anthropocene*, pages 17–19. Elsevier, 2018. doi: 10.1016/B978-0-12-809665-9.05878-X.

[14] R. Davidson-Arnott. *Introduction to Coastal Processes and Geomorphology*. Cambridge University Press, 1st edition, 2010.

[15] R. J. Hallermeier. A profile zonation for seasonal sand beaches from wave climate. *Coastal Engineering*, 4(C):253–277, jan 1980. ISSN 03783839. doi: 10.1016/0378-3839(80)90022-8.

[16] Diane P Horn and Travis Mason. Swash zone sediment transport modes. *Marine Geology*, 120(3-4):309–325, sep 1994. ISSN 00253227. doi: 10.1016/0025-3227(94)90064-7.

[17] Douglas Pender. *A Statistical-Process Based Approach for Modelling Beach Profile Variability*. PhD thesis, University of Glasgow, 2011.

[18] Ian L. Turner and Gerhard Masselink. Swash infiltration-exfiltration and sediment transport. *Journal of Geophysical Research: Oceans*, 103(C13): 30813–30824, dec 1998. ISSN 01480227. doi: 10.1029/98JC02606.

[19] David Pritchard and Andrew J. Hogg. On the transport of suspended sediment by a swash event on a plane beach. *Coastal Engineering*, 52(1):1–23, jan 2005. ISSN 03783839. doi: 10.1016/j.coastaleng.2004.08.002.

[20] José M. Alsina, Iván Cáceres, Maurizio Brocchini, and Tom E. Baldock. An experimental study on sediment transport and bed evolution under different swash zone morphological conditions. *Coastal Engineering*, 68:31–43, oct 2012. ISSN 03783839. doi: 10.1016/j.coastaleng.2012.04.008.

[21] Andrea Ruju, Daniel Conley, Gerd Masselink, and Jack Puleo. Sediment transport dynamics in the swash zone under large-scale laboratory conditions. *Continental Shelf Research*, 120:1–13, jun 2016. ISSN 02784343. doi: 10.1016/j.csr.2016.03.015.

[22] R. Bakhtyar, D. A. Barry, L. Li, D. S. Jeng, and A. Yeganeh-Bakhtiary. Modeling sediment transport in the swash zone: A review. *Ocean Engineering*, 36 (9-10):767–783, 2009. ISSN 00298018. doi: 10.1016/j.oceaneng.2009.03.003.

[23] J.D. Simm. *Beach Management Manual*. CIRIA, 1996.

[24] K Kantamaneni. *Assessing coastal vulnerability: development of a combined physical and economic index*. PhD thesis, University of Wales Trinity Saint David, 2017.

[25] Michael E. Mann, Stefan Rahmstorf, Byron A. Steinman, Martin Tingley, and Sonya K. Miller. The Likelihood of Recent Record Warmth. *Scientific Reports*, 6(1):19831, apr 2016. ISSN 2045-2322. doi: 10.1038/srep19831.

[26] Living with coastal erosion in Europe: Sediment and Space for Sustainability. 2004.

[27] Stephen P. Leatherman. Chapter 8 social and economic costs of sea level rise. In Bruce C. Douglas, Michael S. Kearney, and Stephen P. Leatherman, editors, *Sea Level Rise*, volume 75 of *International Geophysics*, pages 181 – 223. Academic Press, 2001. doi: https://doi.org/10.1016/S0074-6142(01)80011-5.

[28] D. Reeve, A. Chadwick, and C. Fleming. *Coastal Engineering: Processes, Theory and Design Practice*. CRC Press, 2004. ISBN 9780203647356.

[29] J. Fredsøe and R. Deigaard. *Mechanics of Coastal Sediment Transport*. Advanced series on ocean engineering. World Scientific, 1992. ISBN 9789810208417.

[30] R. Soulsby. *Dynamics of Marine Sands: A Manual for Practical Applications*. Telford, 1997. ISBN 9780727725844.

[31] D. Reeve, A. Chadwick, and C. Fleming. *Coastal Engineering: Processes, Theory and Design Practice*. CRC Press, 2015. ISBN 9781498760102.

[32] C.T. Yang. *Sediment Transport: Theory and Practice*. Krieger Publishing Company, 1996. ISBN 9781575242262.

[33] Subhasish Dey. Sediment threshold. *Applied Mathematical Modelling*, 23 (5):399 – 417, 1999. ISSN 0307-904X. doi: http://dx.doi.org/10.1016/S0307-904X(98)10081-1.

[34] A. Shields. Application of Similarity Principles and Turbulence Research to Bed-Load Movement. *Mitt. Preuss. Versuchsanst. Wasserbau Schiffbau*, 26 (5-24):47, 1936.

[35] R.L Soulsby. Threshold of Sediment Motion in Coastal Environments. In *13th Australasian Coastal and Ocean Engineering Conference and the 6th Australasian Port and Harbour Conference*, Christchurch, New Zealand, 1997.

[36] E Meyer-Peter and R Müller. Formulas for Bed-Load transport. In *Report of 2nd Meeting, International Association for Hydraulic and Structural Research*, Stockholm, 1948.

[37] P Nielsen. *Coastal Bottom Boundary Layers and Sediment Transport*. World Scientific Publishing, Singapore, 1992. ISBN 9810204736.

[38] John Lawrence. *Cross-shore morphodynamics of coarse grained beaches and beach /structure interaction: Numerical modelling and large scale measurements*. PhD thesis, University of Plymouth, 2005.

[39] Aronne Armanini and Giampaolo Di Silvio. A one-dimensional model for the transport of a sediment mixture in non-equilibrium conditions. *Journal of Hydraulic Research*, 26(3):275–292, may 1988. ISSN 0022-1686. doi: 10.1080/00221688809499212.

[40] G PENDER and Q LI. NUMERICAL PREDICTION OF GRADED SEDIMENT TRANSPORT. *Proceedings of the Institution of Civil Engineers - Water Maritime and Energy*, 118(4):237–245, dec 1996. ISSN 1753-7819. doi: 10.1680/iwtme.1996.28988.

[41] Robert G. Dean and Robert A. Dalrymple. *Coastal Processes with Engineering Applications*. Cambridge University Press, Cambridge, 2001. ISBN 9780511754500. doi: 10.1017/CBO9780511754500.

[42] XiaoWei Yu. *Sediment Transport Processes and Coastal Management of Mixed Sand and Gravel Beaches*. PhD thesis, The University of Brighton, 2009.

[43] M.R. Phillips. *An Assessment of Processes and Strategies for Management of the Penarth Coast*. Phd thesis, Bath Spa University, 2005.

[44] P.S. Balson and M.B. Collins. *Coastal and Shelf Sediment Transport*. Geological Society special publication Coastal and shelf sediment transport. Geological Society, 2007. ISBN 9781862392175.

[45] Thomas E White. Status of measurement techniques for coastal sediment transport. *Coastal Engineering*, 35(1-2):17–45, oct 1998. ISSN 03783839. doi: 10.1016/S0378-3839(98)00033-7.

[46] J.L. Irish and T.E. White. Coastal engineering applications of high-resolution lidar bathymetry. *Coastal Engineering*, 35(1-2):47–71, oct 1998. ISSN 03783839. doi: 10.1016/S0378-3839(98)00022-2.

[47] Robert A. Morton, Mark P. Leach, Jeffrey G. Paine, and Michael A. Cardoza. Monitoring beach changes using gps surveying techniques. *Journal of Coastal Research*, 9(3):702–720, 1993. ISSN 07490208, 15515036.

[48] Luciana S. Esteves, Jon J. Williams, and Maria A. Lisniowski. Measuring and modelling longshore sediment transport. *Estuarine, Coastal and Shelf Science*, 83(1):47–59, jun 2009. ISSN 02727714. doi: 10.1016/j.ecss.2009.03.020.

[49] L Trim. *Physical modelling of shingle beaches*. PhD thesis, University of Brighton, 2003.

[50] Atilla Bayram, Magnus Larson, Herman C. Miller, and Nicholas C. Kraus. Cross-shore distribution of longshore sediment transport: comparison between predictive formulas and field measurements. *Coastal Engineering*, 44 (2):79–99, dec 2001. ISSN 03783839. doi: 10.1016/S0378-3839(01)00023-0.

[51] C.M. Dohmen-Janssen. *Grain size influence on sediment transport in oscillatory sheet flow; phase lags and mobile-bed effects*. PhD thesis, Delft University of Technology, 1999.

[52] P. Sistermans and O. Nieuwenhuis. South Downs, Sussex County Eurosion Case Study. *DHV Group, Netherlands*, 2001.

[53] Orrin Pilkey and Andrew Cooper. Longshore transport volumes: a critical view. *Journal of Coastal Research*, SI 36:572–580, 2002.

[54] E. Robert Thieler, Jr. Orrin H. Pilkey, Robert S. Young, David M. Bush, and Fei Chai. The use of mathematical models to predict beach behavior for u.s. coastal engineering: A critical review. *Journal of Coastal Research*, 16(1):48–70, 2000.

[55] Tony Thomas. *Coastal processes and morphological change along the Tenby, Pembrokeshire coastline*. Phd thesis, Swansea Metropolitan University, 2012.

[56] Simon Haslett. *Coastal Systems*. Routledge, 2nd edition, 2009. ISBN 0415440602.

[57] Robert J. Hallermeier. Uses for a Calculated Limit Depth to Beach Erosion. In *Coastal Engineering 1978*, pages 1493–1512, New York, NY, aug 1978. American Society of Civil Engineers. ISBN 9780872621909. doi: 10.1061/9780872621909.090.

[58] N.C Kraus, M Larson, and R.A Wise. Depth of Closure in Beach-fill Design. *Coastal Engineering Techinical Note*, CETN II-40, 1998.

[59] Claire Hinton and Robert J. Nicholls. Spatial and Temporal Behaviour of Depth of Closure along the Holland Coast. In *Coastal Engineering 1998*, pages 2913–2925, Reston, VA, apr 1999. American Society of Civil Engineers. ISBN 978-0-7844-0411-9. doi: 10.1061/9780784404119.221.

[60] Robert Sorensen. *Basic Coastal Engineering*. Springer, 2006. ISBN 0387233326.

[61] Stephen P. Leatherman. Modelling shore response to sea-level rise on sedimentary coasts. *Progress in Physical Geography*, 14(4):447–464, 1990. doi: 10.1177/030913339001400402.

[62] Stephen P. Leatherman. Shoreline change mapping and management along the u.s. east coast. *Journal of Coastal Research*, pages 5–13, 2003. ISSN 07490208, 15515036.

[63] M. R. Phillips and A. T. Williams. Depth of Closure and Shoreline Indicators: Empirical Formulae for Beach Management. *Journal of Coastal Research*, 232:487–500, mar 2007. ISSN 0749-0208. doi: 10.2112/05-0593.1.

[64] P Wang and R.A Davis. Depth of Closure and the Equilibrium Beach Profile - A Case Study from Sand key, West-Central Florida. *Shore & Beach*, 67(2): 33–42, 2007.

[65] S. W. Marsh, R. J. Nicholls, A. Kroon, and P. Hoekstra. Assessment of Depth of Closure on a Nourished Beach: Terschelling, The Netherlands. In *Coastal Engineering 1998*, pages 3110–3123, Reston, VA, apr 1999. American Society of Civil Engineers. ISBN 978-0-7844-0411-9. doi: 10.1061/9780784404119.236.

[66] H Karl and A Willig. *Protocols and Architectures for Wireless Sensor Networks*. John Wiley and Sons, 2005. ISBN 978-0-470-09510-2.

[67] S Khan, A Pathan, and N Alrajeh. *Wireless Sensor Networks: Current Status and Future Trends*. CRC Press, 2012.

[68] P. Corke, T. Wark, R. Jurdak, W. Hu, P. Valencia, and D. Moore. Environmental Wireless Sensor Networks. *Proceedings of the IEEE*, 98(11): 1903–1917, 2010. ISSN 00189219. doi: 10.1109/JPROC.2010.2068530.

[69] L.M.L Oliveira and J.J.P.C Rodrigues. Wireless Sensor Networks: a Survey on Environment Monitoring. *Journal of Communications*, 6(2):143–151, 2011. ISSN 1796-2021. doi: 10.4304/jcm.6.2.143-151.

[70] Ala Al-Fuqaha, Mohsen Guizani, Mehdi Mohammadi, Mohammed Aledhari, and Moussa Ayyash. Internet of Things: A Survey on Enabling Technologies, Protocols and Applications. *IEEE Communications Surveys & Tutorials*, 17 (4):2347–2376, 2015. ISSN 1553-877X. doi: 10.1109/COMST.2015.2444095.

[71] V. Raghunathan, C. Schurgers, Sung Park, and M. B. Srivastava. Energy-aware wireless microsensor networks. *IEEE Signal Processing Magazine*, 19 (2):40–50, Mar 2002. ISSN 1053-5888. doi: 10.1109/79.985679.

[72] L. Koval, J. Vanus, and P. Bilik. Distance Measuring by Ultrasonic Sensor. *IFAC-PapersOnLine*, 49(25):153–158, 2016. ISSN 24058963. doi: 10.1016/j.ifacol.2016.12.026.

[73] Ta Yeong Wu, Ningqun Guo, Chee Yang Teh, and Jacqueline Xiao Wen Hay. *Theory and Fundamentals of Ultrasound*, pages 5–12. Springer Netherlands, Dordrecht, 2013. ISBN 978-94-007-5533-8. doi: 10.1007/978-94-007-5533-8_2.

[74] Baldev Raj. *Practical non-destructive testing*. Alpha Science, Oxford, 3rd ed. edition, 2007. ISBN 9781842653753.

[75] P.K. Mittal. *Oscillations, Waves and Acoustics*. I.K. International Publishing House Pvt. Limited, 2010. ISBN 9789380578279.

[76] T. Nelligan. Ultrasonic Flaw Detection. URL `https://www.olympus-ims.com/en/applications-and-solutions/introductory-ultrasonics/introduction-flaw-detection/`.

[77] T. Rossing. *Springer Handbook of Acoustics*. Springer Handbook of Acoustics. Springer New York, 2007. ISBN 9780387304465.

[78] Jack Blitz and Geoff Simpson. *Ultrasonic Methods of Non-destructive Testing*. Chapman & Hall, 1st edition, 1996.

[79] Sang-Jin Shin and Byoung-Jin Jeong. Principle and Comprehension of Ultrasound Imaging. *Journal of the Korean Orthopaedic Association*, 48(5): 325, 2013. ISSN 1226-2102. doi: 10.4055/jkoa.2013.48.5.325.

[80] J.S. Wilson. *Sensor Technology Handbook*. Number v. 1 in Electronics & Electrical. Elsevier Science, 2005. ISBN 9780750677295.

[81] Blind Zone in Ultrasonic Sensors. URL `https://www.levelsensorsolutions.com/blind-zone-i-60.html/`.

[82] D.S. Lin, B.T. Khuri-Yakub, R. Howe, T.W. Kenny, and Stanford University. Department of Mechanical Engineering. *Interface Engineering of Capacitive Micromachined Ultrasonic Transducers for Medical Applications*. Stanford University, 2011.

[83] Seungin Shin, Min-Hyun Kim, and Seibum B. Choi. Ultrasonic Distance Measurement Method With Crosstalk Rejection at High Measurement Rate. *IEEE Transactions on Instrumentation and Measurement*, 68(4):972–979, apr 2019. ISSN 0018-9456. doi: 10.1109/TIM.2018.2863999.

[84] T. Hori, Y. Nishida, T. Kanade, and K. Akiyama. Improving sampling rate with multiplexed ultrasonic emitters. In *SMC'03 Conference Proceedings. 2003 IEEE International Conference on Systems, Man and*

Cybernetics. Conference Theme - System Security and Assurance (Cat. No.03CH37483), volume 5, pages 4522–4527. IEEE. ISBN 0-7803-7952-7. doi: 10.1109/ICSMC.2003.1245696. URL `http://ieeexplore.ieee.org/document/1245696/`.

[85] Qinghao Meng, Fengjuan Yao, and Yuehua Wu. Review of Crosstalk Elimination Methods for Ultrasonic Range Systems in Mobile Robots. In *2006 IEEE/RSJ International Conference on Intelligent Robots and Systems*, pages 1164–1169. IEEE, oct 2006. ISBN 1-4244-0258-1. doi: 10.1109/IROS.2006.281848.

[86] Ehud Galili, Baruch Rosen, and Dov Zviely. Ancient Sounding-Weights and Navigation along the Mediterranean Coast of Israel. *International Journal of Nautical Archaeology*, 38(2):343–368, sep 2009. ISSN 10572414. doi: 10.1111/j.1095-9270.2008.00218.x.

[87] Bathymetry systems. URL `https://woodshole.er.usgs.gov/operations/sfmapping/bathyhist.htm`.

[88] F. Fahy and J. Walker. *Fundamentals of Noise and Vibration*. Taylor & Francis, 1998. ISBN 9780419241805.

[89] Isaac Newton. *The Principia : Mathematical Principles of Natural Philosophy*. CreateSpace Independent Publishing Platform, 1687. ISBN 978-1490592152.

[90] E. McCarthy. *International Regulation of Underwater Sound: Establishing Rules and Standards to Address Ocean Noise Pollution*. Solid Mechanics and Its Applications Series. Springer US, 2007. ISBN 9781402080784.

[91] P Blondel. *Bathymetry and Its Applications*. InTech, Rijeka, Croatia, 2012. ISBN 978-953-307-959-2.

[92] Judith Bell. *A Model for the Simulation of Sidescan Sonar*. PhD thesis, Heriot-Watt University, 1995.

[93] Giuseppe Anastasi, Marco Conti, Mario Di Francesco, and Andrea Passarella. Energy conservation in wireless sensor networks: A survey. *Ad Hoc Networks*, 7(3):537–568, 2009. ISSN 15708705. doi: 10.1016/j.adhoc.2008.06.003.

[94] C.Y. Chong and S.P. Kumar. Sensor networks: Evolution, opportunities, and challenges. *Proceedings of the IEEE*, 91(8):1247–1256, 2003. ISSN 00189219. doi: 10.1109/JPROC.2003.814918.

[95] S. Sitharama Iyengar and R. Brooks. *Distributed Sensor Networks, Second Edition: Sensor Networking and Applications*. CRC Press, 2016. ISBN 1138199516.

[96] A. Shrestha and L. Xing. A performance comparison of different topologies for wireless sensor networks. In *2007 IEEE Conference on Technologies for Homeland Security*, pages 280–285, May 2007. doi: 10.1109/THS.2007.370059.

[97] L. K. Alazzawi, A. M. Elkateeb, A. Ramesh, and W. Aljuhar. Scalability analysis for wireless sensor networks routing protocols. In *22nd International Conference on Advanced Information Networking and Applications - Workshops (aina workshops 2008)*, pages 139–144, March 2008. doi: 10.1109/WAINA.2008.178.

[98] Jolly Soparia and Nirav Bhatt. A Survey on Comparative Study of Wireless Sensor Network Topologies. *International Journal of Computer Applications*, 87(1):40–43, feb 2014. ISSN 09758887. doi: 10.5120/15175-3255.

[99] Alan Mainwaring, David Culler, Joseph Polastre, Robert Szewczyk, and John Anderson. Wireless sensor networks for habitat monitoring. In *Proceedings of the 1st ACM International Workshop on Wireless Sensor Networks and Applications*, WSNA '02, pages 88–97, New York, NY, USA, 2002. ACM. ISBN 1-58113-589-0. doi: 10.1145/570738.570751.

[100] Philo Juang, Hidekazu Oki, Yong Wang, Margaret Martonosi, Li Shiuan Peh, and Daniel Rubenstein. Energy-efficient computing for wildlife tracking: Design tradeoffs and early experiences with zebranet. *SIGARCH Comput. Archit. News*, 30(5):96–107, October 2002. ISSN 0163-5964. doi: 10.1145/635506.605408.

[101] Serena Lucrezi, Melville Saayman, and Peet Van der Merwe. Managing beaches and beachgoers: Lessons from and for the blue flag award. *Tourism Management*, 48:211 – 230, 2015. ISSN 0261-5177. doi: http://dx.doi.org/10.1016/j.tourman.2014.11.010.

[102] S. Burak, E. Dogan, and C. Gazioglu. Impact of urbanization and tourism on coastal environment. *Ocean and Coastal Management*, 47(910):515 – 527, 2004. ISSN 0964-5691. doi: http://dx.doi.org/10.1016/j.ocecoaman.2004.07.007.

[103] J. Davenport and J.L. Davenport. The impact of tourism and personal leisure transport on coastal environments: A review. *Estuarine, Coastal and Shelf Science*, 2006. doi: 10.1016/j.ecss.2005.11.026.

[104] M.R. Phillips and Andrew L. Jones. Erosion and tourism infrastructure in the coastal zone: Problems, consequences and management. *Tourism Management*, 27(3):517–524, 2006. ISSN 02615177. doi: 10.1016/j.tourman.2005.10.019.

[105] IEEE. Wireless LAN Medium Access Control (MAC) and Physical Layer (PHY) Specifications. Technical report, 2012.

[106] Tifenn Rault, Abdelmadjid Bouabdallah, and Yacine Challal. Energy efficiency in wireless sensor networks: A top-down survey. *Computer Networks*, 67:104–122, 2014. ISSN 13891286. doi: 10.1016/j.comnet.2014.03.027.

[107] Jian Shen, Faliu Yi, Sangman Moh, and Ilyong Chung. Energy Efficiency of MAC Protocols in Wireless Sensor Networks. *2011 International Conference on Information Science and Applications*, pages 1–10, 2011. doi: 10.1109/ICISA.2011.5772405.

[108] Siddharth Watwe and R.C. Hansdah. Improving the Energy Efficiency of a Clock Synchronization Protocol for WSNs Using a TDMA-Based MAC Protocol. *2015 IEEE 29th International Conference on Advanced Information Networking and Applications*, pages 231–238, 2015. doi: 10.1109/AINA.2015.190.

[109] Mandeep Singh Bandral and Susma Jain. Energy Efficient Protocol For Wireless Sensor Network. In *IEEE International Conference on Recent Advances and Innovations in Engineering*, pages 7–12. IEEE, 2014. ISBN 9781479940400.

[110] J. Heidemann, J. Wills, and A. Syed. Research challenges and applications for underwater sensor networking. *IEEE Wireless Communications and Networking Conference, 2006. WCNC 2006.*, 1:228–235, 2006. ISSN 1525-3511. doi: 10.1109/WCNC.2006.1683469.

[111] Carlene E-A Campbell, Ibrar A Shah, and Kok-Keong Loo. Medium Access Control and Transport protocol for Wireless Sensor Networks : An overview. *International Journal of Applied Research on Information Technology and Computing*, 1(1):79–92, 2010.

[112] X. Chen, K. Makki, K. Yen, and N. Pissinou. Sensor network security: a survey. *IEEE Communications Surveys Tutorials*, 11(2):52–73, Second 2009. ISSN 1553-877X. doi: 10.1109/SURV.2009.090205.

[113] X. Che, I. Wells, P. Kear, G. Dickers, X. Gong, and M. Rhodes. A Static Multi-Hop Underwater Wireless Sensor Network Using RF Electromagnetic Communications. *Icdcs: 2009 International Conference on Distributed Computing Systems Workshops*, pages 460–463, 2009. ISSN 1545-0678. doi: 10.1109/ICDCSW.2009.36.

[114] ASTEC. URL `http://www.internet-engineering.co.uk/`.

[115] I. Wells, A. Davies, X. Che, P. Kear, G. Dickers, X. Gong, and M. Rhodes. Node pattern simulation of an undersea sensor network using RF electromagnetic communications. In *2009 International Conference on Ultra Modern Telecommunications & Workshops*, pages 1–4. IEEE, oct 2009. ISBN 978-1-4244-3942-3. doi: 10.1109/ICUMT.2009.5345555.

[116] X Che, I Wells, G Dickers, P Kear, and X Gong. Re-Evaluation of RF Electromagnetic Communication in Underwater Sensor Networks. *IEEE Communications Magazine*, pages 143–151, 2010.

[117] Ian F. Akyildiz, Dario Pompili, and Tommaso Melodia. Underwater acoustic sensor networks: research challenges. *Ad Hoc Networks*, 3(3):257–279, may 2005. ISSN 15708705. doi: 10.1016/j.adhoc.2005.01.004.

[118] Khalid Mahmood Awan, Peer Azmat Shah, Khalid Iqbal, Saira Gillani, Waqas Ahmad, and Yunyoung Nam. Underwater Wireless Sensor Networks: A Review of Recent Issues and Challenges. *Wireless Communications and Mobile Computing*, 2019:1–20, jan 2019. ISSN 1530-8669. doi: 10.1155/2019/6470359.

[119] X Che, I Wells, P Kear, G Dickers, and X Gong. Failure Tolerance Analysis of a Small Scale Underwater Sensor Network with EM Technology. *Unpublished*, 2009.

[120] I Wells, X Che, P Kear, G Dickers, X Gong, and M Rhodes. Undersea Sensor Network using Electromagnetic Very Low Frequency Communications. *Unpublished*, 2010.

[121] M Rhodes and B Hyland. Dispersion control in underwater electromagnetic communications systems.

[122] L Russell. Unpublished Summary Report of ASTEC Sea Trials at Port Edgar Marina. Technical report, Wireless Fibre Systems.

[123] J. Heidemann, M. Stojanovic, and M. Zorzi. Underwater sensor networks: applications, advances and challenges. *Philosophical Transactions of the Royal Society A: Mathematical, Physical and Engineering Sciences*, 370 (1958):158–175, jan 2012. ISSN 1364-503X. doi: 10.1098/rsta.2011.0214.

[124] Melike Erol-Kantarci, Hussein Mouftah, and Sema Oktug. Localization techniques for underwater acoustic sensor networks. *IEEE Communications Magazine*, 48(12):152–158, dec 2010. ISSN 0163-6804. doi: 10.1109/MCOM.2010.5673086.

[125] Kuna Nageswararao and U Devee Prasan. A survey on underwater sensor networks localization techniques. 2012.

[126] Gianluca Dini and Marco Tiloca. Considerations on Security in ZigBee Networks. In *2010 IEEE International Conference on Sensor Networks, Ubiquitous, and Trustworthy Computing*, pages 58–65. IEEE, 2010. ISBN 978-1-4244-7087-7. doi: 10.1109/SUTC.2010.15.

[127] E. Ferro and F. Potorti. Bluetooth and wi-fi wireless protocols: a survey and a comparison. *IEEE Wireless Communications*, 12(1):12–26, feb 2005. ISSN 1536-1284. doi: 10.1109/MWC.2005.1404569.

[128] C. Gehrmann, J. Persson, and B. Smeets. *Bluetooth Security*. Artech House computer security series. Artech House, 2004. ISBN 9781580538855.

[129] ZigBee Specification. Technical report, ZigBee Standards Organization, 2012.

[130] R. Wilson. ZigBee wireless operates like a location system, 2013. URL `https://www.electronicsweekly.com/news/design/communications/zigbee-wireless-operates-like-a-location-system-2013-07/`.

[131] Matt Hillman. An Overview of ZigBee Networks: A guide for implementers and security testers. Technical report, MWR InfoSecurity.

[132] Atmel. ATmega328/P Datasheet, 2016.

[133] Digi. XCTU Configuration and Test Utility Software, User Guide, 2018.

[134] A.R. Pinto, L. Bolzani, C. Montez, and F. Vargas. Power Optimization for Wireless Sensor Networks. In *Wireless Sensor Networks - Technology and Applications*. InTech, jul 2012. doi: 10.5772/50603.

[135] Kofi Sarpong Adu-Manu, Nadir Adam, Cristiano Tapparello, Hoda Ayatollahi, and Wendi Heinzelman. Energy-Harvesting Wireless Sensor Networks (EH-WSNs). *ACM Transactions on Sensor Networks*, 14(2):1–50, apr 2018. ISSN 15504859. doi: 10.1145/3183338.

Appendix 1: Publications

The following publications directly incorporate material from this thesis:

- Watt, A.J., Campbell, C.E.-A., Hole, S., Wells, I. and Phillips, M.R. (2016) A Comparative Assessment of Floating and Submerged Sensor Network Deployments for Monitoring Underwater Sediment Transport Processes, Journal of Computer and Communications, 4, pp. 41-46. http://dx.doi.org/10.4236/jcc.2016.45006

- Watt, A.J., Phillips, M.R., Campbell, C.E.-A., Wells, I., and Hole, S. (2019) Wireless Sensor Networks for Monitoring Underwater Sediment Transport, Science of the Total Environment, 667, pp. 160-165, https://doi.org/10.1016/j.scitotenv.2019.02.369

Appendix 2. Raw Data for Initial Tank Measurements

Sensor 1	Frame ID	Time	Reading (cm)	Actual (cm)
	3	10:15:22	30	31
	7	10:15:27	30	31
	11	10:15:32	30	31
	15	10:15:37	30	31
	19	10:15:42	30	31
	23	10:15:47	30	31
	27	10:15:52	29	31
	31	10:15:57	29	31
	35	10:16:02	29	31
	39	10:16:07	29	31
	42	10:16:12	29	31
	47	10:16:17	29	31
	51	10:16:22	29	31
	55	10:16:27	29	31
	59	10:16:32	29	31
	63	10:16:37	29	31
	67	10:16:42	30	31
	71	10:16:47	29	31

	75	10:16:52	29	31
	79	10:16:57	29	31
	83	10:17:02	29	31
	87	10:17:07	30	31
	91	10:17:12	30	31
	95	10:17:17	30	31
	99	10:17:22	30	31
	103	10:17:27	30	31
	107	10:17:32	30	31
	111	10:17:37	30	31
	115	10:17:42	30	31
	119	10:17:47	30	31
	123	10:17:52	30	31
	127	10:17:57	30	31
	132	10:18:02	30	31
	136	10:18:07	30	31
	141	10:18:12	30	31
	145	10:18:17	30	31
	149	10:18:22	30	31
	153	10:18:27	30	31
	157	10:18:32	29	31
	161	10:18:37	29	31
	165	10:18:42	29	31
	169	10:18:47	29	31
	173	10:18:52	29	31
	177	10:18:57	29	31
	181	10:19:02	29	31

	185	10:19:07	29	31
	189	10:19:12	29	31
	193	10:19:17	29	31
	197	10:19:22	29	31
	201	10:19:27	29	31
	205	10:19:32	29	31
	209	10:19:37	29	31
	213	10:19:42	29	31
	217	10:19:47	29	31
	221	10:19:52	29	31
	225	10:19:57	29	31
	229	10:20:02	28	31
	233	10:20:07	28	31
	237	10:20:12	29	31
	241	10:20:17	29	31
		Average	**29.36666667**	**31**
		Std. Dev	**0.551320961**	
		Std. Error	**0.07117523**	
Sensor 2	**Frame ID**	**Time**	**Reading (cm)**	**Actual (cm)**
	0	10:15:20	28	30
	4	10:15:25	28	30
	8	10:15:30	28	30
	13	10:15:35	28	30
	17	10:15:40	28	30
	21	10:15:45	28	30
	25	10:15:50	28	30
	29	10:15:55	28	30

	34	10:16:00	28	30
	38	10:16:05	28	30
	42	10:16:11	28	30
	46	10:16:16	28	30
	50	10:16:21	28	30
	54	10:16:26	28	30
	58	10:16:31	28	30
	62	10:16:36	28	30
	66	10:16:41	28	30
	70	10:16:46	28	30
	74	10:16:51	28	30
	78	10:16:56	28	30
	82	10:17:01	28	30
	86	10:17:06	28	30
	90	10:17:11	28	30
	94	10:17:16	28	30
	98	10:17:21	28	30
	102	10:17:26	28	30
	106	10:17:31	28	30
	110	10:17:36	28	30
	114	10:17:41	28	30
	118	10:17:46	28	30
	122	10:17:51	28	30
	126	10:17:56	28	30
	130	10:18:01	28	30
	134	10:18:06	28	30
	138	10:18:11	28	30

	142	10:18:16	28	30
	146	10:18:21	28	30
	150	10:18:26	28	30
	154	10:18:31	28	30
	158	10:18:36	28	30
	162	10:18:41	28	30
	166	10:18:46	28	30
	170	10:18:51	28	30
	174	10:18:56	28	30
	178	10:19:01	28	30
	182	10:19:06	28	30
	186	10:19:11	28	30
	190	10:19:16	28	30
	194	10:19:21	28	30
	198	10:19:26	28	30
	204	10:19:31	28	30
	208	10:19:36	28	30
	212	10:19:41	28	30
	216	10:19:46	28	30
	220	10:19:51	28	30
		Average	**28**	**30**
		Std. Dev	**0**	
		Std. Error	**0**	

Appendix 3. Raw Data for Datum Measurements

Sand Datum

Sensor 1	Frame ID	Time	Reading (cm)	Actual (cm)
	0	16:08:01	28	29
	4	16:08:06	28	29
	8	16:08:11	28	29
	12	16:08:16	28	29
	16	16:08:21	28	29
	20	16:08:26	28	29
	24	16:08:31	28	29
	28	16:08:36	28	29
	32	16:08:41	28	29
	36	16:08:46	28	29
	40	16:08:51	28	29
	44	16:08:56	28	29
	48	16:09:01	28	29
	52	16:09:06	28	29
	56	16:09:11	28	29
	60	16:09:16	28	29

	64	16:09:21	28	29
	68	16:09:26	28	29
	72	16:09:31	28	29
	76	16:09:36	28	29
	80	16:09:41	28	29
	84	16:09:46	28	29
	88	16:09:51	28	29
	93	16:09:56	28	29
	97	16:10:01	28	29
	101	16:10:06	28	29
	105	16:10:11	28	29
	109	16:10:16	28	29
	113	16:10:21	28	29
	117	16:10:26	28	29
	121	16:10:31	28	29
	125	16:10:36	28	29
	129	16:10:41	28	29
	133	16:10:46	28	29
	137	16:10:51	28	29
	141	16:10:56	28	29
	145	16:11:01	28	29
	149	16:11:06	28	29
	153	16:11:11	28	29
	157	16:11:16	28	29
	160	16:11:21	28	29
	164	16:11:26	28	29
	168	16:11:31	28	29

	172	16:11:36	28	29
	176	16:11:41	28	29
	180	16:11:46	28	29
	184	16:11:51	28	29
	188	16:11:56	28	29
	192	16:12:01	28	29
	196	16:12:06	28	29
	200	16:12:11	28	29
	204	16:12:16	28	29
	208	16:12:21	28	29
	212	16:12:26	28	29
	217	16:12:31	28	29
	221	16:12:36	28	29
	225	16:12:41	28	29
	229	16:12:46	28	29
	233	16:12:51	28	29
	237	16:12:56	28	29
		Average	**28**	**29**
		Std. Dev	**0**	
		Std. Error	**0**	
Sensor 2	**Frame ID**	**Time**	**Reading (cm)**	**Actual (cm)**
	2	16:08:02	29	30
	6	16:08:07	30	30
	10	16:08:12	30	30
	14	16:08:17	30	30
	17	16:08:22	30	30
	21	16:08:27	30	30

	25	16:08:32	30	30
	29	16:08:37	31	30
	33	16:08:42	29	30
	38	16:08:47	29	30
	42	16:08:52	29	30
	46	16:08:57	29	30
	50	16:09:02	29	30
	54	16:09:07	30	30
	58	16:09:12	30	30
	62	16:09:17	29	30
	66	16:09:22	29	30
	70	16:09:27	29	30
	74	16:09:32	30	30
	78	16:09:38	30	30
	82	16:09:43	29	30
	86	16:09:48	29	30
	90	16:09:53	29	30
	94	16:09:58	29	30
	98	16:10:03	29	30
	102	16:10:08	29	30
	106	16:10:13	29	30
	110	16:10:18	30	30
	115	16:10:24	30	30
	119	16:10:29	29	30
	123	16:10:34	29	30
	127	16:10:39	29	30
	131	16:10:44	29	30

	135	16:10:49	29	30
	139	16:10:54	29	30
	143	16:10:59	30	30
	147	16:11:04	29	30
	151	16:11:09	29	30
	155	16:11:14	29	30
	159	16:11:19	29	30
	163	16:11:24	29	30
	167	16:11:29	29	30
	171	16:11:34	29	30
	175	16:11:39	29	30
	179	16:11:44	29	30
	183	16:11:49	29	30
	187	16:11:54	29	30
	191	16:11:59	29	30
	195	16:12:04	29	30
	199	16:12:09	29	30
	203	16:12:14	29	30
	207	16:12:19	29	30
	211	16:12:24	29	30
	215	16:12:29	29	30
	219	16:12:35	29	30
	223	16:12:40	29	30
	227	16:12:45	29	30
	231	16:12:50	29	30
		Average	**29.25**	**30**
		Std. Dev	**0.47389479**	

		Std. Error	**0.06117955**	

Shingle Datum

Sensor 1	**Frame ID**	**Time**	**Reading (cm)**	**Actual (cm)**
	1	12:21:45	29	29
	5	12:21:50	29	29
	9	12:21:55	29	29
	13	12:22:00	29	29
	17	12:22:05	29	29
	21	12:22:10	29	29
	26	12:22:15	29	29
	30	12:22:20	29	29
	34	12:22:25	29	29
	38	12:22:30	29	29
	42	12:22:35	29	29
	46	12:22:40	29	29
	50	12:22:45	29	29
	54	12:22:50	29	29
	58	12:22:55	29	29
	62	12:23:00	29	29
	66	12:23:05	29	29
	70	12:23:10	29	29
	74	12:23:15	29	29
	78	12:23:20	29	29
	82	12:23:25	29	29
	86	12:23:30	29	29

	90	12:23:35	29	29
	94	12:23:40	29	29
	98	12:23:45	29	29
	102	12:23:50	29	29
	106	12:23:55	29	29
	110	12:24:00	29	29
	114	12:24:05	29	29
	118	12:24:10	29	29
	122	12:24:15	29	29
	126	12:24:20	29	29
	130	12:24:25	29	29
	134	12:24:30	29	29
	138	12:24:35	28	29
	142	12:24:40	28	29
	146	12:24:45	28	29
	150	12:24:50	28	29
	154	12:24:55	29	29
	158	12:25:00	29	29
	162	12:25:05	28	29
	166	12:25:10	28	29
	169	12:25:15	29	29
	173	12:25:20	29	29
	177	12:25:25	28	29
	181	12:25:30	29	29
	185	12:25:35	29	29
	189	12:25:40	29	29
	193	12:25:45	32	29

	197	12:25:50	32	29
	201	12:25:55	32	29
	205	12:26:00	32	29
	209	12:26:05	32	29
	213	12:26:10	32	29
	217	12:26:15	32	29
	221	12:26:20	32	29
	225	12:26:25	32	29
	230	12:26:30	32	29
	234	12:26:35	30	29
	238	12:26:40	30	29
		Average	**29.4166667**	**29**
		Std. Dev	**1.22532136**	
		Std. Error	**0.15818831**	
Sensor 2	**Frame ID**	**Time**	**Reading (cm)**	**Actual (cm)**
	3	12:21:47	27	28
	7	12:21:52	27	28
	11	12:21:57	27	28
	15	12:22:03	27	28
	19	12:22:08	27	28
	23	12:22:13	27	28
	27	12:22:18	27	28
	31	12:22:23	27	28
	35	12:22:28	27	28
	39	12:22:33	27	28
	44	12:22:38	27	28
	48	12:22:43	27	28

	52	12:22:48	27	28
	56	12:22:53	27	28
	60	12:22:58	27	28
	64	12:23:03	27	28
	69	12:23:09	27	28
	73	12:23:14	27	28
	77	12:23:19	27	28
	81	12:23:24	27	28
	85	12:23:29	27	28
	89	12:23:34	27	28
	93	12:23:39	27	28
	97	12:23:44	27	28
	101	12:23:49	27	28
	105	12:23:55	27	28
	109	12:24:00	27	28
	113	12:24:05	27	28
	117	12:24:10	27	28
	121	12:24:15	27	28
	125	12:24:20	27	28
	129	12:24:25	27	28
	133	12:24:30	27	28
	137	12:24:35	27	28
	141	12:24:40	27	28
	145	12:24:45	27	28
	149	12:24:50	27	28
	153	12:24:55	27	28
	157	12:25:00	27	28

	161	12:25:05	27	28
	165	12:25:10	27	28
	170	12:25:15	27	28
	174	12:25:20	27	28
	178	12:25:25	27	28
	182	12:25:30	27	28
	186	12:25:35	27	28
	190	12:25:40	27	28
	194	12:25:45	27	28
	198	12:25:50	27	28
	202	12:25:55	27	28
	206	12:26:00	27	28
	210	12:26:05	27	28
	214	12:26:10	27	28
	218	12:26:15	27	28
	223	12:26:20	27	28
	227	12:26:25	27	28
	231	12:26:30	27	28
	235	12:26:35	27	28
	239	12:26:40	27	28
	243	12:26:45	27	28
		Average	**27**	28
		Std. Dev	**0**	
		Std. Error	**0**	

Sand/Shingle Mix Datum

Sensor 1	**Frame ID**	**Time**	**Reading (cm)**	**Actual (cm)**
	2	12:08:36	27	27
	6	12:08:41	27	27
	10	12:08:46	26	27
	14	12:08:51	26	27
	18	12:08:56	26	27
	22	12:09:01	26	27
	26	12:09:06	26	27
	30	12:09:11	26	27
	34	12:09:16	26	27
	38	12:09:21	26	27
	42	12:09:26	26	27
	46	12:09:31	26	27
	50	12:09:36	26	27
	54	12:09:41	26	27
	58	12:09:46	26	27
	62	12:09:51	26	27
	66	12:09:56	26	27
	70	12:10:01	26	27
	74	12:10:06	26	27
	78	12:10:11	26	27
	82	12:10:16	26	27
	86	12:10:21	26	27
	90	12:10:26	26	27
	94	12:10:31	26	27
	99	12:10:36	26	27
	103	12:10:41	26	27
	107	12:10:46	26	27

	111	12:10:51	26	27
	115	12:10:56	26	27
	119	12:11:01	26	27
	123	12:11:06	26	27
	127	12:11:11	26	27
	131	12:11:16	26	27
	135	12:11:21	26	27
	139	12:11:26	25	27
	143	12:11:31	25	27
	147	12:11:36	25	27
	151	12:11:41	25	27
	153	12:11:46	25	27
	157	12:11:51	25	27
	161	12:11:56	25	27
	165	12:12:01	25	27
	169	12:12:06	25	27
	173	12:12:11	25	27
	177	12:12:16	25	27
	182	12:12:21	25	27
	186	12:12:26	25	27
	190	12:12:31	25	27
	194	12:12:36	25	27
	198	12:12:41	25	27
	202	12:12:46	25	27
	206	12:12:51	25	27
	210	12:12:56	25	27
	214	12:13:01	25	27

	218	12:13:06	25	27
	222	12:13:11	25	27
	226	12:13:16	25	27
	230	12:13:21	25	27
	234	12:13:26	25	27
	238	12:13:31	25	27
		Average	**25.6**	**27**
		Std. Dev	**0.55844821**	
		Std. Error	**0.07209535**	
Sensor 2	**Frame ID**	**Time**	**Reading (cm)**	**Actual (cm)**
	3	12:08:37	26	26
	7	12:08:41	25	26
	11	12:08:47	25	26
	15	12:08:51	25	26
	19	12:08:56	26	26
	23	12:09:02	26	26
	27	12:09:07	26	26
	31	12:09:12	26	26
	36	12:09:17	26	26
	40	12:09:22	26	26
	44	12:09:27	26	26
	48	12:09:33	26	26
	52	12:09:38	26	26
	56	12:09:43	26	26
	60	12:09:48	25	26
	64	12:09:54	26	26
	69	12:09:59	26	26

	73	12:10:04	26	26
	77	12:10:09	26	26
	81	12:10:14	26	26
	85	12:10:19	26	26
	89	12:10:24	26	26
	93	12:10:28	26	26
	97	12:10:33	25	26
	101	12:10:39	25	26
	105	12:10:44	25	26
	109	12:10:48	26	26
	113	12:10:53	26	26
	117	12:10:58	25	26
	121	12:11:04	25	26
	125	12:11:09	25	26
	129	12:11:13	26	26
	133	12:11:19	26	26
	137	12:11:23	26	26
	141	12:11:28	26	26
	145	12:11:33	25	26
	149	12:11:39	26	26
	155	12:11:47	26	26
	156	12:11:50	26	26
	159	12:11:53	26	26
	163	12:11:59	26	26
	168	12:12:04	26	26
	172	12:12:09	26	26
	176	12:12:14	26	26

	180	12:12:19	26	26
	184	12:12:24	26	26
	188	12:12:29	26	26
	192	12:12:34	26	26
	196	12:12:39	26	26
	200	12:12:44	26	26
	204	12:12:49	26	26
	208	12:12:54	26	26
	212	12:12:59	26	26
	216	12:13:04	26	26
	220	12:13:10	26	26
	224	12:13:15	26	26
	229	12:13:20	26	26
	233	12:13:25	26	26
	237	12:13:30	26	26
	241	12:13:35	26	26
		Average	**25.8166667**	
		Std. Dev	**0.39020493**	
		Std. Error	**0.05037524**	

Appendix 4. Raw Sensor Data for Sediment Movement

Shingle Movement

Sensor 1	Frame ID	Time	Reading (cm)	Actual (cm)
0 mins	2	12:36:36	26	26
	6	12:36:41	26	26
	10	12:36:46	25	26
	14	12:36:51	25	26
	18	12:36:56	26	26
	22	12:37:01	26	26
	26	12:37:06	26	26
	30	12:37:11	25	26
	34	12:37:16	25	26
	38	12:37:21	25	26
	42	12:37:26	26	26
	46	12:37:31	26	26
	50	12:37:36	25	26
	54	12:37:41	25	26
	58	12:37:46	25	26
	63	12:37:51	25	26

	67	12:37:56	25	26
	71	12:38:01	25	26
	75	12:38:06	25	26
	79	12:38:11	25	26
	83	12:38:16	25	26
	87	12:38:21	25	26
	91	12:38:26	25	26
	95	12:38:31	25	26
Reading Avg.			**25.29166667**	
Std. Deviation			**0.464305621**	
Std. Error			**0.094775988**	
2 mins	99	12:38:36	25	25
	103	12:38:41	25	25
	107	12:38:46	31	25
	111	12:38:51	30	25
	115	12:38:56	26	25
	119	12:39:01	26	25
	123	12:39:06	26	25
	127	12:39:11	26	25
	131	12:39:16	27	25
	135	12:39:21	30	25
	139	12:39:26	30	25
	143	12:39:31	30	25
	147	12:39:36	31	25
	151	12:39:41	30	25
	155	12:39:46	30	25

	159	12:39:51	30	25
	163	12:39:56	30	25
	167	12:40:01	30	25
	171	12:40:06	30	25
	175	12:40:11	27	25
	179	12:40:16	30	25
	183	12:40:21	26	25
	187	12:40:26	26	25
	191	12:40:31	26	25
Reading Avg.			**28.25**	
Std. Deviation			**2.171955641**	
Std. Error			**0.443348589**	
4 mins	195	12:40:36	27	28
	199	12:40:41	27	28
	203	12:40:46	27	28
	207	12:40:51	27	28
	211	12:40:56	27	28
	215	12:41:01	27	28
	219	12:41:06	27	28
	224	12:41:11	27	28
	228	12:41:16	27	28
	232	12:41:21	27	28
	236	12:41:26	27	28
	240	12:41:31	27	28
	244	12:41:36	27	28
	248	12:41:41	27	28

	252	12:41:46	27	28
	257	12:41:51	27	28
	261	12:41:56	27	28
	265	12:42:01	27	28
	269	12:42:06	27	28
	273	12:42:11	27	28
	277	12:42:16	27	28
	280	12:42:21	27	28
	284	12:42:26	27	28
	288	12:42:31	27	28
Reading Avg.			**27**	
Std. Deviation			**0**	
Std. Error			**0**	
6 mins	292	12:42:36	27	26
	296	12:42:41	26	26
	300	12:42:46	27	26
	304	12:42:51	27	26
	308	12:42:56	27	26
	312	12:43:01	27	26
	316	12:43:06	27	26
	320	12:43:11	27	26
	324	12:43:16	27	26
	332	12:43:21	27	26
	336	12:43:26	27	26
	340	12:43:31	27	26
	344	12:43:36	27	26

	348	12:43:41	27	26
	352	12:43:46	27	26
	356	12:43:51	27	26
	360	12:43:56	27	26
	364	12:44:01	26	26
	369	12:44:06	26	26
	373	12:44:11	26	26
	377	12:44:16	26	26
	381	12:44:21	27	26
	385	12:44:26	27	26
	389	12:44:31	19	26
Reading Avg.			**26.45833333**	
Std. Deviation			**1.64129235**	
Std. Error			**0.335027398**	
8 mins	393	12:44:36	20	21
	397	12:44:41	21	21
	401	12:44:46	20	21
	405	12:44:51	20	21
	409	12:44:56	20	21
	413	12:45:01	20	21
	417	12:45:06	20	21
	421	12:45:11	20	21
	425	12:45:16	20	21
	429	12:45:21	20	21
	433	12:45:26	20	21
	437	12:45:31	20	21

	441	12:45:36	20	21
	445	12:45:41	20	21
	449	12:45:46	20	21
	453	12:45:51	20	21
	458	12:45:56	20	21
	462	12:46:01	20	21
	466	12:46:06	20	21
	470	12:46:11	20	21
	474	12:46:16	20	21
	478	12:46:21	20	21
	482	12:46:26	20	21
	486	12:46:31	20	21
Reading Avg.			**20.04166667**	
Std. Deviation			**0.204124145**	
Std. Error			**0.041666667**	
Sensor 2	**Frame ID**	**Time**	**Reading (cm)**	**Actual (cm)**
0 mins	1	12:36:34	27	27
	5	12:36:40	27	27
	9	12:36:45	27	27
	13	12:36:51	27	27
	17	12:36:56	27	27
	21	12:37:01	27	27
	25	12:37:06	27	27
	29	12:37:10	27	27
	33	12:37:16	27	27
	37	12:37:21	27	27

	41	12:37:26	27	27
	45	12:37:31	27	27
	49	12:37:36	27	27
	56	12:37:41	27	27
	60	12:37:46	27	27
	64	12:37:51	27	27
	68	12:37:56	28	27
	72	12:38:01	27	27
	76	12:38:07	27	27
	80	12:38:12	27	27
	84	12:38:17	27	27
	88	12:38:22	27	27
	92	12:38:27	27	27
	96	12:38:33	27	27
Reading Avg.			**27.0416667**	
Std. Deviation			**0.20412415**	
Std. Error			**0.04166667**	
2 mins	100	12:38:38	25	24
	104	12:38:43	25	24
	108	12:38:48	25	24
	112	12:38:53	25	24
	116	12:38:58	25	24
	120	12:39:03	25	24
	124	12:39:08	25	24
	128	12:39:13	25	24
	132	12:39:18	25	24

	136	12:39:23	25	24
	140	12:39:28	25	24
	144	12:39:33	25	24
	148	12:39:38	25	24
	152	12:39:43	25	24
	156	12:39:48	25	24
	160	12:39:53	25	24
	166	12:39:58	25	24
	170	12:40:03	25	24
	174	12:40:08	25	24
	178	12:40:13	25	24
	182	12:40:18	25	24
	186	12:40:23	25	24
	190	12:40:28	25	24
	194	12:40:33	25	24
Reading Avg.			**25**	
Std. Deviation			**0**	
Std. Error			**0**	
4 mins	198	12:40:38	25	25
	202	12:40:43	25	25
	206	12:40:49	25	25
	210	12:40:54	25	25
	214	12:41:00	25	25
	218	12:41:05	24	25
	222	12:41:10	25	25
	226	12:41:15	25	25

	230	12:41:20	25	25
	234	12:41:25	25	25
	238	12:41:30	25	25
	242	12:41:35	25	25
	247	12:41:40	25	25
	251	12:41:45	25	25
	255	12:41:50	25	25
	260	12:41:56	25	25
	264	12:42:01	25	25
	268	12:42:06	25	25
	272	12:42:11	25	25
	276	12:42:16	25	25
	281	12:42:22	25	25
	285	12:42:27	25	25
	289	12:42:32	25	25
	293	12:42:37	25	25
Reading Avg.			**24.9583333**	
Std. Deviation			**0.20412415**	
Std. Error			**0.04166667**	
6 mins	297	12:42:42	25	25
	301	12:42:47	25	25
	305	12:42:52	25	25
	309	12:42:57	24	25
	313	12:43:02	24	25
	317	12:43:07	24	25
	321	12:43:12	24	25

	326	12:43:18	24	25
	330	12:43:23	24	25
	334	12:43:28	24	25
	338	12:43:33	24	25
	342	12:43:38	24	25
	346	12:43:43	24	25
	350	12:43:48	24	25
	354	12:43:53	24	25
	358	12:43:58	24	25
	362	12:44:03	24	25
	366	12:44:08	24	25
	370	12:44:13	24	25
	374	12:44:18	24	25
	378	12:44:23	24	25
	382	12:44:28	24	25
	387	12:44:33	24	25
	391	12:44:38	30	25
Reading Avg.			**24.375**	
Std. Deviation			**1.24455335**	
Std. Error			**0.25404339**	
8 mins	395	12:44:43	30	31
	399	12:44:48	30	31
	403	12:44:53	30	31
	407	12:44:58	29	31
	411	12:45:03	29	31
	415	12:45:08	29	31

	419	12:45:13	29	31
	423	12:45:18	29	31
	427	12:45:24	29	31
	431	12:45:29	29	31
	436	12:45:34	29	31
	440	12:45:39	29	31
	444	12:45:44	29	31
	448	12:45:49	29	31
	452	12:45:54	29	31
	456	12:45:59	29	31
	460	12:46:04	29	31
	464	12:46:09	29	31
	468	12:46:14	29	31
	472	12:46:20	29	31
	476	12:46:25	29	31
	480	12:46:30	29	31
	484	12:46:35	29	31
	488	12:46:40	29	31
Reading Avg.			**29.125**	
Std. Deviation			**29.125**	
Std. Error			**0.33783196**	

Sand Movement

Sensor 1	**Frame ID**	**Time**	**Reading (cm)**	**Actual (cm)**
0 mins	1	16:15:26	28	29

	5	16:15:31	28	29
	9	16:15:36	28	29
	13	16:15:41	28	29
	17	16:15:46	28	29
	21	16:15:51	28	29
	25	16:15:56	28	29
	29	16:16:01	28	29
	33	16:16:06	28	29
	37	16:16:11	28	29
	41	16:16:16	28	29
	45	16:16:21	28	29
	49	16:16:26	28	29
	53	16:16:31	28	29
	57	16:16:36	28	29
	60	16:16:41	28	29
	64	16:16:46	28	29
	68	16:16:51	28	29
	72	16:16:56	28	29
	76	16:17:01	28	29
	80	16:17:06	28	29
	84	16:17:11	28	29
	88	16:17:16	28	29
	92	16:17:21	28	29
Reading Avg.			**28**	
Std. Deviation			**0**	
Std. Error			**0**	

2 mins	96	16:17:26	29	32
	100	16:17:31	33	32
	104	16:17:36	31	32
	108	16:17:41	33	32
	112	16:17:46	33	32
	116	16:17:51	33	32
	120	16:17:56	33	32
	124	16:18:01	33	32
	128	16:18:06	33	32
	132	16:18:11	33	32
	136	16:18:16	33	32
	140	16:18:21	33	32
	145	16:18:26	33	32
	149	16:18:31	33	32
	153	16:18:36	33	32
	157	16:18:41	33	32
	161	16:18:46	33	32
	165	16:18:51	33	32
	169	16:18:56	33	32
	173	16:19:01	33	32
	176	16:19:06	33	32
	180	16:19:11	33	32
	184	16:19:16	33	32
	188	16:19:21	33	32
Reading Avg.			**32.75**	
Std. Deviation			**0.896854406**	
Std. Error			**0.183069639**	

4 mins	192	16:19:26	30	32
	196	16:19:31	31	32
	200	16:19:36	31	32
	204	16:19:41	32	32
	208	16:19:46	31	32
	212	16:19:51	31	32
	216	16:19:56	31	32
	220	16:20:01	31	32
	224	16:20:06	31	32
	228	16:20:11	31	32
	232	16:20:16	32	32
	236	16:20:21	31	32
	240	16:20:26	31	32
	244	16:20:31	31	32
	248	16:20:37	31	32
	252	16:20:42	31	32
	256	16:20:46	32	32
	260	16:20:52	31	32
	265	16:20:57	31	32
	269	16:21:02	31	32
	273	16:21:07	31	32
	277	16:21:12	31	32
	281	16:21:17	31	32
	285	16:21:22	32	32
Reading Avg.			**31.125**	
Std. Deviation			**0.448427203**	

Std. Error			**0.09153482**	
6 mins	289	16:21:27	31	32
	293	16:21:32	31	32
	297	16:21:37	31	32
	301	16:21:42	31	32
	305	16:21:47	31	32
	309	16:21:52	31	32
	313	16:21:57	31	32
	317	16:22:02	31	32
	321	16:22:07	31	32
	325	16:22:12	31	32
	329	16:22:17	31	32
	333	16:22:22	31	32
	337	16:22:27	31	32
	341	16:22:32	31	32
	345	16:22:37	31	32
	350	16:22:42	31	32
	354	16:22:47	31	32
	358	16:22:52	31	32
	362	16:22:57	31	32
	366	16:23:02	31	32
	370	16:23:07	31	32
	374	16:23:12	31	32
	378	16:23:17	30	32
	382	16:23:22	30	32
Reading Avg.			**30.91666667**	

Std. Deviation			**0.282329851**	
Std. Error			**0.05763034**	
8 mins	386	16:23:27	31	31
	390	16:23:32	31	31
	394	16:23:37	30	31
	398	16:23:42	34	31
	402	16:23:47	34	31
	406	16:23:52	34	31
	410	16:23:57	32	31
	414	16:24:02	32	31
	418	16:24:07	32	31
	422	16:24:12	32	31
	426	16:24:17	32	31
	430	16:24:22	32	31
	434	16:24:27	35	31
	438	16:24:32	32	31
	442	16:24:37	31	31
	446	16:24:42	32	31
	450	16:24:47	32	31
	454	16:24:52	32	31
	458	16:24:57	31	31
	462	16:25:02	32	31
	466	16:25:07	31	31
	470	16:25:12	31	31
	474	16:25:17	31	31
	478	16:25:23	31	31

Reading Avg.			**31.95833333**	
Std. Deviation			**1.197067673**	
Std. Error			**0.244350416**	
Sensor 2	**Frame ID**	**Time**	**Reading (cm)**	**Actual (cm)**
0 mins	2	16:15:28	29	30
	7	16:15:33	29	30
	11	16:15:38	29	30
	15	16:15:43	29	30
	19	16:15:48	29	30
	23	16:15:53	29	30
	27	16:15:58	29	30
	31	16:16:03	29	30
	35	16:16:08	29	30
	39	16:16:13	29	30
	43	16:16:18	29	30
	47	16:16:23	29	30
	51	16:16:28	29	30
	55	16:16:33	29	30
	59	16:16:38	29	30
	62	16:16:43	29	30
	66	16:16:49	29	30
	70	16:16:54	29	30
	74	16:16:59	29	30
	78	16:17:04	29	30
	82	16:17:09	29	30
	86	16:17:14	29	30

	90	16:17:19	29	30
	94	16:17:24	29	30
Reading Avg.			**29**	
Std. Deviation			**0**	
Std. Error			**0**	
2 mins	98	16:17:29	28	28
	102	16:17:34	28	28
	106	16:17:39	28	28
	110	16:17:44	28	28
	114	16:17:50	28	28
	118	16:17:55	28	28
	122	16:18:00	28	28
	126	16:18:05	28	28
	130	16:18:10	28	28
	135	16:18:15	28	28
	139	16:18:20	28	28
	143	16:18:25	28	28
	147	16:18:30	28	28
	151	16:18:35	28	28
	155	16:18:40	28	28
	159	16:18:45	28	28
	163	16:18:50	28	28
	168	16:18:56	28	28
	172	16:19:01	28	28
	177	16:19:07	28	28
	181	16:19:12	28	28

	185	16:19:17	28	28
	189	16:19:22	28	28
	193	16:19:27	25	28
Reading Avg.			**27.875**	
Std. Deviation			**0.61237244**	
Std. Error			**0.125**	
4 mins	197	16:19:32	25	26
	201	16:19:37	25	26
	205	16:19:42	25	26
	209	16:19:47	25	26
	213	16:19:52	25	26
	217	16:19:57	25	26
	221	16:20:02	25	26
	225	16:20:07	26	26
	229	16:20:12	26	26
	233	16:20:17	26	26
	237	16:20:22	26	26
	242	16:20:28	26	26
	246	16:20:33	26	26
	250	16:20:38	26	26
	254	16:20:43	26	26
	258	16:20:48	26	26
	262	16:20:53	26	26
	266	16:20:58	26	26
	270	16:21:03	26	26
	274	16:21:08	26	26

	278	16:21:13	26	26
	282	16:21:18	26	26
	286	16:21:23	26	26
	290	16:21:28	25	26
Reading Avg.			**25.6666667**	
Std. Deviation			**0.48154341**	
Std. Error			**0.09829464**	
6 mins	294	16:21:33	24	24
	298	16:21:38	24	24
	303	16:21:43	24	24
	307	16:21:48	24	24
	311	16:21:53	24	24
	315	16:21:58	24	24
	319	16:22:03	24	24
	323	16:22:08	24	24
	327	16:22:13	24	24
	331	16:22:18	24	24
	335	16:22:24	24	24
	339	16:22:29	24	24
	344	16:22:35	24	24
	348	16:22:40	24	24
	352	16:22:45	24	24
	356	16:22:50	24	24
	360	16:22:55	24	24
	364	16:23:00	24	24
	368	16:23:05	24	24

	372	16:23:10	24	24
	376	16:23:15	24	24
	380	16:23:20	24	24
	384	16:23:25	24	24
	388	16:23:30	24	24
Reading Avg.			**24**	
Std. Deviation			**0**	
Std. Error			**0**	
8 mins	392	16:23:35	25	21
	396	16:23:40	25	21
	400	16:23:45	26	21
	404	16:23:50	26	21
	408	16:23:55	25	21
	412	16:24:00	21	21
	416	16:24:05	22	21
	420	16:24:10	22	21
	424	16:24:15	22	21
	429	16:24:20	22	21
	433	16:24:25	21	21
	437	16:24:31	21	21
	441	16:24:36	22	21
	445	16:24:41	22	21
	449	16:24:45	22	21
	453	16:24:50	21	21
	457	16:24:55	22	21
	461	16:25:00	22	21

	465	16:25:05	22	21
	469	16:25:10	22	21
	472	16:25:15	22	21
	476	16:25:20	22	21
	480	16:25:25	22	21
	484	16:25:30	22	21
Reading Avg.			**22.5416667**	
Std. Deviation			**1.55979839**	
Std. Error			**0.31839251**	

Sand/Shingle Mix Movement

Sensor 1	**Frame ID**	**Time**	**Reading (cm)**	**Actual (cm)**
0 mins	2	12:16:41	25	27
	7	12:16:46	25	27
	11	12:16:51	25	27
	15	12:16:56	25	27
	19	12:17:01	25	27
	23	12:17:06	25	27
	27	12:17:11	25	27
	31	12:17:16	25	27
	35	12:17:21	25	27
	39	12:17:26	25	27
	43	12:17:31	25	27
	47	12:17:36	25	27
	50	12:17:41	25	27

	54	12:17:46	25	27
	58	12:17:51	25	27
	62	12:17:56	25	27
	66	12:18:01	25	27
	70	12:18:06	25	27
	74	12:18:11	25	27
	78	12:18:16	33	27
	82	12:18:21	29	27
	86	12:18:26	25	27
	90	12:18:31	25	27
	94	12:18:36	25	27
Reading Avg.			**25.5**	
Std. Deviation			**1.793708813**	
Std. Error			**0.366139278**	
2 mins	98	12:18:41	26	29
	102	12:18:46	30	29
	106	12:18:51	30	29
	110	12:18:56	30	29
	113	12:19:01	30	29
	117	12:19:06	27	29
	121	12:19:11	30	29
	125	12:19:16	30	29
	130	12:19:21	30	29
	134	12:19:26	30	29
	138	12:19:31	30	29
	142	12:19:36	30	29

	146	12:19:41	30	29
	150	12:19:46	30	29
	154	12:19:51	30	29
	158	12:19:56	30	29
	162	12:20:01	30	29
	166	12:20:06	30	29
	170	12:20:11	30	29
	174	12:20:16	30	29
	178	12:20:21	30	29
	182	12:20:26	30	29
	186	12:20:31	30	29
	190	12:20:36	30	29
Reading Avg.			**29.70833333**	
Std. Deviation			**0.999093792**	
Std. Error			**0.203939166**	
4 mins	194	12:20:41	28	29
	198	12:20:46	28	29
	202	12:20:51	27	29
	206	12:20:56	28	29
	210	12:21:01	28	29
	214	12:21:06	27	29
	218	12:21:11	27	29
	222	12:21:16	28	29
	226	12:21:21	27	29
	230	12:21:26	27	29
	234	12:21:31	28	29

	238	12:21:36	27	29
	242	12:21:41	27	29
	246	12:21:46	28	29
	250	12:21:51	28	29
	254	12:21:56	27	29
	258	12:22:01	27	29
	262	12:22:06	28	29
	266	12:22:11	28	29
	270	12:22:16	27	29
	274	12:22:21	27	29
	278	12:22:26	28	29
	282	12:22:31	27	29
	286	12:22:36	28	29
Reading Avg.			**27.5**	
Std. Deviation			**0.510753918**	
Std. Error			**0.104257207**	
6 mins	290	12:22:41	23	24
	294	12:22:46	25	24
	298	12:22:51	25	24
	302	12:22:56	24	24
	306	12:23:01	31	24
	310	12:23:06	24	24
	314	12:23:11	24	24
	318	12:23:16	24	24
	322	12:23:21	24	24
	326	12:23:26	24	24

	330	12:23:31	24	24
	334	12:23:36	24	24
	339	12:23:41	24	24
	343	12:23:46	24	24
	347	12:23:51	24	24
	351	12:23:56	24	24
	355	12:24:01	24	24
	359	12:24:06	24	24
	363	12:24:11	24	24
	367	12:24:16	24	24
	371	12:24:21	24	24
	375	12:24:26	25	24
	379	12:24:31	24	24
	383	12:24:36	24	24
Reading Avg.			**24.375**	
Std. Deviation			**1.468880082**	
Std. Error			**0.299833891**	
8 mins	387	12:24:41	19	23
	391	12:24:47	22	23
	395	12:24:52	22	23
	399	12:24:57	22	23
	403	12:25:02	22	23
	407	12:25:07	22	23
	411	12:25:12	22	23
	415	12:25:17	22	23
	419	12:25:22	23	23

	424	12:25:27	27	23
	428	12:25:32	22	23
	432	12:25:37	22	23
	435	12:25:42	22	23
	439	12:25:47	22	23
	443	12:25:52	22	23
	447	12:25:57	22	23
	451	12:26:02	22	23
	455	12:26:07	22	23
	459	12:26:12	22	23
	463	12:26:17	22	23
	467	12:26:22	22	23
	471	12:26:27	22	23
	475	12:26:32	22	23
	479	12:26:37	22	23
Reading Avg.			**22.125**	
Std. Deviation			**1.226961606**	
Std. Error			**0.250452489**	
Sensor 2	**Frame ID**	**Time**	**Reading (cm)**	**Actual (cm)**
0 mins	1	12:16:40	26	26
	5	12:16:45	26	26
	9	12:16:49	26	26
	13	12:16:55	26	26
	17	12:17:00	25	26
	21	12:17:05	26	26
	25	12:17:10	26	26

	29	12:17:15	26	26
	33	12:17:20	26	26
	38	12:17:26	26	26
	42	12:17:31	26	26
	46	12:17:36	26	26
	51	12:17:42	26	26
	55	12:17:47	26	26
	59	12:17:52	26	26
	63	12:17:57	26	26
	67	12:18:02	26	26
	71	12:18:07	26	26
	75	12:18:12	25	26
	79	12:18:17	27	26
	83	12:18:22	27	26
	87	12:18:27	26	26
	91	12:18:32	26	26
	95	12:18:37	25	26
Reading Avg.			**25.9583333**	
Std. Deviation			**0.46430562**	
Std. Error			**0.09477599**	
2 mins	99	12:18:42	26	25
	103	12:18:47	25	25
	107	12:18:52	25	25
	111	12:18:57	25	25
	115	12:19:02	25	25
	119	12:19:07	25	25

	123	12:19:12	25	25
	127	12:19:17	25	25
	131	12:19:22	25	25
	135	12:19:27	25	25
	139	12:19:32	25	25
	143	12:19:37	25	25
	147	12:19:41	25	25
	151	12:19:47	25	25
	155	12:19:52	25	25
	159	12:19:57	25	25
	163	12:20:02	25	25
	167	12:20:07	25	25
	171	12:20:12	25	25
	175	12:20:17	25	25
	180	12:20:22	25	25
	184	12:20:27	25	25
	188	12:20:32	25	25
	192	12:20:37	25	25
Reading Avg.			**25.0416667**	
Std. Deviation			**0.20412415**	
Std. Error			**0.04166667**	
4 mins	196	12:20:42	22	21
	200	12:20:47	21	21
	204	12:20:52	21	21
	208	12:20:57	21	21
	212	12:21:02	21	21

	215	12:21:07	22	21
	219	12:21:12	21	21
	223	12:21:17	23	21
	227	12:21:22	22	21
	231	12:21:27	21	21
	235	12:21:33	21	21
	239	12:21:38	21	21
	243	12:21:43	21	21
	247	12:21:48	21	21
	251	12:21:53	21	21
	255	12:21:58	21	21
	259	12:22:03	21	21
	264	12:22:09	21	21
	268	12:22:14	21	21
	272	12:22:19	21	21
	276	12:22:24	21	21
	280	12:22:29	21	21
	284	12:22:34	21	21
	288	12:22:39	21	21
Reading Avg.			**21.2083333**	
Std. Deviation			**0.50897738**	
Std. Error			**0.10389457**	
6 mins	292	12:22:44	26	26
	296	12:22:49	26	26
	300	12:22:54	26	26
	304	12:22:59	26	26

	309	12:23:04	26	26
	313	12:23:09	26	26
	317	12:23:14	26	26
	321	12:23:19	26	26
	325	12:23:24	26	26
	329	12:23:29	26	26
	333	12:23:35	26	26
	337	12:23:40	26	26
	341	12:23:45	25	26
	345	12:23:50	26	26
	349	12:23:55	26	26
	353	12:24:00	26	26
	357	12:24:05	26	26
	361	12:24:10	25	26
	365	12:24:15	26	26
	369	12:24:20	25	26
	373	12:24:25	26	26
	377	12:24:30	26	26
	381	12:24:35	25	26
	385	12:24:40	26	26
Reading Avg.			**25.8333333**	
Std. Deviation			**0.38069349**	
Std. Error			**0.07770873**	
8 mins	389	12:24:45	30	31
	394	12:24:51	30	31
	398	12:24:55	30	31

	402	12:25:00	30	31
	406	12:25:06	30	31
	410	12:25:10	29	31
	414	12:25:15	30	31
	418	12:25:20	30	31
	422	12:25:26	30	31
	426	12:25:31	29	31
	430	12:25:36	29	31
	436	12:25:42	29	31
	440	12:25:47	29	31
	444	12:25:52	29	31
	448	12:25:57	29	31
	452	12:26:02	29	31
	456	12:26:07	29	31
	460	12:26:13	29	31
	464	12:26:18	29	31
	468	12:26:23	29	31
	472	12:26:28	29	31
	476	12:26:33	29	31
	480	12:26:38	29	31
	484	12:26:43	29	31
Reading Avg.			**29.3333333**	
Std. Deviation			**0.48154341**	
Std. Error			**0.09829464**	